Revisiting hydro-ecological impacts of climate change on a restored floodplain wetland via hydrological / hydraulic modelling and the UK Climate Projections 2018 scenarios

Julian R. Thompson[1] · Hannah M. Clilverd[1,2] · Jiaxuan Zheng[1] · Honeyeh Iravani[1] · Carl D. Sayer[1] · Catherine M. Heppell[3] · Jan C. Axmacher[1]

Abstract

The hydro-ecological impacts of 40 UK Climate Projections 2018 scenarios on a restored lowland England river floodplain are assessed using a MIKE SHE / MIKE 11 model. Annual precipitation declines for 60% of scenarios (range: -26%–21%, with small, <5%, declines for the central probability level). Potential evapotranspiration increases for all probability levels except the most extreme, very unlikely, 10% level (range: -4%–43%, central probability 9%–20%) Mean, peak and low river discharges are reduced for all but the extreme 90% probability level. Reduced frequency of bankfull discharge dominates (at least halved for the central probability level). Floodplain inundation declines for over 97% of 320 scenario-events. Winter water table levels still intercept the surface, while mean and summer low levels are reduced. Declines in mean summer floodplain water table levels for the central probability level (0.22 m and 0.28 m for the 2050s and 2080s, respectively) are twice as large as those in the more dynamic riparian area. Declines reach 0.39 m for some 10% probability level scenarios. Simulated hydrological changes differ subtly from a previous assessment using earlier UK climate projections. A soil aeration stress index demonstrates that, under baseline conditions, prolonged high winter floodplain water tables drive long periods of low root-zone oxygen, in turn favouring vegetation communities adapted to waterlogged conditions. Climate change reduces aeration stress and the extent of appropriate conditions for these plant communities in favour of communities less tolerant of wet conditions.

Keywords Climate change; floodplain · MIKE SHE · UKCP18 · Aeration stress

Introduction

Intensification of the global hydrological cycle in response to a warming climate is projected to drive changes in precipitation and evapotranspiration (e.g. IPCC 2014, 2018). These will, in turn, impact catchment hydrological processes with implications that include changes to river flows, soil moisture and groundwater levels (Kundzewicz et al. 2007;

Bates et al. 2008; Jiménez Cisneros et al. 2014). There is, however, uncertainty in the hydrological impacts of climate change (e.g. Wilby and Dessai 2010). Studies have demonstrated hydrological responses that vary spatially across the globe (e.g. Arnell and Gosling 2013; Gosling et al. 2017; Do et al. 2020), for different parts of the same catchment (e.g. Thompson et al. 2014, 2017a), and contrasting impacts on high, mean and low flows (Giuntoli et al. 2015; Chan et al. 2020). Notwithstanding this uncertainty, climate-change driven modifications to hydrological conditions clearly have major implications for global aquatic ecosystems (Döll and Zhang 2010; Thompson et al. 2021a). Such changes have significant potential to drive wetland loss and degradation (Ramsar Convention on Wetlands 2018, 2021; Xi et al. 2020), given the dominant influence of hydrology upon wetland functioning (e.g. Baker et al. 2009). Climate change will impose additional stresses on environments which, in many cases, have already been strongly modified

✉ Julian R. Thompson
   j.r.thompson@ucl.ac.uk

1   UCL Department of Geography, University College London, Gower Street, London WC1E 6BT, UK

2   UK Centre for Ecology and Hydrology, Bush Estate, Penicuik, Midlothian EH26 0QB, UK

3   School of Geography, Queen Mary University of London, Mile End Road, London E1 4NS, UK

by human actions (Tickner et al. 2020). Many ecosystem services are underpinned by hydro-ecological conditions. Climate change-driven changes to hydrology therefore have broader consequences for human populations (Maltby et al. 2011; Okruszko et al. 2011).

Floodplain wetlands exemplify the important influence of hydrology on ecological conditions and ecosystem service provision. Exchanges of water between rivers and their floodplains via overbank inundation, as well as through the hyporheic zone, play important roles in driving habitat heterogeneity including, for example, variability in shallow groundwater levels (Ward 1998; Gowing et al. 2002a; Thompson et al. 2004). This heterogeneity, characterised by small-scale microhabitat mosaics, is further enhanced by the disturbance provided by floods and associated sediment, nutrient and propagule deposition (Junk et al. 1989; Naiman et al. 2010; Nilsson et al. 2010). Hydrological conditions, in particular water table depth and flooding regime (i.e. frequency, duration and depth of inundation), therefore exert dominant controls on the composition and zonation of plants within floodplain wetlands (e.g. Toogood et al. 2008; Wheeler et al. 2009). Root zone aeration stress, which is strongly influenced by the depth to the water table, has been identified as an important determinant of plant species distribution (Silvertown et al. 1999; Gowing et al. 2002a, 2002b; Dwire et al. 2006; Clilverd et al. 2022). Similarly, the hydrological regime of floodplains and associated wetlands influences habitat suitability for animals. For example, water table depth and soil wetness impact upon wading birds via controls on habitat suitability for invertebrate prey (Plum 2005; Eglington et al. 2010) and soil penetrability by birds' beaks (Ausden et al. 2001; Smart et al. 2008).

The dominant influence of hydrological conditions on floodplain wetlands is further evidenced by ecological declines that have accompanied river regulation (e.g. Ward and Stanford 1995; Nilsson and Svedmark 2002). Extent, frequency and duration of inundation have often been reduced via the construction of embankments, often combined with widening and deepening of rivers, designed to protect surrounding land from flooding and improve agricultural productivity (e.g. Wyżga 2001; Tockner and Stanford 2002; Antheunisse et al. 2006). Re-establishing connections between rivers and floodplains via embankment removal and channel reconfiguration has expanded in response to widespread recognition of the damage inflicted by river regulation (e.g. Acreman et al. 2003; Bernhardt et al. 2005). In combination with other restoration measures (e.g. Meynell et al. 2012), such approaches aim to establish more natural flood-pulse ecosystems with benefits to biodiversity and ecosystem services such as floodwater storage and nutrient retention (e.g. Blackwell and Maltby 2006; Pescott and Wentworth 2011). Appreciation of the need to restore floodplains is, however, coincident with concerns about the hydro-ecological impacts of climate change. Floodplains are likely to be severely impacted by climate change-related modifications to local meteorological conditions (i.e. precipitation and evaporation) and changing river flows in response to climatic change over their wider catchments (Thompson et al. 2016, 2021b; Rahman et al. 2020).

Robust evaluation of hydro-ecological impacts of climate change requires hydrological models capable of representing complex, inter-related processes within floodplains and similar wetlands. This includes inundation from rivers and other water bodies, infiltration of floodwater and resulting water table rises, drainage of surface water to river channels, and further bi-directional subsurface exchanges between river channels, water bodies and shallow groundwater (e.g. Rahman et al. 2016; Jones et al. 2019). Process simulation should ideally be undertaken at sufficiently high spatial resolution to characterise variability in hydrological conditions across individual wetlands, and at a sufficiently fine vertical resolution to link results to the sensitive water table requirements of floodplain vegetation (e.g. Gowing et al. 2002b; Tattersfield and McInnes 2003; Wheeler et al. 2004). Such water level requirements enable the translation of hydrological changes to ecological responses. The MIKE SHE / MIKE 11 coupled hydrological / hydraulic modelling system has been successfully employed in simulating floodplain and other wetland environments (e.g. Al-Khudhairy et al. 1999; Refsgaard et al. 1998; Thompson 2004; Hammersmark et al. 2008; Dai et al. 2010; House et al. 2016b; Gardner et al. 2019; Duranel et al. 2021). A number of studies have combined high resolution projections of changing hydrological conditions provided by MIKE SHE / MIKE 11 models of UK floodplain wetlands with water requirements of plants and animals in order to assess ecological responses (e.g. Thompson 2009; House et al. 2016a, 2017).

These earlier studies employed UKCIP02 or UKCP09, UK-wide climate change projections developed by the UK Climate Impacts Programme (UKCIP). These, and more recent UKCIP projections superseding them, provide high-resolution projections of climate change suitable for impact assessment. UKCP18 (Lowe et al. 2018), the latest generation of projections used in our study, employs the four 'Representative Concentration Pathways' (RCPs) that feature extensively in international climate change research (Moss et al. 2010). The RCPs are associated with radiative forcing targets of between 2.6 and 8.5 Wm^2 by 2100. As such they encompass a range of assumptions concerning future global population, economic development and greenhouse gas mitigation measures (Moss et al. 2010). The climate modelling methodology adopted by UKCP18 provides probability functions for change in a range of meteorological parameters for each RCP thereby providing insights into uncertainties in future UK climate (Lowe et al. 2018).

Updating and expansion of climate projections at global, regional, or national levels enable the re-assessment of studies on the hydro-ecological impacts on wetlands. However, such re-evaluations are relatively rare (see Thompson et al. 2016, 2017a for one example), at least in part because they often require substantial numerical modelling (Kay et al. 2020). The current study provides such a re-evaluation, in this case for a river floodplain (Hunworth Meadow, River Glaven) restored by embankment removal in North Norfolk, eastern England, UK (Clilverd et al. 2016). It builds upon and expands a climate change impact assessment of the site by Thompson et al. (2017b) that employed 30 UKCP09 scenarios. This earlier study identified a dominance of drier conditions which were characterised by lower water tables, especially in summer, and a reduction in the frequency and extent of inundation. A preliminary analysis suggested that declining root zone soil aeration stress could have implications for floodplain vegetation.

The current study employs a total of 40 scenarios from the UKCP18 projections that encompass different future time periods over the current century, alternative levels of radiative forcing and varied levels of uncertainty. These projections are used to perturb the meteorological inputs to a high resolution coupled hydrological / hydraulic model of Hunworth Meadow as well as a rainfall-runoff model of the wider catchment that, in turn, provides estimates of changes in river discharge upstream of Hunworth. The hydrological impacts of climate change are initially re-evaluated using the new climate change scenarios and approaches adopted in the earlier assessment (Thompson et al. 2017b). These comprise reviews of modifications to river flows and the frequency of bankfull discharges, the extent of inundation during flood events and simulated water table levels at representative locations that coincide with observation wells. Assessments of the hydrological impacts of the UKCP18 scenarios are subsequently extended to high resolution, site-wide analysis of changes in water table elevations that include mean conditions as well as extreme low and high levels. The novel combination of distributed water tables across the meadow with an aeration stress index enables a review of potential climate change impacts on an important hydrological control of the vegetation. Comparisons of this stress index with tolerance ranges finally provides insights into spatial patterns for current and scenario water table suitability for five floodplain / wet grassland plant communities.

Methods

Study Area

Hunworth Meadow is located on the floodplain of the River Glaven (Fig. 1), a small (17 km long) lowland river draining a chalk catchment (total area: 115 km^2). From a geomorphological and hydrological standpoint, the Glaven is a typical small UK lowland coastal river. However, the river is of high importance due to the occurrence of species of UK and European-level conservation concern, including Brook Lamprey (*Lampetra planeri)*, European Bullhead (*Cottus gobio)* and the critically endangered White-clawed Crayfish (*Austropotamobius pallipes)*. Floodplain restoration work on Hunworth Meadow (described below) is characteristic of many schemes developed for UK lowland rivers (e.g. The River Restoration Centre 2023). While comprehensive studies are lacking for many of these UK river-floodplain re-connection projects, the Glaven's Hunworth Meadow site has been widely studied, covering multiple physical, hydrological and biological elements (Clilverd et al. 2013; Sayer 2014; Champkin et al. 2018). As such, it is of high importance for understanding restoration outcomes and hence developing future conservation work. The datasets established through these studies permit the application of robust scientific approaches including the high-resolution numerical modelling reported in the current study.

Chalk bedrock in the Glaven catchment is overlain by chalk-rich sandy till and glaciogenic sand and gravel (Moorlock et al. 2002), whilst floodplain soils are alluvial and characteristically up to 2 m thick (Clilverd et al. 2013). The catchment is dominated by arable agriculture interspersed with deciduous and coniferous woodland, and by grazing meadows. Mean annual catchment rainfall (1985–2015) of 620 mm exceeds annual potential evapotranspiration (PET) by, on average, 20 mm. Seasonality in differences between precipitation and PET is reflected in stream discharge; largest flows occur in winter, while low flows dominate in summer. Mean discharge at a gauging station immediately upstream of Hunworth Meadow for the period 2001–2010 was 0.26 m^{3}s^{-1}, whilst the largest recorded discharge was 3.1 m^{3}s^{-1} (Clilverd et al. 2016).

The meadow is approximately 400 m long, 40–80 m wide and covers an area of nearly 3 ha. It is bounded to the south by the River Glaven, whilst its north-east boundary is defined by the start of an arable and wooded hillslope (Fig. 1). Elevation declines very gradually in a downstream direction with a total fall of no more than 1 m along the length of the meadow. An agricultural ditch runs along the floodplain, parallel to the river and close to the hillslope. It was blocked at its downstream end throughout the current study, producing near-permanent water within a shallow pond on the lowest part of the floodplain. Pre-restoration vegetation comprised a degraded *Holcus lanatus-Juncus effusus* rush-pasture community (represented by MG10, with constant species *Agrostis stolonifera*, *Holcus lanatus*, *Juncus effusus*, and *Ranunculus repens*, according to the UK National Vegetation Classification, NVC, Rodwell 1992), typical of consistently moist soils (Clilverd 2016; Clilverd et al. 2022).

Fig. 1 Hunworth Meadow, north Norfolk and locations of shallow groundwater monitoring wells and the automatic weather station
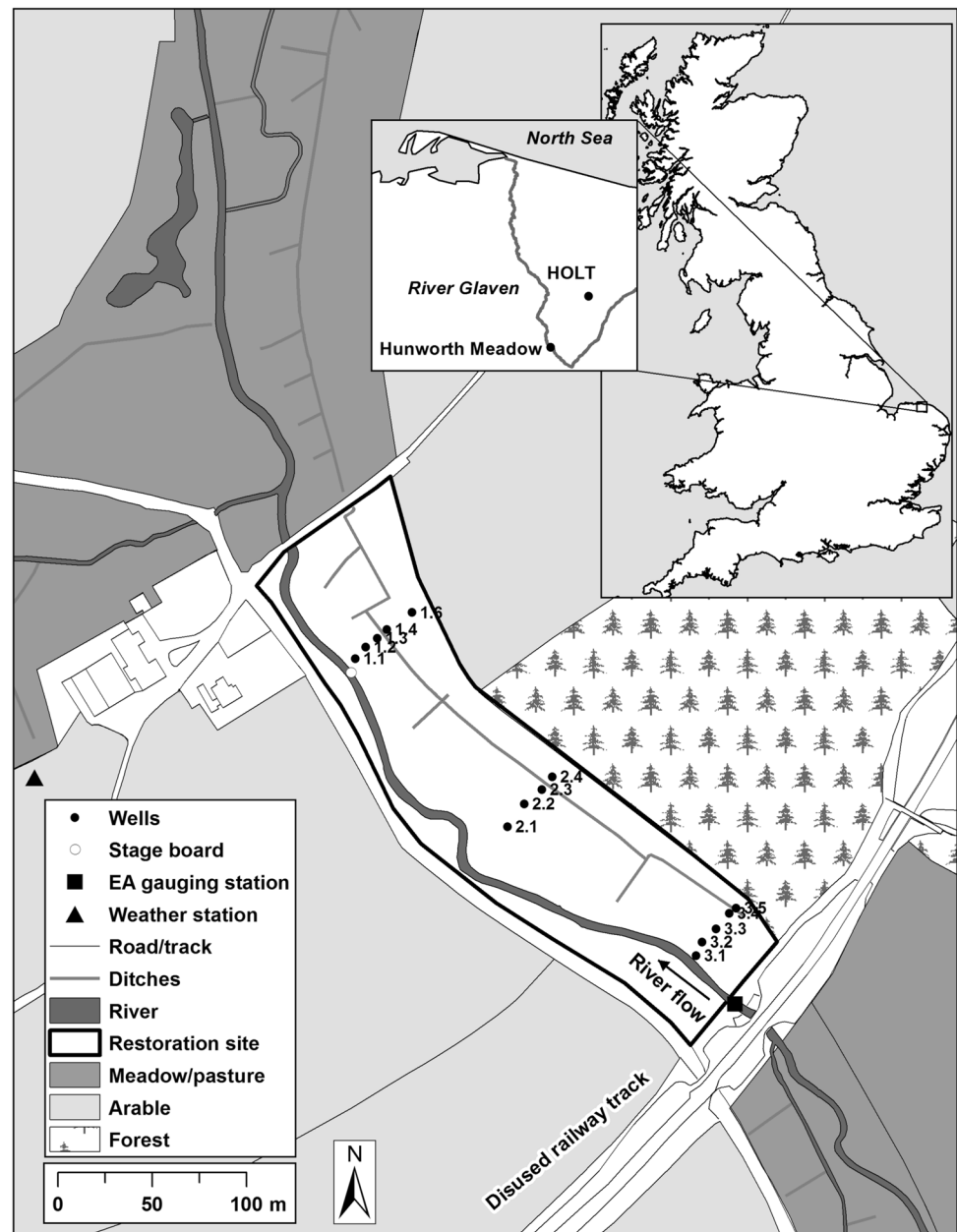
In common with many reaches along the Glaven, the river channel at Hunworth was historically straightened and constrained by embankments ranging in height from 0.4 m to 1.1 m above the meadow surface (Clilverd et al. 2013). The embankments were designed to limit overbank flows onto the floodplain. They may also have restricted drainage from the floodplain back to the river, especially towards its downstream limit, thus contributing to waterlogging of the floodplain (Thompson et al. 2017b). As described by Clilverd et al. (2016), restoration works for Hunworth Meadow focussed on restoring river-floodplain connections, thereby providing temporary flood storage during periods of high river flow and establishing a hydrological regime that could enable diversification of wet meadow vegetation (e.g. Hammersmark et al. 2008; Castellarin et al. 2010; Viers et al. 2012). In March 2009, embankments were removed along the entire length of the Hunworth reach except for a short (c. 20 m) section which was retained to protect European Water Vole (*Arvicola amphibious*) burrows. Riverbank elevations were lowered to the level of the adjacent floodplain, whilst the depth and cross-sectional area of the channel were reduced by, on average, 44% and 60%, respectively (Clilverd et al. 2013).

Hydrological / hydraulic modelling

Clilverd et al. (2016) provided a detailed description of the MIKE SHE / MIKE 11 modelling of Hunworth Meadow. Consequentially, the model is reviewed relatively briefly herein. The model domain included Hunworth Meadow and extended to the top of the hillsides on either side of the river. The upstream boundary coincided with a disused railway embankment, whilst the downstream boundary was defined by a smaller embankment carrying an agricultural track. The domain was discretised using a 5 m × 5 m grid (total number of cells: 5,308). Grid cell elevations were derived from dGPS surveys (Leica Geosystems SR530 base station receiver and Series 1200 rover receiver, Milton Keynes, UK), undertaken before and after embankment removal (Clilverd et al. 2013) so that two distinct models were developed representing conditions pre- and post-restoration. The spatial resolution of the model enabled retention of the floodplain ditch within the topographic data. Spatially uniform precipitation and PET were applied across the model. An automatic weather station (AWS; MiniMet SDL 5400, Skye, Powys, UK) installed in a field 100 m from the meadow (Fig. 1) provided daily precipitation with gaps filled using the Mannington Hall UK Met Office meteorological station (<10 km from the site). The AWS also provided air temperature, net radiation, relative humidity, and wind speed data which were used to calculate daily Penman-Monteith PET (Monteith 1965).

The 3D finite difference saturated zone model comprised a single layer representing the alluvial and glacial soils that are separated from the underlying chalk by low-permeability boulder clay. Horizontal and vertical hydraulic conductivity of this layer were calibration terms with initial values guided by piezometer slug tests (Surridge et al. 2005). Lower hydraulic conductivity was specified in the location of the pond at the downstream end of the meadow. Based on assumptions that the groundwater divide follows the topographic divide and foundations of the upstream railway embankment limit subsurface flows, a zero-flow boundary was specified around most of the model. The exception was the downstream boundary where a constant head was specified using mean groundwater elevation from a well transect (see below) to permit subsurface flow perpendicular to the river and towards the next section of floodplain. The MIKE SHE drainage option represented the likely small volume of relatively rapid runoff along the base of the hillside and along the ditch, with its two parameters defining depth and size of the drains being varied during calibration.

The unsaturated zone was represented using the conceptual two-layer water balance method (e.g. Thompson 2012). A uniform soil type was specified across the model domain with its parameterisation (infiltration rate, soil water content at saturation, field capacity and wilting point, and the ET depth) informed by piezometer slug tests, water release characteristics derived from sandbox experiments (Eijkelkamp, Giesbeek, The Netherlands), soil porosity and the literature (Chubarova 1972; Das 2002; DHI 2007; Zotarelli et al. 2010). Parameterisation of root depth and Leaf Area Index (LAI), including temporal variations to reflect seasonal vegetation development, for three land covers (riparian grassland, mixed deciduous/coniferous woodland, and arable land) was based on values from the literature (Canadell et al. 1996; Hough and Jones 1997; Herbst et al. 2008; Thorup-Kristensen et al. 2009; FAO 2013). Root depth and LAI for the small extent of roads and buildings were assigned values of 0. Manning's roughness for overland flow was distributed throughout the model using the four land cover classes, with initial values taken from the literature and varied during calibration (USDA 1986; Thompson 2004).

MIKE 11 models of the River Glaven immediately upstream, through and downstream of Hunworth Meadow represented original embanked conditions and those following embankment removal. These models were dynamically coupled to the respective MIKE SHE model using the methodology described by Thompson et al. (2004). Channel location was digitised from 1:10,000 Ordnance Survey LandLine.Plus data digital map data with cross sections specified every 10 m along the channel. Cross sections were derived from the pre- and post-restoration dGPS surveys. Time varying Manning's n roughness was specified through both MIKE 11 models to represent seasonal in-stream macrophyte growth (Clilverd et al. 2013; House et al. 2016b). MIKE SHE grid cells covering the immediate riparian area (cells containing the river channel, the embankments in the case of the pre-restoration model and a zone up to 10 m from the river onto the meadow) were specified as being potentially directly flooded by MIKE 11. The MIKE SHE / MIKE 11 coupling simulates inundation of these cells if MIKE 11 water levels exceed their elevation and thereafter the MIKE SHE overland flow component simulates water movement across the floodplain (Thompson et al. 2004). Daily mean discharge from the gauging station above Hunworth Meadow was specified as the upstream MIKE 11 boundary condition. The lower boundary comprised a constant water level just above the river bed with the MIKE 11 model extended downstream beyond the floodplain so that the boundary did not impact simulated water levels within the reach adjacent to Hunworth Meadow.

A three-stage calibration and validation approach was employed. In each stage, model performance was assessed via comparison of simulated water table levels with observations from 10 shallow (1–2 m deep) wells installed in three transects across the floodplain (Fig. 1; Clilverd et al. 2013). Mean daily water table levels were obtained from pressure transducers (Levelogger Gold 3.0 corrected for atmospheric pressure using a Barologger Gold, Solist, Ontario, Canada)

installed in each well to match the frequency with which MIKE SHE results were stored. The root mean square error (RMSE), Pearson correlation coefficient (r) and Nash-Sutcliffe efficiency coefficient (NSE; Nash and Sutcliffe 1970) were used to evaluate model performance. The pre-restoration model (i.e. using topography and cross-sections that included the embankments) was first calibrated for the period 22/02/2007–14/03/2008. An automatic procedure (Madsen 2000, 2003) was initially employed using a 15 m × 15 m model grid to reduce computation time, with parameter values then being refined manually using the 5 m × 5 m grid. Validation using the pre-restoration model employed the period 15/03/2008–15/03/2009. The end of this second period coincided with embankment removal, so a further validation employed the post-restoration model (i.e. revised

topography and cross-sections) with values of the calibration parameters established in the previous step and the period 29/03/2009–25/05/2010. Good agreement between observed and simulated groundwater levels was achieved (e.g. Fig. 2). This included reproduction of observed seasonal fluctuations and relatively rapid responses to high magnitude rainfall events, particularly at locations close to the river. Across the different wells, the mean values of r for the calibration and pre- and post-restoration validation periods were 0.85, 0.80 and 0.85, respectively. Mean error (ME) was typically less than ± 0.05 m whilst, for most wells, NSE values were normally in the range 0.50—0.80 (see Clilverd et al. 2016).

Clilverd et al. (2016) compared results for the pre- and post-restoration models for an extended simulation period (2001–2010) to evaluate the impacts of embankment
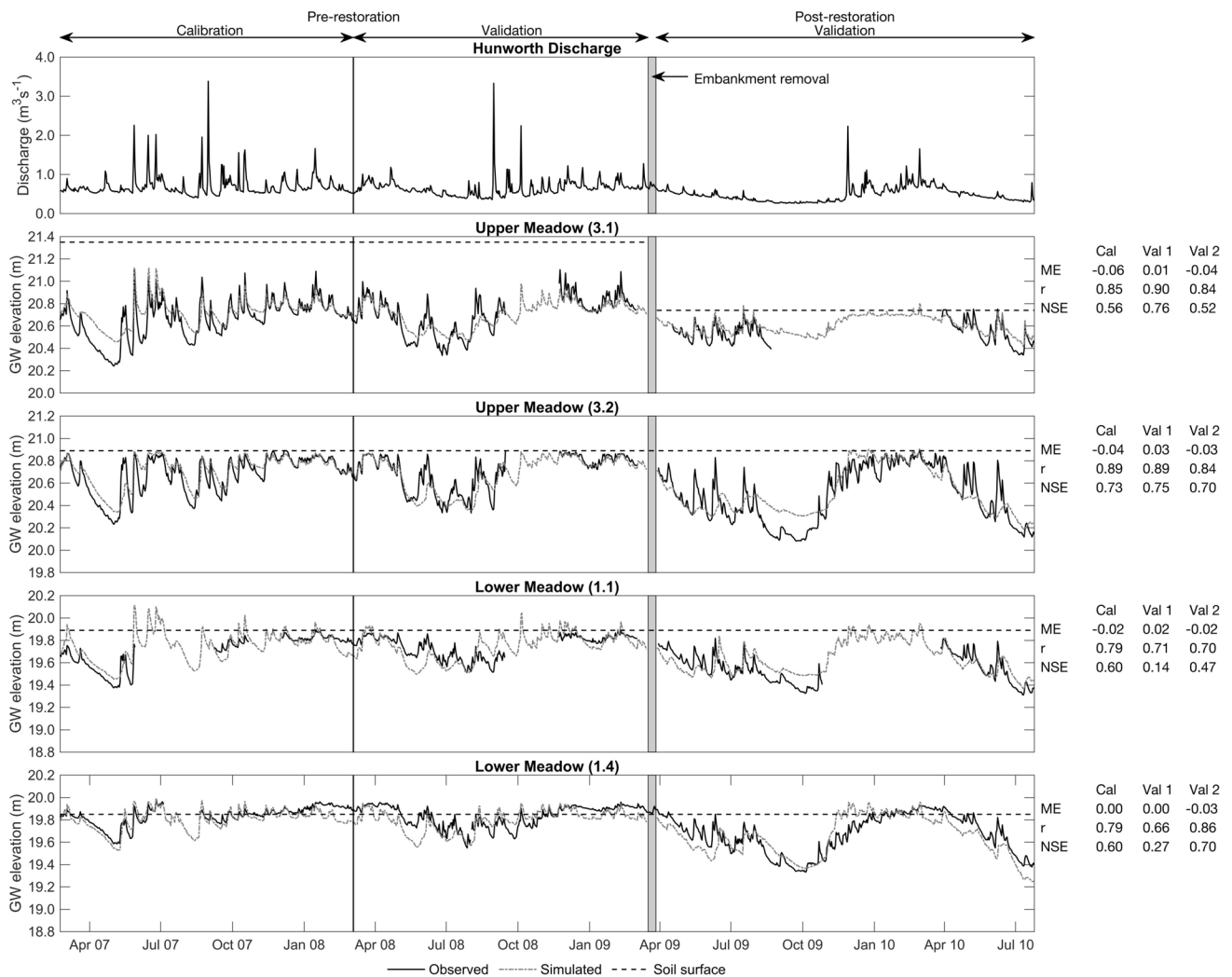
Fig. 2 Observed and simulated groundwater depths for four representative wells installed in Hunworth Meadow and corresponding river discharge at the Hunworth gauging station for the calibration and validation periods. Values of mean error (ME), Pearson correla-

tion coefficient (r) and Nash-Sutcliffe efficiency coefficient (NSE) are provided for the calibration and two validation periods. Embankment removal in March 2009 is indicated. Well locations are shown in Figure 1.

removal over a range of climate and river flow conditions. Whilst river flow data for the gauging station above Hunworth Meadow were available for the upstream MIKE 11 boundary condition, the AWS was not in operation for most of this period. Consequently, precipitation and Penman-Monteith PET were established using data from the Mannington Hall meteorological station. Following the approach of Thompson et al. (2017b), the current study employs the post-restoration MIKE SHE / MIKE 11 model forced with these data for the same ten-year period as a baseline to re-assess the impacts of climate change using UKCP18, the current UK-wide climate projections.

Simulation of the hydrological impacts of climate change

Monthly changes (delta factors) for precipitation (%), minimum, mean and maximum temperatures (°C), relative humidity (%) and total downward surface shortwave flux (W m^2) with respect to a 30-year baseline (1981–2010, containing the extended simulation period) were acquired for the 25 km × 25 km UKCP18 grid cell containing Hunworth Meadow and the upstream Glaven catchment for four RCPs and two future time slices (2040–2069 and 2070–2099). The two time slices represent conditions towards the middle (2050s) and end (2080s) of the 21st century, respectively. Changes in each of the climate variables were obtained from the respective probability distribution functions for probabilities of between 10% and 90% in 20% increments (Thompson 2012; Thompson et al. 2017b), resulting in 40 scenarios overall (20 for each time slice). In this way, the range of probabilities includes the central estimate of change (i.e. 50% probability level, representing change that is as likely as not to be exceeded) and is bounded by changes that are very likely (10% probability) and very unlikely (90% probability) to be exceeded. The scenarios are referred to in the form 2050-4.5$_{50}$ (i.e. 2050s time slice, RCP4.5, 50% probability level). Scenario precipitation was derived by multiplying the original precipitation data for 2001–2010 by the monthly percentage changes from UKCP18. The delta factors for the remaining meteorological variables were used to perturb the corresponding time series which were, in turn, employed in the recalculation of Penman-Monteith PET for each scenario (Thompson et al. 2009, 2014, 2017b).

Scenario discharges at the gauging station above Hunworth Meadow were established using a MIKE NAM rainfall-runoff model developed by Thompson et al. (2017b) following the methodology established by House et al. (2016a). MIKE NAM is a deterministic, lumped conceptual model that represents storage within, and flows between, interrelated catchment stores (surface, soil, groundwater; DHI 2009; Hafezparast et al. 2013). The MIKE NAM model of the 37.6 km^2 catchment above Hunworth was initially calibrated against observed discharge

for the period 2001–2010. Calibration was undertaken using a combination of automatic optimisation routines and manual fine tuning of parameters that included maximum water content in the surface and root zone stores, the overland flow runoff coefficient, time constants for interflow, routing overland flow and routing baseflow, and the root zone zone threshold values for overland flow, interflow and groundwater recharge. Performance was considered appropriate, especially at a monthly time step for which values of bias (differences between observed and simulated mean discharge when expressed as a percentage), and NSE were classed as "excellent" and "very good", respectively, according to the classification scheme of Henriksen et al. (2008) (see Thompson et al. 2017b for details). Within the current study, the calibrated MIKE NAM model was forced with perturbed precipitation and PET for each of the UKCP18 climate change scenarios. Monthly delta factors for discharge were established as the percentage differences between baseline and scenario mean monthly discharges. These were then applied to the records from the gauging station above Hunworth Meadow.

Each of the UKCP18 climate change scenarios were simulated by substituting the original precipitation, PET, and discharge times series used to force the coupled MIKE SHE / MIKE 11 post-restoration model with those developed using the approaches described above. The extended 2001–2010 simulation period was used for each scenario, with the results compared with those from the model forced with the original hydrometeorological inputs (i.e. the baseline). The focus of this hydrological comparison was simulated groundwater levels at representative points on the floodplain corresponding to well locations, as well as across the whole of the meadow, and floodplain inundation during a number of representative flood events.

Hydrological change impacts on floodplain vegetation

An aeration stress index was used to evaluate potential floristically relevant changes in hydrological conditions within Hunworth Meadow due to climate change. The Sum Exceedance Values for aeration stress (SEV$_{as}$) index indicating waterlogging was originally proposed by Sieben (1965) and subsequently adapted to wet grassland communities by Gowing et al. (1998b)). It employs water table position as a proxy for aeration stress under shallow water table conditions - i.e. where the water table is less than 1 m below the soil surface (Gowing et al. 1998a; Silvertown et al. 1999). Aeration stress is calculated as the integral of the difference between modelled and a reference water table depth:

$$SEV_{as} = \int_{1}^{N} (D_{ref} - D_W) dt \qquad (1)$$

where SEV_{as} is sum exceedance value (number of weeks when the reference depth is exceeded, multiplied by the height by which the water table exceeded it) and increases in value with aeration stress; N is the number of weeks in the active growing season for grasses (taken to be March–September inclusive; Gowing et al. 2002b); D_W is simulated depth to the water table (m) and D_{ref} is the reference water table (m) where air filled porosity at the surface = 0.1 (the threshold porosity expected for aeration stress in plants; Wesseling and van Wijk 1975; Gowing et al. 1998a). D_{ref} was established by Clilverd et al. (2016) using sandbox measurements (Eijkelkamp, Giesbeek, The Netherlands) of soil samples and the approach of Barber et al. (2004). The established value for D_{ref} of 0.34 m was very close to that employed by Gowing et al. (1998a) to calculate SEV_{as} within a UK peat-based wet grassland. In this study, the integral was solved numerically at one-week intervals, and only positive values were included in the integration. Annual values of SEV_{as} were first calculated from simulated water table depths in each of the MIKE SHE grid cells covering the meadow and immediate riparian area (n = 1059) for the baseline and each of the 40 climate change scenarios. A mean SEV_{as} across all years of the simulation period was then established for each of these cells.

The values of mean SEV_{as} were compared against SEV_{as} tolerance ranges (minimum and maximum; Table 1) for five NVC floodplain / wet mesotrophic grassland (MG) plant communities (Rodwell 1992). Ranges were taken from figures of mean water-regime (± 95% CI) of plant communities and differential tolerances to SEV_{as} from presence-absence data in Gowing et al. (2002a, 2002b). The communities include those of high conservation interest with free-draining soils and limited tolerance to waterlogging (low SEV_{as}; MG4 species-rich grass and broad-leaved herb floodplain meadow characterised by *Alopecurus pratensis* and *Sanguisorba officinalis*), through those which occupy less well-drained soils and are tolerant of fluctuating soil moisture conditions (mid SEV_{as}; species-rich MG7C *Lolium perenne - Alopecurus pratensis – Festuca pratensis* flood-pasture; and MG8 *Cynosurus cristatus – Caltha palustris* water meadow), to those which can tolerate extended periods of high water tables and hence soil aeration stress and tend to be species-poor assemblages (high SEV_{as}; MG13 *Agrostis stolonifera – Alopecurus geniculatus* inundation grassland; and AG/Cx water meadow characterized by *Agrostis/Carex* grassland) (see Table 1). This analysis was undertaken for all floodplain / riparian cells for the baseline and each of the 40 climate change scenarios. Subsequent baseline-scenario comparison of the number and distribution of cells with tolerable values of SEV_{as} provided a basis for evaluating how climate change-driven modifications to the simulated hydrological regime might induce vegetation responses.

Results

Climate change-impacts on hydrometeorological forcing

Mean annual precipitation declines for probability levels between 10% and 50% across all four RCPs and both time slices. It increases for all 70% and 90% probability scenarios (Table 2). Declines for 50% probability are small, and for a given time slice they are slightly larger with progression from RCP2.6 to RCP8.5 (2050s: 3%–4%; 2080s: 2%–4%). Inter-time slice differences for a given RCP at this level of probability are also small with, on average, declines for the 2050s being around 1% larger than those for the 2080s. Declines for the 10% probability (very likely to be exceeded) are larger, and those for 30% are intermediate. There is, again, a general increase in the magnitude of declines with radiative forcing, although inter-RCP differences are small - declines range between 22% (20%) and 24% (26%) for RCP2.6 and RCP8.5, respectively for the 2050s (2080s). Similarly, inter-time slice differences are modest (≤ 2%),

Table 1 NVC vegetation communities (outlined in Rodwell 1992) and the SEV_{as} ranges employed in assessing water level regime suitability under baseline conditions and each climate change scenario

NVC community	Community name	Vegetation type	SEV_{as} range (m weeks)	
			Minimum	Maximum
MG4	*Alopecurus pratensis - Sanguisorba officinalis* grassland	Floodplain meadow	0.0	1.0
MG7C	*Lolium perenne - Alopecurus pratensis - Festuca pratensis* grassland (species-rich variant)	Flood pasture	1.5	2.7
MG8	*Cynosurus cristatus - Caltha palustris* grassland	Water meadow	1.6	4.1
MG13	*Agrostis stoloniofera - Alopecurus geniculatus* grassland (*Alopecurus pratensis* variant)	Inundation grassland	3.3	5.0
AG/Cx	*Agrostis / Carex* grassland (both variants)	Water meadow	4.1	6.8

Table 2 Mean annual precipitation, potential evapotranspiration (PET) and net precipitation (precipitation – PET) (mm), and number (% of 120 months) of months when precipitation > PET (i.e. net pre- cipitation is positive) for the baseline and each UCKIP18 scenario for the period 2001–2010. Shaded cells indicate reductions compared to the baseline

Mean Annual Precipitation: Baseline 774						
		10%	30%	50%	70%	90%
2050	2.6	607	688	745	807	896
	4.5	600	682	742	804	897
	6.0	602	684	741	804	897
	8.5	587	674	739	804	904
2080	2.6	617	698	757	819	909
	4.5	604	692	755	819	915
	6.0	597	685	751	819	919
	8.5	574	673	745	821	938

Mean Annual PET: Baseline 509						
		10%	30%	50%	70%	90%
2050	2.6	489	525	555	582	622
	4.5	490	527	556	585	626
	6.0	488	526	554	583	624
	8.5	496	540	570	603	651
2080	2.6	491	531	559	589	631
	4.5	496	540	573	606	658
	6.0	496	544	582	619	674
	8.5	506	566	610	656	727

Mean Annual Net Precipitation: Baseline 265						
		10%	30%	50%	70%	90%
2050	2.6	118	163	189	225	274
	4.5	111	155	187	219	271
	6.0	115	158	187	221	273
	8.5	91	134	170	201	253
2080	2.6	126	167	198	230	278
	4.5	108	152	182	213	257
	6.0	101	141	170	200	245
	8.5	67	106	136	165	211

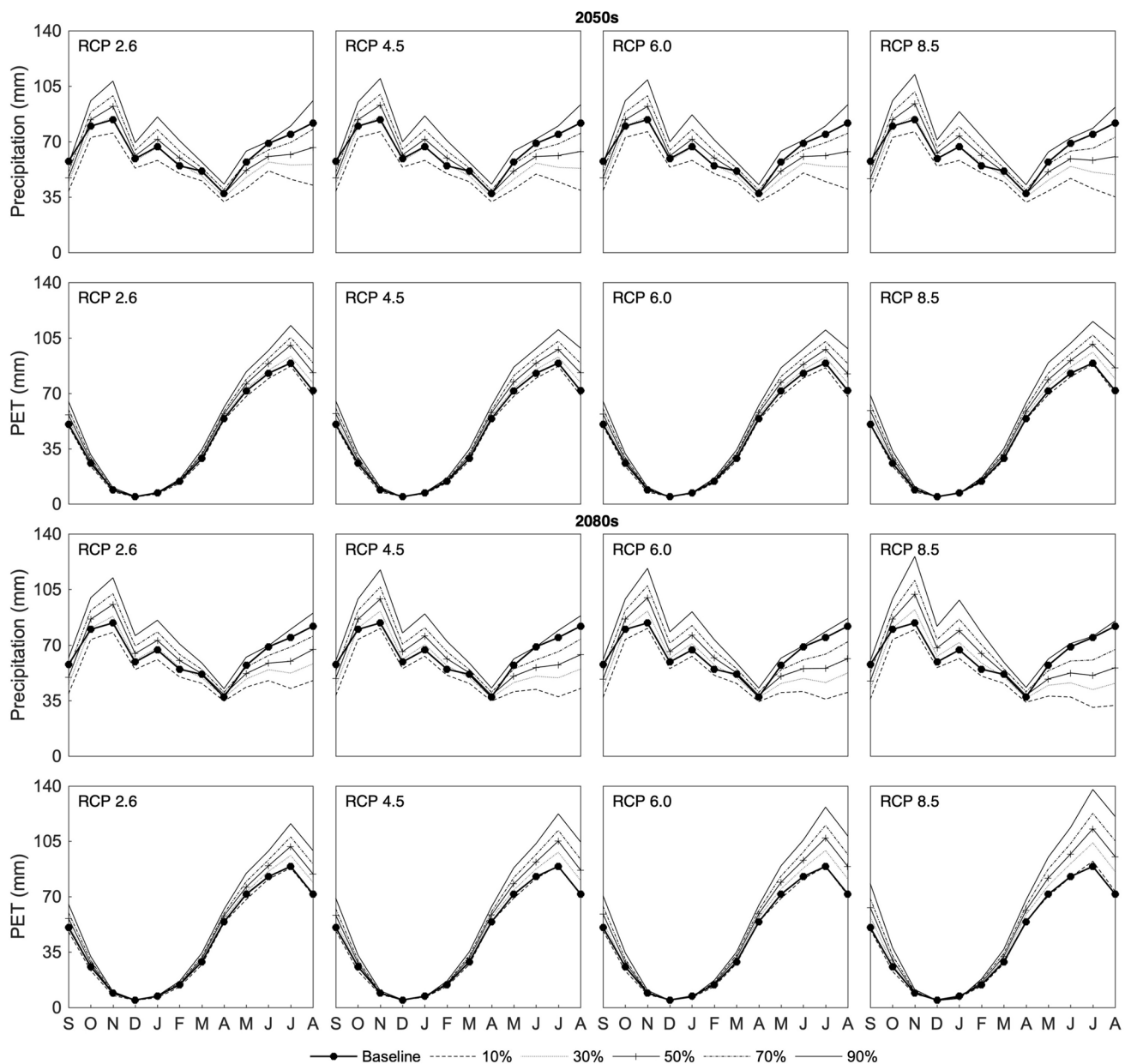| Months where Precipitation > PET: Baseline 76 (63%)						
		10%	30%	50%	70%	90%
2050	2.6	65 (54%)	67 (56%)	68 (57%)	72 (60%)	73 (61%)
	4.5	65 (54%)	67 (56%)	69 (58%)	70 (58%)	72 (60%)
	6.0	65 (54%)	67 (56%)	68 (57%)	71 (59%)	73 (61%)
	8.5	63 (53%)	65 (54%)	67 (56%)	68 (57%)	71 (59%)
2080	2.6	67 (56%)	67 (56%)	69 (58%)	71 (59%)	73 (61%)
	4.5	66 (55%)	67 (56%)	67 (56%)	69 (58%)	70 (58%)
	6.0	65 (54%)	66 (55%)	67 (56%)	68 (57%)	69 (58%)
	8.5	62 (52%)	62 (52%)	65 (54%)	65 (54%)	66 (55%)

Fig. 3 Mean monthly precipitation and potential evapotranspiration for the baseline and each UKCP18 scenario for the 2050s and 2080s

with changes for the 2050s slightly exceeding those for the 2080s for RCP2.6 and RCP4.5, but with a reverse trend for RCP6.0 and RCP8.5. At the other extreme probability (i.e. 90%, very unlikely to be exceeded), gains in annual precipitation increase with radiative forcing, while inter-RCP differences remain small, especially for the closer time slice (2050s: 16%–17%; 2080s: 18%–21%). For a given RCP, larger increases are projected for the 2080s, although the difference remains modest (mean difference: nearly 3%). This is repeated for 70% probability, although increases for a given time slice/RCP are, on average, less than a third the size of those for the 90% probability level.

For the 50% probability level, increases in precipitation are concentrated between October and April, with very small declines ($\leq$ 1%) in March in the 2050s (Fig. 3). The largest increases are consistently projected for November, the wettest baseline month (84 mm). In both time slices, increases are larger with higher radiative forcing, although differences are small for the 2050s (RCP2.6 vs RCP8.5: 10% vs 12% in the 2050s, 14% vs 21% in the 2080s). Declining precipitation for the rest of the year accounts for overall reductions in annual totals. Declines in July and August range from a mean of 18% (19%) for RCP2.6 to 24% (32%) for RCP8.5 in the 2050s (2080s). The number of months in which mean

precipitation increases constricts for the next lowest probability (30%). Whilst increases are projected for the five months between October and February for all RCPs in the 2080s, increases are limited to two (RCP2.6 and RCP4.5), three (RCP6.0) and four (RCP8.5) of these months in the 2050s. The largest increases still occur in November, but they are between a third and a half the size of those for 50% probability. Declines in most of the other months are at least 10 percentage points larger. Mean precipitation declines in every month for the lowest (10%) probability. In most cases, the smallest reductions are projected for November whilst large declines occur in June–August. For a given time slice, the magnitude of these declines grows with radiative forcing. For example, reductions in August for RCP2.6 and RCP8.5 equal 48% (42%) and 57% (61%), respectively, for the 2050s (2080s). For the 70% probability, increases occur between October–April in all scenarios (and May for 2050-2.6$_{10}$), whilst for 90%, increases are projected for every month in both time slices (except September for the 2050s; declines ≤ 3%). The largest increases are again projected for November (RCP2.6 vs RCP8.5: 29% vs 34% in the 2050s, 34% vs 50% in the 2080s). This larger magnitude of increases with higher radiative forcing is mirrored by a decline in the size of the gains in summer precipitation (e.g. increases in August for RCP2.6 and RCP8.5 are 17% and 12%, respectively for the 2050s. The corresponding figures for the 2080s are 10% and 4%).

Annual total PET is projected to increase for 32 of the 40 scenarios (Table 2). Declines are restricted to the 10% probability level and are relatively small (RCP2.6 vs RCP8.5: 4% vs 3% in the 2050s, 4% vs 1% in the 2080s). Across the other scenarios, the magnitude of increases for a given probability generally increase with radiative forcing, and inter-RCP differences are greater for the 2080s than the 2050s. For 50% probability in the 2050s, increases in mean annual PET range from 9% (RCP2.6) to 12% (RCP8.5). The corresponding figures for the 2080s are 10% and 20%, respectively. In absolute terms, PET increases for the 2050s are in most cases over 50% larger than declines in annual precipitation, whilst for the 2080s, they are over three times the size. The disparity in the size of PET increases between the two time slices is repeated for other probability levels and is most notable for 90%; increases for the 2050s range between 22% (RCP2.6) and 28% (RCP8.5) compared to 24% and 43% for the same RCPs in the 2080s.

Figure 3 shows that the largest increases in mean monthly PET are projected for June–September (especially the two central months of this period), when baseline values peak and the largest declines in precipitation are projected. Inter-RCP and time slice differences follow trends in annual PET with, for example, gains in August (baseline: 72 mm) for the 50% probability level being in the range 16%–20% (RCP2.6 and RCP8.5, respectively) for the 2050s and 18%–33% (same RCPs) for the 2080s. With the exception of 10% probability,

declines in monthly PET are concentrated in autumn and winter (in particular November–January). Baseline PET is low at this time, so that absolute changes are small and barely discernible in Fig. 3. For 10% probability, declines in mean monthly PET are also small, but occur across many more months (although not every month in most scenarios). The largest declines in August for the 2050s and 2080s are 5% and 1%, respectively (for RCP6.0 in both cases) whilst 2080-8.5$_{10}$ projects a small (2%) increase in this month. At the other extreme (90% probability), mean monthly PET increases in most months (all 12 for RCP2.6 in both time slices). Declines are restricted to January and/or December and are very small in absolute terms. The largest increases occur in summer, with gains in August ranging between 37% (RCP2.6) and 45% for the 2050s (RCP8.5). The corresponding range for the 2080s is 38%–68% (same RCPs).

Mean annual net precipitation (i.e. precipitation – PET) for each scenario further demonstrates the projected dominance of drier conditions (Table 2). In the 2050s, increases compared to the baseline are limited to the three lower radiative forcing scenarios (i.e. RCP2.6, RCP4.5 and RCP6.0) and the 90% probability, whilst in the 2080s, just one scenario (2080-8.5$_{90}$) produces an increase. Increases in annual precipitation for 70% probability described above are more than offset by elevated PET, resulting in declining net precipitation. The magnitudes of these declines increase with progressively smaller probability levels. For a given time slice and probability level, declines are generally larger with magnitude of radiative forcing. The exception is RCP6.0 for the 2050s, which produces very similar, but slightly larger, net annual precipitation to RCP4.5. Whilst reductions in mean annual net precipitation for RCP2.6 are, for each probability, larger for the 2050s compared to the 2080s, from RCP4.5 onwards, declines are larger for the more distant time slice. For example, at the 50% probability level, annual net precipitation for RCP2.6 declines by 28% in the 2050s compared to 25% in the 2080s. In contrast, declines for RCP8.5 at this probability are equivalent to 36% and 49% for the 2050s and 2080s, respectively. The frequency with which monthly net precipitation is positive (i.e. precipitation > PET; Table 2) further confirms the drying trend, with all scenarios producing a decline in this metric. Although inter-scenario differences are relatively small, there is a general increase in the magnitude of drying with higher radiative forcing, reduction in probability level and more distant time slice.

Table 3 summarises the climate change impacts on River Glaven discharge above Hunworth Meadow. It first provides the mean, as well as the Q5 and Q95 discharges (discharges exceeded for 5% and 95% of the time and indicative of high and low flows, respectively) for the baseline and each scenario. Increases in mean, Q5 and Q95 discharges are limited to the 90% probability with just one exception; very small (<0.1%) increase in Q5 for 2080-2.6$_{10}$ whilst Q95 discharge

Table 3 Baseline and UKCIP18 scenario mean, Q5 and Q95 discharges (m³s⁻¹) and frequency of discharge exceeding post-restoration discharge thresholds associated with widespread (1.67 m³s⁻¹) and localized (0.60 m³s⁻¹) inundation for the period 2001–2010. Scenario discharges are based on perturbing observations by the delta factors established using the NAM model forced with scenario precipitation and PET. Frequency is specified as days for both thresholds (and number of discrete events for localized inundation). Shaded cells indicate reductions compared to the baseline

Q5 discharge (m³s⁻¹): Baseline 0.499		10%	30%	50%	70%	90%
2050	2.6	0.334	0.396	0.436	0.486	0.553
	4.5	0.328	0.388	0.434	0.481	0.552
	6.0	0.332	0.391	0.433	0.482	0.555
	8.5	0.315	0.374	0.425	0.471	0.546
2080	2.6	0.347	0.405	0.452	0.500	0.567
	4.5	0.335	0.397	0.444	0.493	0.563
	6.0	0.328	0.391	0.436	0.484	0.556
	8.5	0.308	0.368	0.417	0.467	0.549
Mean discharge (m³s⁻¹): Baseline 0.278		10%	30%	50%	70%	90%
2050	2.6	0.185	0.220	0.243	0.272	0.313
	4.5	0.181	0.215	0.241	0.268	0.311
	6.0	0.183	0.217	0.241	0.269	0.313
	8.5	0.173	0.207	0.235	0.262	0.307
2080	2.6	0.191	0.225	0.250	0.277	0.318
	4.5	0.184	0.220	0.245	0.272	0.313
	6.0	0.181	0.215	0.241	0.268	0.309
	8.5	0.168	0.202	0.229	0.257	0.303
Q95 discharge (m³s⁻¹): Baseline 0.137		10%	30%	50%	70%	90%
2050	2.6	0.077	0.096	0.109	0.125	0.148
	4.5	0.074	0.093	0.107	0.122	0.147
	6.0	0.075	0.094	0.107	0.123	0.147
	8.5	0.069	0.087	0.103	0.118	0.142
2080	2.6	0.080	0.098	0.111	0.126	0.148
	4.5	0.074	0.093	0.107	0.121	0.143
	6.0	0.072	0.089	0.103	0.118	0.140
	8.5	0.065	0.080	0.094	0.109	0.134
Widespread inundation threshold exceedance (days): Baseline 8		10%	30%	50%	70%	90%
2050	2.6	1	2	4	6	9
	4.5	1	2	4	5	9
	6.0	1	2	4	6	9
	8.5	1	1	3	5	9
2080	2.6	1	2	4	6	9
	4.5	1	2	4	5	9
	6.0	1	2	3	5	9
	8.5	1	1	3	4	7
Localised inundation threshold exceedance (days / events): Baseline 97 (57)		10%	30%	50%	70%	90%
2050	2.6	29 (21)	44 (30)	64 (36)	86 (50)	133 (71)
	4.5	26 (20)	43 (29)	62 (36)	82 (47)	133 (71)
	6.0	28 (21)	43 (29)	63 (36)	83 (47)	135 (71)
	8.5	25 (19)	37 (25)	54 (34)	77 (44)	128 (69)
2080	2.6	30 (21)	46 (31)	73 (41)	91 (53)	141 (74)
	4.5	28 (21)	44 (29)	68 (39)	86 (51)	137 (72)
	6.0	27 (20)	43 (29)	61 (37)	80 (46)	135 (70)
	8.5	18 (16)	36 (24)	50 (31)	75 (43)	124 (66)

declines by 2% for 2080-8.5$_{90}$. Declines are projected for probability levels between 10% and 70%, with the magnitude of changes increasing as probabilities decline. For example, across the four RCPs, mean discharge for the 2050s declines by, on average, 35% for the 10% probability level, reducing to declines of 23% and 14% for 30% and 50% probability, respectively. The 70% probability level is associated with a mean decline of 4% with, on average, an increase of 12% projected for the 90% probability level. In percentage terms, changes tend to increase in magnitude from Q5, through mean discharge to Q95, with the latter experiencing notably larger percentage changes, at least when declines are projected. For example, mean changes in Q5 across the four RCPs in the 2050s for the 10%, 50% and 90% probability levels are -38%, -13% and 11%, respectively (all within one percentage point of those for mean discharge). The corresponding changes in Q95 are -46%, -22% and 7%, respectively (all more than five, and as much as ten, percentage points higher than those for the mean). For a given time slice and probability projecting reduced discharges, larger changes tend to be associated with enhanced radiative forcing (slightly smaller increases for 90% probability) although these inter-RCP differences are relatively small (especially for the 2050s). Lower radiative forcing (RCP2.5 and RCP4.5) often produce larger declines in the 2050s compared to the 2080s, but this reverses for RCP6.0 and RCP8.5.

For example, for the 50% probability level in the 2050s, mean discharge declines by between 13% (RCP2.6) and 15% (RCP8.5), whilst the corresponding figures for the same scenarios in the 2080s are 10% and 18%. Similar trends are evident for the two extreme discharge metrics (Q5 and Q95).

Declines in mean discharge are projected in all months for the vast majority of 10%–50% probability scenarios (Fig. 4). In percentage terms the largest changes are projected for summer and early autumn (June–October). The magnitude of changes follows trends established for Q95 with generally larger reductions for the more distant time slice, higher radiative forcing and lower probability levels. For example, across these three probabilities, the smallest decline in mean discharge for August is 21% (2080-2.6$_{50}$), whilst the largest is 55% (2080-8.5$_{10}$). Reductions in discharge during the winter peak are smaller, echoing the smaller reductions in Q5. Across all 10%–50% probability levels, reductions in February (the baseline highest monthly mean discharge: 0.327 m^{3}s^{-1}) range between 1% (2080-2.6$_{50}$) and 29% (2080-8.5$_{10}$). It is also notable that across these scenarios, and repeated for the 70% and 90% probabilities, mean discharge declines more in November and December compared to January and February, so that the period of the highest flows is more concentrated. At the 70% probability scenarios, increased mean monthly discharge is projected for January and February, with the average increase ranging between 5% (2050-8.5$_{70}$)
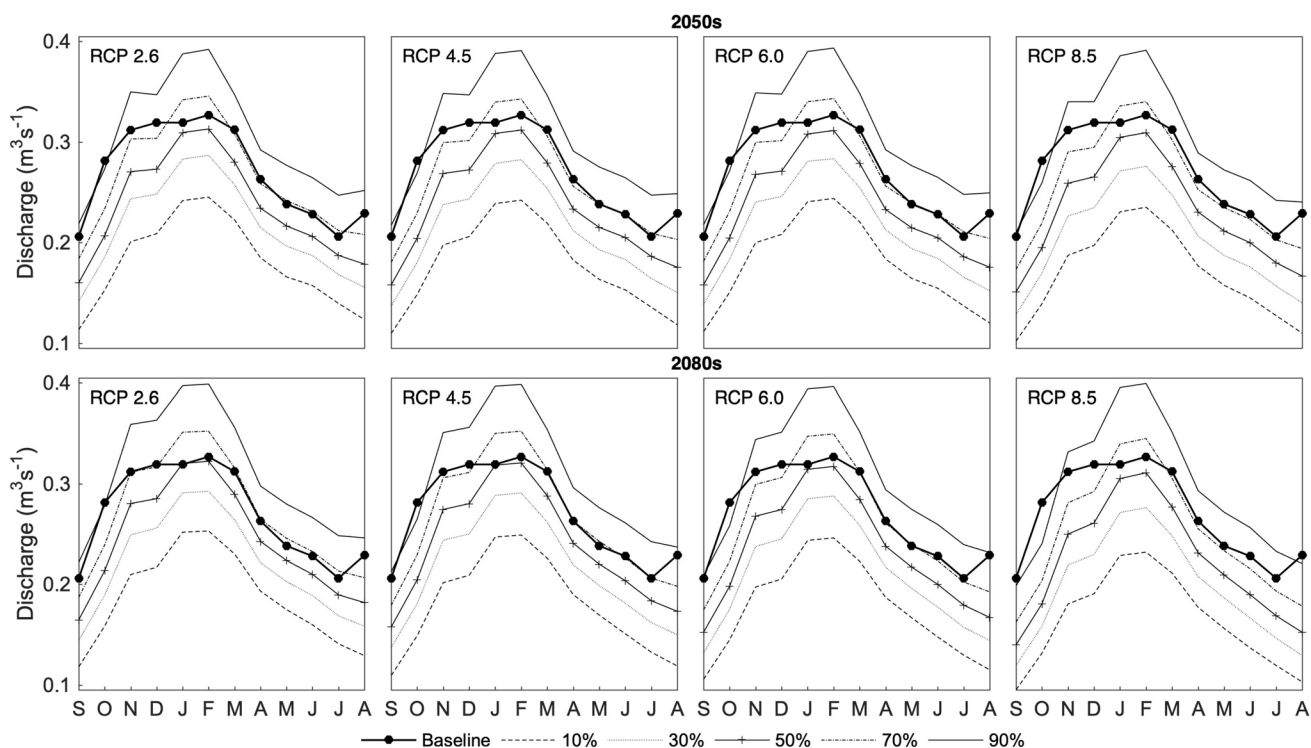

Fig. 4 Mean monthly discharge at Hunworth for the baseline and each UKCP18 scenario for the 2050s and 2080s. Scenario discharges are based on perturbing observations by the delta factors established using the NAM model forced with scenario precipitation and PET

and 9% ($2080\text{-}2.6_{70}$). A number of 70% probability scenarios, typically those with smaller radiative forcing (RCP2.6 and RCP4.5), also project increases in some of the months between March and April, but they are characteristically small (in most cases <2%). Discharge still declines in summer, although to a smaller extent compared to lower probability scenarios. The 90% probability scenarios project increases in mean discharges in most, but not all months (declines in October for all scenarios, as well as August and September for $2080\text{-}8.5_{90}$). The largest increases are again projected for winter, with the mean change for January and February ranging between +20% ($2050\text{-}8.5_{70}$) and +23% ($2080\text{-}2.6_{70}$). Increases in summer are smaller and, including the decline for $2080\text{-}8.5_{90}$, changes range between -4% and 10% ($2050\text{-}2.6_{90}$). Across all scenarios, the range of mean monthly discharges (i.e. difference between the largest and smallest values in Fig. 4 for a given scenario) increases compared to the baseline (0.12 m^{3}s^{-1}), although inter-RCP differences are small for a given probability level. For example, at 50% probability this range varies between 0.15 m^{3}s^{-1} and 0.16 m^{3}s^{-1} for the 2050s, increasing very slightly to between 0.16 m^{3}s^{-1} and 0.17 m^{3}s^{-1} for the 2080. The corresponding mean ranges for the two extreme probability levels (i.e. 10% and 90%) are 0.13 m^{3}s^{-1} and 0.18 m^{3}s^{-1} for the 2050s compared to 0.14 m^{3}s^{-1} and 0.19 m^{3}s^{-1} for the 2080s.

Climate change impacts on floodplain inundation

A preliminary indication of the impacts of climate change on river-floodplain inundation is possible by assessing the frequency with which baseline and scenario discharges exceed two thresholds (Clilverd et al. 2016; Table 3). The first (1.67 m^{3}s^{-1}) is the post-restoration channel capacity beyond which widespread inundation occurs, whilst the second (0.60 m^{3}s^{-1}) is associated with localised flooding in the riparian area. Periods of exceedance for the larger threshold are limited to one day, whilst for some events, discharges exceed the lower threshold for a number of consecutive days (Thompson et al. 2017b). Consequentially, both the total number of days and number of discrete events when discharges exceed the second threshold are evaluated. For both threshold discharges, increases in frequency are limited to the 90% probability level (in most cases a single additional event for the largest threshold, with larger increases for the smaller threshold, albeit declining from RCP2.6 to RPC8.5). The frequency of the larger threshold discharge being exceeded is at least halved for the 50% probability level, whilst across all 10% scenarios, exceedance is limited to a single event. The incidence of more localised inundation follows these trends with, for example, the number of days (events) of exceedance

for the 50% level declining by 34%–44% (37%–40%) for the 2050s and 25%–49% (28%–46%) for the 2080s.

Implications of climate change on simulated flood extent within Hunworth Meadow are initially demonstrated using simulated total inundated area for the eight events when baseline river discharge exceeded the 1.67 m^{3}s^{-1} post-restoration channel capacity (Table 4). As noted by Thompson et al. (2017b), the changing number of events that exceed specific threshold discharges does impact such direct comparisons with, for example, the one additional event for all but one of the 90% probability level scenarios being excluded from the analysis. Similarly, as reported above, for progressively lower probability levels there is a consistent reduction in the incidence of events that exceed this threshold discharge, so that inundation that does occur is more likely associated with high water tables. Notwithstanding these caveats, a dominant trend of declining flood extent is demonstrated. Increases are limited to just two summer (July or August) events for some 90% probability scenarios, although in percentage terms, increases are very small (<2%). Declines are projected in all other cases and, following the trends reported above for river discharge, the magnitude of the declines increases into the future (i.e. 2050s vs. 2080s) and with progressively lower probability levels. There is also considerable inter-event variability for a given scenario. For 50% probability in the 2050s, the mean decline across the four RCPs and eight events is 22.3% (overall range: -45% to -5%). This increases to a mean decline of 25% (-54% to -5%) for the 2080s. At the extreme low (10%) probability the equivalent mean declines are 47% (-75% to -13%) and 48% (-78% to -14%), respectively. The magnitude of reductions in flood extent generally increases with radiative forcing (although results for RCP4.5 and RCP6.0 are very similar). For example, in the case of the 50% probability level in the 2050s, the mean decline across the eight events for RCP2.6 is 21%, increasing to 25% for RCP8.5. The equivalent figures for the 2080s indicate mean declines in flood extent of 20% and 32%, respectively.

Climate change impacts on floodplain inundation are further detailed using the two events employed by Clilverd et al. (2016) to illustrate the consequences of embankment removal. The first (18/07/2001) is associated with the largest discharge (3.1 m^{3}s^{-1}) recorded at Hunworth during the simulation period, whilst the second (28/05/2007) coincides with a smaller discharge of 1.9 m^{3}s^{-1}. Figure 5 shows the simulated extent and depth of surface water across Hunworth Meadow for these two events under the baseline and the 10%, 50% and 90% probability levels for both RCP4.5 and RCP8.5. These two RCPs represent

Table 4 Baseline and UKCIP18 scenario total areas of inundation (m^2) within Hunworth Meadow for the eight events when baseline discharge exceeded the 1.67 m^{3}s^{-1} threshold associated with widespread inundation. Inundation is defined as the presence of surface water of any depth within a MIKE SHE grid cell and may result from both flooding from the river and high water tables. Shaded cells indicate reductions compared to the baseline

	2050s					2080s				
	10%	30%	50%	70%	90%	10%	30%	50%	70%	90%
18/07/2001: Baseline 21400										
2.6	18650	19550	20275	21125	21700	18475	19500	20300	21100	21700
4.5	18500	19425	20250	21050	21700	17975	19125	19850	20825	21525
6.0	18575	19425	20225	21100	21700	17775	18800	19675	20575	21375
8.5	17675	19000	19925	20825	21575	16950	18450	18925	20025	21000
15/10/2002: Baseline 16400										
2.6	4900	7950	10100	12925	15400	5750	8200	11225	13325	15525
4.5	4575	7575	9600	12600	15175	4600	7600	9600	12425	14700
6.0	4775	7775	9750	12725	15325	4350	7200	8975	12275	14175
8.5	4075	6400	9025	11350	14300	3775	5425	7475	9375	12850
13/08/2004: Baseline 19125										
2.6	12050	15675	16875	18125	19300	12825	15850	17000	18025	19100
4.5	11175	15175	16800	17950	19250	11200	15175	16675	17775	18750
6.0	11375	15325	16800	18000	19300	10650	14725	16325	17600	18575
8.5	9775	14225	16325	17675	18950	8800	12800	15350	16850	18375
15/10/2004: Baseline 23075										
2.6	16700	18350	19350	20600	22525	17200	18350	19675	20625	22275
4.5	16225	18100	19225	20300	21100	16150	18125	19100	20125	21275
6.0	16575	18250	19300	20325	22325	15425	17850	18725	19825	20775
8.5	14625	17700	18775	19850	21225	13025	16225	17675	18800	19975
28/05/2007: Baseline 24450										
2.6	13225	16175	17200	18300	20050	14100	16450	17450	18375	19975
4.5	12750	15725	17125	18075	19875	13425	16075	17125	18150	19675
6.0	12925	15900	17100	18175	19950	12975	15825	17025	17875	19500
8.5	11250	15400	16825	17950	19625	10700	14975	16475	17525	19100
25/06/2007: Baseline 25800										
2.6	16600	21525	22950	24625	25250	16075	21275	22600	24375	25175
4.5	16200	21125	22750	24350	25275	14500	18400	21775	22950	24850
6.0	16575	21225	22750	24375	25250	13725	17350	21125	22575	24825
8.5	14400	19100	22050	23575	25200	11000	15550	18125	21525	23775
23/08/2007: Baseline 21575										
2.6	7475	12875	15125	17050	19325	8700	13100	15350	16875	18800
4.5	6975	12300	14875	16775	19100	6975	11900	14325	16125	17925
6.0	7050	12575	14875	16850	19125	6150	11025	13525	15700	17600
8.5	5775	10225	13725	16125	18250	4650	8425	11950	14250	16850
05/10/2008: Baseline 22500										
2.6	10250	14750	16900	18325	20400	11500	15175	17200	18000	20450
4.5	9375	13875	16675	18075	20175	9375	14000	16400	17775	19650
6.0	9675	14350	16700	18150	20100	9000	13200	15625	17400	19050
8.5	8025	12775	15450	17475	19400	6800	10700	13200	15575	17625
Percentage changes across the eight events and four RCPs										
Maximum	-13	-9	-5	-1	1	-14	-9	-5	-1	1
Mean	-47	-31	-22	-15	-7	-48	-34	-25	-18	-10
Minimum	-75	-61	-45	-31	-20	-78	-67	-54	-43	-22

intermediate/mid-range and more extreme emissions scenarios, respectively (van Vuuren et al. 2011) whilst the selected probability levels encompass the central and two extremes of the projected changes. Supplementary Material figures S1 and S2 shows results for all scenarios in the 2050s and 2080s, respectively, whilst Supplementary Material figures S3 and S4 map changes in surface water depth compared to the baseline, again for the two time slices, respectively. Total flood extent for the two events, as well as the area of surface water for three depth classes are summarised for the baseline and each scenario in Table 5.

Baseline flooding for both events is concentrated towards the downstream end of the meadow, especially
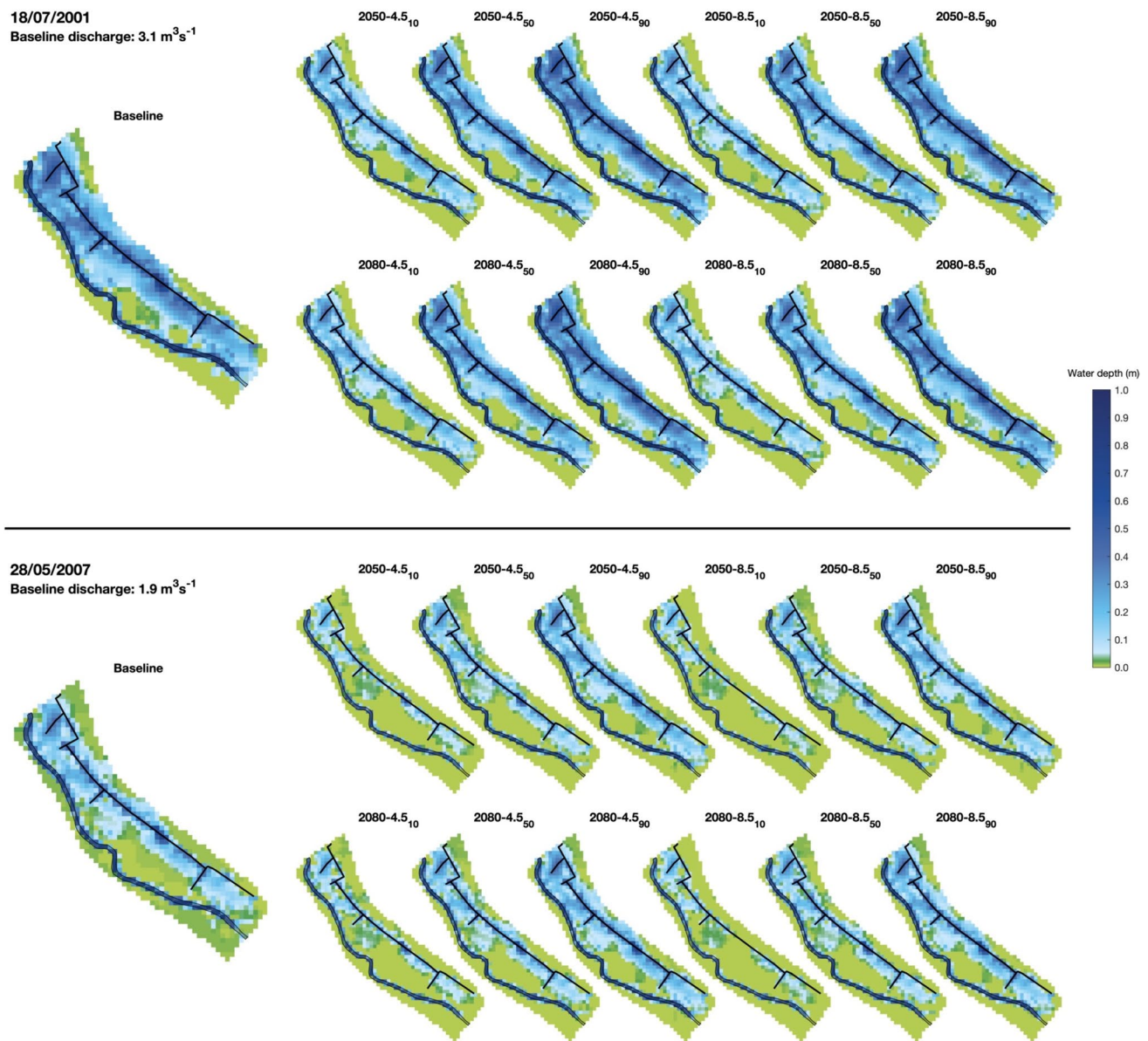
Fig. 5 Simulated surface water extents and depths within Hunworth Meadow during two events for the baseline and 10%, 50% and 90% probability levels for the RCP4.5 and RCP8.5 scenarios in the 2050s and 2080s. Discharge values refer to the baseline mean daily discharge on the date of the event

on 28/05/2007, as well as around the ditch running perpendicular to the river (Fig. 5). Whilst Table 5 shows that the total flood extent for the second event, associated with a smaller peak discharge, exceeds that which occurs at the time of the largest recorded discharge (i.e. 18/07/2001), a much larger proportion of the inundated area is covered with relatively shallow water which may be due to groundwater flooding rather than inundation from the river. For example, whilst 13% of the area flooded on 18/07/2001 is covered in water less than 0.05 m deep, this increases

to 44% for 28/05/2007. Conversely, 23% of the inundated area for the first, larger, event has water over 0.4 m deep, this drops to 11% for 28/05/2007.

The 18/07/2001 event is one for which flood extent increases for some 90% probability scenarios (all RCPs in the 2050s, RCP2.6 and RCP4.5 in the 2080s), although, as previously noted, such increases are no more than 2% of the baseline area (Fig. 5). Spatial differences in the simulated change in flood depth for these scenarios are relatively small across most of the floodplain (Supplementary Material

Table 5 Baseline and UKCP18 scenario total flooded area and extent of areas flooded to different depth ranges (m²) for two events. Discharges are the baseline mean daily discharge on the date of the event. Shaded cells indicate reductions compared to the baseline

			10%	30%	50%	70%	90%
18/07/2001 ($3.1\ \mathrm{m^3 s^{-1}}$)		Total flooded area: Baseline 21400					
	2050	RCP 2.6	18650	19550	20275	21125	21700
		RCP 4.5	18500	19425	20250	21050	21700
		RCP 6.0	18575	19425	20225	21100	21700
		RCP 8.5	17675	19000	19925	20825	21575
	2080	RCP 2.6	18475	19500	20300	21100	21700
		RCP 4.5	17975	19125	19850	20825	21525
		RCP 6.0	17775	18800	19675	20575	21375
		RCP 8.5	16950	18450	18925	20025	21000
		Flooded area < 0.05 m depth: Baseline 2750					
	2050	RCP 2.6	2950	2275	2325	2325	2000
		RCP 4.5	3250	2425	2350	2275	1975
		RCP 6.0	3175	2325	2325	2325	1975
		RCP 8.5	3075	2275	2175	2275	1925
	2080	RCP 2.6	2675	2125	2175	2250	1975
		RCP 4.5	2975	2225	2050	2175	1850
		RCP 6.0	3050	2075	1950	2025	1800
		RCP 8.5	3175	2375	1550	1775	1675
		Flooded area 0.05 m – 0.4 m depth: Baseline 13825					
	2050	RCP 2.6	12500	13300	13475	13800	13550
		RCP 4.5	12100	13175	13425	13900	13575
		RCP 6.0	12225	13250	13425	13825	13575
		RCP 8.5	11675	13100	13500	13800	13575
	2080	RCP 2.6	12600	13400	13650	13800	13550
		RCP 4.5	11900	13150	13425	13825	13600
		RCP 6.0	11675	13075	13500	13800	13600
		RCP 8.5	11025	12775	13400	13675	13600
		Flooded area > 0.4 m depth (m²): Baseline 4825					
	2050	RCP 2.6	3200	3975	4475	5000	6150
		RCP 4.5	3150	3825	4475	4875	6150
		RCP 6.0	3175	3850	4475	4950	6150
		RCP 8.5	2925	3625	4250	4750	6075
	2080	RCP 2.6	3200	3975	4475	5050	6175
		RCP 4.5	3100	3750	4375	4825	6075
		RCP 6.0	3050	3650	4225	4750	5975
		RCP 8.5	2750	3300	3975	4575	5725
28/05/2007 ($1.9\ \mathrm{m^3 s^{-1}}$)		Total flooded area: Baseline 24450					
	2050	RCP 2.6	13225	16175	17200	18300	20050
		RCP 4.5	12750	15725	17125	18075	19875
		RCP 6.0	12925	15900	17100	18175	19950
		RCP 8.5	11250	15400	16825	17950	19625
	2080	RCP 2.6	14100	16450	17450	18375	19975
		RCP 4.5	13425	16075	17125	18150	19675
		RCP 6.0	12975	15825	17025	17875	19500
		RCP 8.5	10700	14975	16475	17525	19100
		Flooded area < 0.05 m depth: Baseline 10825					
	2050	RCP 2.6	4925	5775	5650	4650	4825
		RCP 4.5	4750	5500	5600	4650	4775
		RCP 6.0	4800	5600	5625	4675	4800
		RCP 8.5	4225	5575	5525	4775	4600
	2080	RCP 2.6	5150	5675	5300	4500	4600
		RCP 4.5	4900	5550	5200	4475	4525
		RCP 6.0	4575	5450	5475	4350	4400
		RCP 8.5	3975	5175	5375	4450	4075
		Flooded area 0.05 m – 0.4 m depth: Baseline 10950					
	2050	RCP 2.6	6650	8300	9150	10975	12075
		RCP 4.5	6450	8125	9125	10800	11975
		RCP 6.0	6500	8200	9100	10850	12000
		RCP 8.5	5675	7825	8950	10650	11900
	2080	RCP 2.6	7150	8550	9675	11150	12225
		RCP 4.5	6775	8325	9475	10975	12025
		RCP 6.0	6750	8275	9150	10850	11975
		RCP 8.5	5400	7800	8750	10550	11925
		Flooded area >0.4 m depth: Baseline 2675					
	2050	RCP 2.6	1650	2100	2400	2675	3150
		RCP 4.5	1550	2100	2400	2625	3125
		RCP 6.0	1625	2100	2375	2650	3150
		RCP 8.5	1350	2000	2350	2525	3125
	2080	RCP 2.6	1800	2225	2475	2725	3150
		RCP 4.5	1750	2200	2450	2700	3125
		RCP 6.0	1650	2100	2400	2675	3125
		RCP 8.5	1325	2000	2350	2525	3100

figures S3 and S4). The most obvious exceptions to this uniformity are the riparian area at the very top of the floodplain, where the embankment was removed (larger increases in water depth compared to the adjacent floodplain), and at another slightly higher riparian area further downstream (smaller increases in water depth compared to the adjacent floodplain). It is also notable that even for this extreme scenario, two small riparian patches, which include the area where embankments were not removed due to water vole burrows, remain dry.

Total flood extent for the 18/07/2001 event declines for all other scenarios. Reductions are small for the 70% probability level (1%–3% for the 2050s and 1%–6% for the 2080s with the extremes provided by RCP2.6 and RCP8.5). The declines are despite widespread increases in water depth for most scenarios in the 2050s (the exception being 2080-8.5$_{70}$) and 2080-2.6$_{70}$ (Supplementary Material figures S3 and S4). However, magnitudes of increased water depths are small (on average no more than 0.7 cm). For the 50% probability level declines in total flood extent range between 5% and 7% (2050s) and 5% and 12% (2080s), with RCP2.6 and RCP8.5 accounting for the extremes. In common with the baseline, the whole width of the lower meadow is inundated and declines in total flood extent are predominantly associated with an area between the river and the ditch midway down the floodplain (Fig. 5, Supplementary Material figures S1 and S2). Declines in water depth across most of the floodplain are relatively consistent for a given scenario, although an increase in the magnitude of declines is evident with higher probability level for a single time slice and when comparing the 2050s and 2080s (Supplementary Material figures S3 and S4). Increases in water depth for 50% probability scenarios are limited to a few grid cells close to the river. Total flood extent declines further for the 30% and then the 10% probability level scenarios. For the latter, reductions range between 13%–17% (2050s) and 14%–21% (2080s). RCP2.6 and RCP8.5 again produce the smallest and largest declines, respectively. There is a further expansion of the mid-floodplain area which is not inundated although flooding is retained along the ditch and the low-lying downstream end of the site. Differences in the magnitude of declines in surface water depth across the meadow are more evident, especially for higher radiative forcing (e.g. RCP8.5 compared to RCP4.5) and more the distant time slice (Supplementary Material figures S3 and S4). The largest declines are focussed around the ditch (in particular around and upstream of its midpoint) and at the downstream end of the floodplain, both areas which, under baseline conditions, experience some of the deepest inundation.

Table 5 shows that for the 18/07/2001 event, only the 10% probability scenarios (with the exception of 2080-2.6$_{10}$) project increases in the absolute extent of shallow (<0.05 m) inundation, although these areas make up a slightly larger proportion of the total (15%–19%, mean 17% compared to the baseline 13%). The absolute extent of this shallow inundation declines for the remaining scenarios, as does its relative extent (accounting for, on average, 11% and 9% of the total across the 50% and 90% probability scenarios, respectively). Most scenarios produce a decline in the absolute extent of intermediary flooding (i.e. 0.05m–0.4m), the exceptions being 2050-6.0$_{70}$, 2080-4.5$_{70}$ (no change) and 2050-45$_{70}$ (increase equivalent to three grid cells). Whilst flooding of this depth tends to account for a larger proportion of the total flooded area than under the baseline, differences are small (predominantly less than 3%). Both the absolute and relative extent of the deepest inundation (>0.4 m) decline for all 10%, 30% and 50% probability scenarios. At 50% probability, declines in absolute extent are, on average, 9% and 12% for the 2050s and 2080s, respectively. The largest declines are projected for RCP8.5 (12% and 18%, respectively). A very slightly smaller proportion of the total flooded area is inundated to a least 0.4 m (mean for both time slices is 22% compared to 23% for the baseline). Declines in the area (and proportion of total) of this deeper water are larger for the 10% probability level, with mean declines of 36% (17%) and 37% (17%) for the 2050s and 2080s, respectively. Whilst four of the 70% probability scenarios project an increase in the extent of the deepest flooding and three project declines (no change for 2080-6.0$_{70}$), the magnitude of the changes are small (equivalent to <10 model grid cells). Larger increases are projected for all 90% probability scenarios. An almost consistent increase of 27% (26% for 2050-8.5$_{90}$) is projected for the 2050s, whilst for the 2080s the magnitude of increases declines consistently from RCP2.6 (28%) to RCP8.5 (19%). Across the eight 90% probability scenarios the deepest flooding accounts for between 27% and 28% of the total inundated area (an increase from 23% for the baseline).

The total extent of inundation on 28/05/2007 declines for all scenarios with, in percentage terms, the magnitude of declines being considerably larger than those for the 18/07/2001 flood. For the 50% probability level in the 2050s, declines range between 30% (RCP2.6) and 31% (RCP8.5) and in the 2080s between 29% and 33% (same scenarios). Declines for an individual scenario are, in percentage terms, at least 2.5 times (and in most cases over four times) as large as those for 18/07/2001. Whilst surface water is still concentrated in the same areas as under baseline conditions, the width of the band of inundation around the ditch constricts, especially in the upstream half of the floodplain, and the area of very shallow inundation mid-way across this part of the floodplain is eliminated (Fig. 5). In areas that are still inundated, the magnitude of declines in water depth is relatively uniform for a given 50% probability scenario (Supplementary Material figures S3 and S4). These trends, albeit elevated in magnitude, are repeated for the 30% probability level. In contrast, for the

10% probability scenarios, declines in water depth vary across the meadow and are particularly pronounced (>0.15 m) adjacent to the ditch in the centre of the floodplain. For both RCP8.5$_{10}$ scenarios, the continuous flooding along the ditch for the baseline and all other scenarios (albeit with a reduction in width) is interrupted by a stretch that is no longer inundated (Fig. 5). Declines in the total area inundated for 10% probability scenarios are in the range 46%–54% (2050s) and 42%–56% (2080s), with the extremes being simulated by RCP2.6 and RCP8.5. The widespread, but very small (<1 cm) increases in surface water depth for some 70% probability scenarios that characterised results for 18/07/2001 are repeated in some cases (RCP2.6 in the 2050s and both RCP2.6 and RCP4.5 in the 2080s; Supplementary Material figures S3 and S4), but overall flood extent still declines (Table 5). At the most extreme high probability (90%), total extent of inundation declines (by 18%–20% and 18%–22% for the 2050s and 2080s, respectively), despite more widespread increases in water depth around the ditch and in the lower part of the floodplain. These, at first sight, contradictory results are due to the decline in the extent of very shallow water within the middle part of the floodplain.

Simulated shallow flooding (<0.05 m deep) declines for all scenarios during the 28/05/2007 event (Table 5). Whilst the largest declines in percentage terms are associated with the extreme probability scenarios (average declines of 57% and 58% across the 10% and 90% scenarios, respectively compared to 50% for 50% probability), shallow inundation makes up a progressively larger proportion of the total area as probability level declines, although it is smaller for all scenarios than for the baseline (44.3%). On average, shallow inundation accounts for 23% of the total area across the 90% probability scenarios. This increases to 32% and 37% for the 50% and 10% scenarios, respectively. The extent of intermediate depth (0.05m–0.4m) flooding declines for all 10%–50% probability scenarios, with the magnitude of absolute reductions increasing with probability and, in most cases, radiative forcing. Declines for the 10% probability level are in the range 39%–48% for the 2050s and 35%–51% in the 2080s (RCP2.6 and RCP8.5 accounting for the smallest and largest declines). While the RCP2.6 scenarios (joined by RCP4.5 in the 2080s), project increases in the extent of intermediate flooding for the 70% probability level, no increases are larger than 2% in absolute terms. Similarly, decreases for the remaining 70% scenarios are all small (<4%). Increases in the extent of intermediate depth flooding are larger for 90% probability, with the magnitude of changes declining slightly with radiative forcing (10%–9% for 2050-2.6$_{90}$ and 2050-8.5$_{90}$, 12%–9% for 2080-2.6$_{90}$ and 2080-8.5$_{90}$). Across all scenarios, flooding of this range of depths makes up a larger proportion of the total compared to the 45% for the baseline (on average 51% for 10% probability, increasing to 61% for 90%). Inter-scenario differences in the direction of change in deeper (>0.4m)

flooding for 28/05/2007 are almost identical to those for intermediate flood depths. Declines for the 50% probability scenarios in the 2050s range between 10% (RCP2.6 and RCP4.5) and 12% (RCP8.5), with the corresponding range for the 2080s being declines of 8%–12% (RCP2.6 and RCP8.5). Reductions are larger for the lower probability levels (e.g. for 10% - 2050s: 38–50%; 2080s: 33%–51%). At the other extreme (90% probability), the absolute extent of the deepest flooding increases for all scenarios but the inter-scenario ranges are small (2050s: 17%; 2080s: 16%–18%). As for inundation of intermediate depth, deeper flooding makes up a slightly larger proportion of the declining total flood extent during the 28/05/2007 event. Compared to 11% for the baseline, the mean proportion increases to 13%, 14% and 16% for the 10%, 50% and 90% probability scenarios, respectively (inter-RCP and inter-time slice ranges are all <1%).

Climate change impacts on floodplain groundwater levels

Climate change impacts on shallow floodplain groundwater are first demonstrated using results for MIKE SHE grid cells corresponding with locations of shallow wells installed within Hunworth Meadows. Figures 6 and 7 show simulated daily water table levels at Well 1.1 and Well 1.4, respectively. The latter is representative of conditions across much of the floodplain whilst Well 1.1 is located closer to the river (see Fig. 1 for locations). Results are provided for the baseline and the 10%, 50% and 90% probability levels for each scenario. In the interests of clarity, 30% and 70% levels are excluded, given that they lie mid-way between adjacent probabilities. This is demonstrated in Fig. 8, which shows mean monthly water table elevations (the water table regime) for all scenarios for these two wells and two additional wells located towards the upstream limit of Hunworth Meadow, but at approximately the same positions across the floodplain (i.e. Well 3.1 close to the river, Well 3.2 on the floodplain – Fig. 1). Simulated daily water table levels for these two wells are provided in Supplementary Material figures S5 and S6. The temporal patterns in water table elevation at these wells are similar to those on the lower part of the meadow, but they are overall slightly higher given the gradual downstream decline in surface elevation.

Under baseline conditions, seasonal variations in groundwater levels are evident at all wells with sustained high water tables in winter and early spring. This is most evident towards the centre of the floodplain (Well 1.4, Fig. 7), where mean monthly water tables are at, or very close to, the ground surface between November and March (Fig. 8). Whilst baseline water tables closer to the river are high during this period, they exhibit much more variability (repeated throughout the year) with repeated short-term rises and falls (e.g. Well 1.1; Fig. 6). Baseline water table levels at all wells

decline through spring reaching, on average, the lowest levels in July (Fig. 8) although there is considerable inter-annual variability in the lowest summer levels (e.g. contrast 2005 and 2006 for Well 1.4; Fig. 7). The magnitude of summer drawdowns under the baseline is relatively small close to the river. The overall range in groundwater levels is therefore smaller compared to further onto the floodplain. This is quantified by comparing differences in WTE-5 and WTE-95 (water table elevations exceeded for 5% and 95% of the time and indicative of high and low water levels, respectively) for wells 1.1 and 1.4 (Table 6, Supplementary Material Table S1 provides corresponding data for wells 3.1 and 3.2). For Well 1.1 this difference is 0.44 m compared to 0.52 m for Well 1.4 (0.22 m and 0.59 m for wells 3.1 and 3.2, respectively).

Seasonality in water table levels is retained and, in most, cases enhanced with climate change. This is predominantly due to lower summer levels, with very limited changes in the peak winter water table. At a daily resolution these impacts are most evident in wells further from the river (i.e. wells 1.4 and 3.2). Summer levels decline in each year for every scenario, although the magnitude and duration of declines varies year-on-year. Some of the largest reductions (>0.20 m in many scenarios) are projected for those years which, under the baseline, experience the largest drawdowns (e.g. 2002, 2003 and 2009 for Well 1.4; Fig. 7), although declines of similar magnitude occur in some wetter years (e.g. 2005) when baseline levels are relatively high. In some years, the autumn/winter rise in groundwater levels is also delayed (especially for the 10% probability level), so that high water table periods are shortened. A general increase in the magnitude of summer drawdown accompanies progression from the highest to lowest probability levels, increasing radiative forcing (although differences are relatively small, especially for the 2050s) and more distant time slice. As an illustration, the lowest water table at Well 1.4 across all scenarios is simulated in early October 2003 (Fig. 7). The mean decline across the first ten days of this month (from the baseline mean of 19.23 m above OD) for 50% probability in the 2050s (2080s) varies between 0.21 m and 0.27 m (0.21 m and 0.40 m) for RCP2.6 and RCP8.5, respectively. For 2050-4.5, these declines range from 0.26 m (10%) to 0.17 m (90%) with the corresponding figures for 2080-4.5 being 0.30 m and 0.24 m, respectively.

Inter-scenario differences in groundwater levels, as well as variability in the climate change signal with location, are further demonstrated by the water table regimes (Fig. 8) and quantified by the values of mean groundwater elevation, WTE-5 and WTE-95 (Table 6 and Supplementary Material Table S1). Increases in mean monthly water table elevations, when they occur, are limited to winter. For the lowest probabilities (10% and 30%), declines are projected throughout the year for all wells, although they are extremely small (< cm) in mid-winter. At 50% probability, increases at wells 1.1

and 1.4 are projected for January and February for all RCPs in both the 2050s and 2080s (largely repeated for wells 3.1 and 3.2, although for some scenarios very small declines occur in one or more months). The period of increasing mean monthly water tables centred on January and February extends with higher probability (70%: predominantly three or four months although at some wells and higher RCPs it is still limited to the same two months; 90%: mostly between four and six months and as many as nine months in some cases for Well 3.1). However, even for the most extreme probabilities changes in mean winter water table elevations are very small with the largest increase being only 0.04 m (January for Well 1.1 and 2080-8.5$_{90}$). The very small inter-scenario differences in peak winter water tables are also evident in the values of WTE-5 for all wells. Whilst this metric declines for the lower probabilities (10%–50% in all cases, 70% for some) and increases thereafter, changes are only in the range -0.06m–0.02 m across all wells and scenarios (for Well 1.4 no more than 0.01 m in both directions).

Projected declines in groundwater levels, especially in summer, for all scenarios are larger than any winter increases and more variable between scenarios and wells (Fig. 8). All scenarios project declining water tables in at least August–October for the 90% probability level (more months for most wells / scenarios) with the duration of declining levels progressively increasing with lower probability (all months for 10% and 30%). The largest declines are almost always projected for August and September, whilst in many cases the seasonal drawdown extends for one month (in some cases two months). When this does not occur, it is predominantly associated with the higher probability levels (70% and in particular, 90%). Figure 8 demonstrates that, for a given RCP, the magnitude of summer drawdown progressively increases with a reduction in probability level, whilst larger changes are projected for higher radiative forcing and the more distant time slice. For example, the smallest reduction in mean August or September groundwater levels for Well 1.1 is 0.04 m (August for 2050-2.6$_{90}$), whilst the largest is 0.27 m (August for 2080-8.5$_{10}$). The corresponding figures for Well 1.4 are 0.09 and 0.48 m (in August and September for 2050-2.6$_{90}$ and 2080-8.5$_{10}$, respectively). The differences between these two wells are repeated for wells 3.1 and 3.2 (<0.01–0.24 m and 0.05–0.39 m for the same scenarios, respectively).

WTE-95 for the four wells (Table 6, Supplementary Material Table S1) declines from the respective baseline with changes echoing the previously described inter-scenario and inter-well differences in summer water table levels. Again, differences from the baseline tend to increase with radiative forcing (although for an individual probability level they are often small) and future time slice. Conversely, they decline with progressively higher probability. Declines that are as likely as not to be exceeded (i.e 50% probability) for
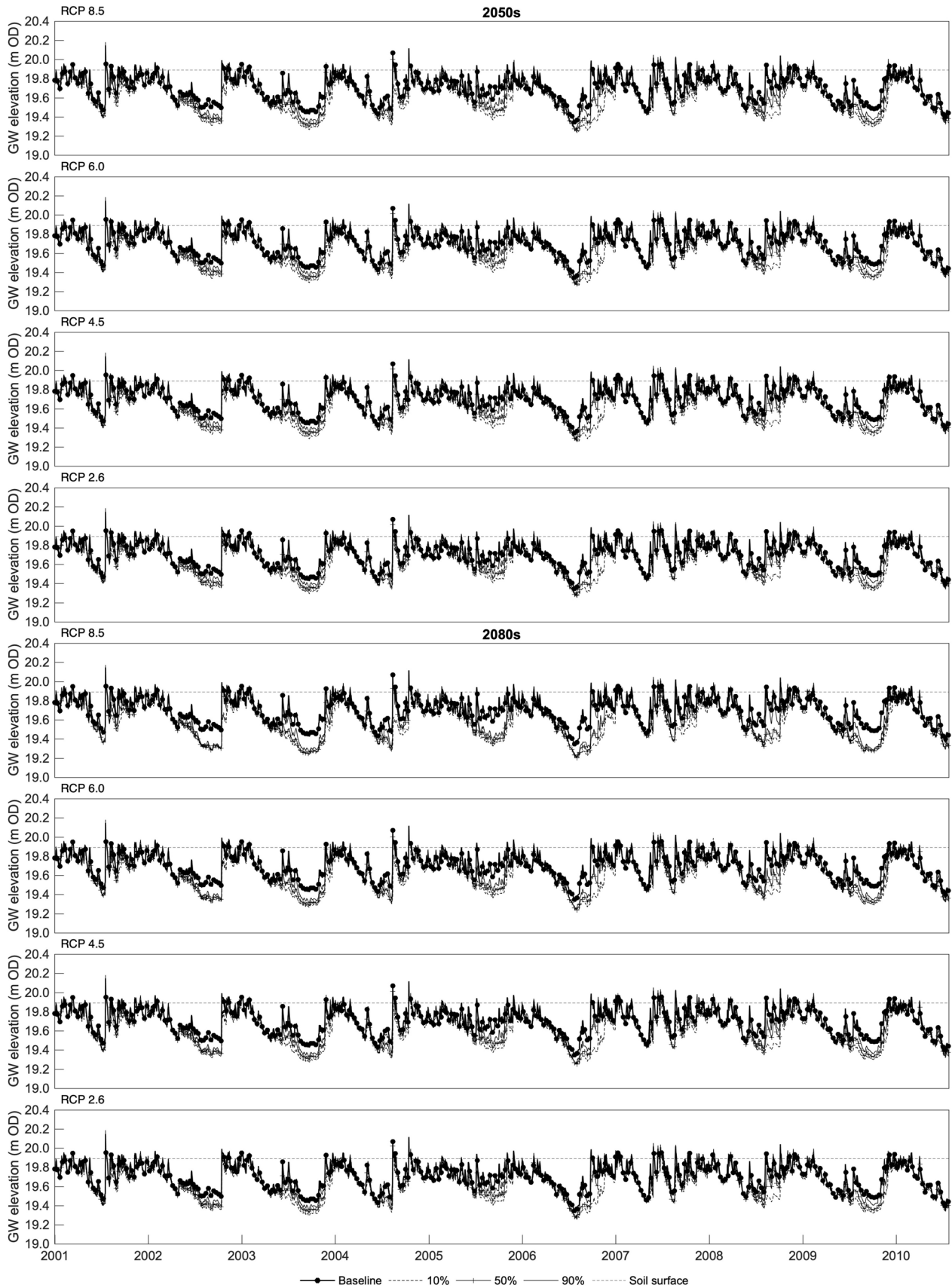
Fig. 6 Simulated daily water table elevation (m OD) at Well 1.1 for the baseline and selected UKCP18 scenarios for the 2050s and 2080s
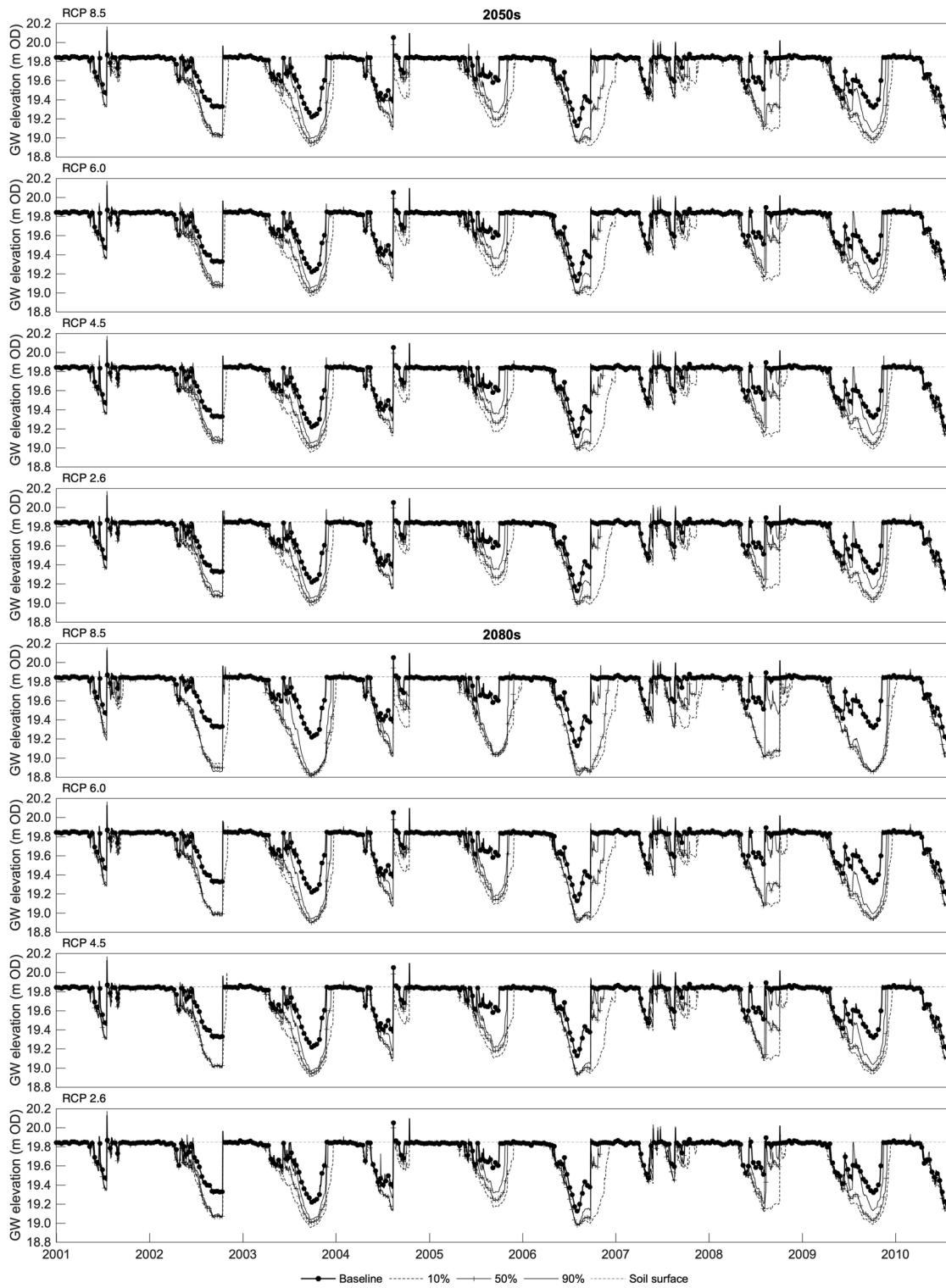
Fig. 7 Simulated daily water table elevation (m OD) at Well 1.4 for the baseline and selected UKCP18 scenarios for the 2050s and 2080s (Note: the absolute y-axis range differs from the corresponding figure for Well 1.1 shown in Figure 6 but covers the same range)

Well 1.4 range between 0.26 m and 0.31 m for the 2050s (RCP2.6 and RCP8.5 respectively) and between 0.27 m and 0.44 m for the 2080s (same RCPs). These compare with ranges of 0.09–0.12 m and 0.10–0.18 m closer to the river (i.e. Well 1.1). Across all scenarios, declines in WTE-95 for Well 1.4 are at least twice as large as those for Well 1.1 (over three times as large for some 70% and all 90% probability scenarios). The ranges of the central 90% of groundwater levels (i.e. differences between WTE-5 and WTE-95) also increase, especially for wells on the floodplain. For example, at Well 1.4 this range for the 50% probability level in the 2050s (2080s) is between 0.77 m (0.78 m) and 0.82 m (0.95 m), compared to 0.52 m for the baseline. It increases very slightly (by no more than 0.05 m and in most cases only a few cm) for lower probability levels and decreases (by at most 0.09 m) for higher levels. Declines of the same direction are projected for wells closer to the river (e.g. Well 1.1) but, as previously noted, baseline water tables vary less at these locations and changes in the scenario ranges are all also smaller.

The dominance of lower summer water tables and the relatively small changes in either direction for winter peak levels drives declines in mean WTE for the overwhelming majority of scenarios (Table 6, Supplementary Material Table S1). Increases are restricted to Well 3.1 at the highest probability level for some scenarios (all <1 cm). The magnitudes of changes for different RCPs, probability levels and time slices follow the trends for WTE-95, although they are naturally smaller. For example, 50% probability scenarios project declines for Well 1.4 of between 0.08 m (RCP2.6) and 0.11 m (RCP8.5) in the 2050s and 0.08 m and 0.17 m in the 2080s. On average across the four RCPs, mean WTE declines by an additional 0.06 m (0.05 m) for the 10% probability scenarios in the 2050s (2080s) whilst declines for 90% probability are smaller (by on average 0.05 m and 0.04 m for the 2050s and 2080s, respectively). Similar trends are evident for other wells, with those closer to the river experiencing smaller changes (e.g. for the 50% probability level declines in mean WTE for Well 1.1 are around half those for Well 1.4). The overwhelming trend towards drier conditions is further demonstrated by the number of days in which simulated water tables at the different wells are lower than those of the baseline (Table 6 and Supplementary Material Table S1).

Climate change impacts on water table elevations across Hunworth Meadow are illustrated in Fig. 9. This firstly maps baseline WTE-5, mean WTE and WTE-95 for each MIKE SHE grid cell covering the meadow and the immediate areas on either side of the river. It demonstrates the general downstream decline in water table elevations that follows the surface topography, as well as the progressively lower groundwater

levels with movement from the river onto the floodplain. Changes in these three water table elevation indices are shown for the 10%, 50% and 90% probability scenarios for RCP4.5 and RCP8.5. These two RCPs are used given the relatively small differences in many of the changes described above for the three lower RCPs. Supplementary Material figures S7 and S8 provide the results for all probability levels and RCPs for the 2050s and 2080s, respectively. Scenario impacts are quantified by evaluating the mean changes in WTE-5, mean WTE and WTE-95 across the MIKE SHE grid cells covering the immediate riparian area (two grid cells from the river) and the rest of the floodplain to the north of the river (Table 7, the two areas are defined in Supplementary Material Figure S9).

Mean values of mean WTE and WTE-95 decline on both the meadow and riparian area for all scenarios except riparian mean WTE for RCP2.6_{90} in both time slices (mean increases are <1 cm). Increases in WTE-95 are limited to two cells adjacent to the river for 2050-4.5_{90}, whilst increases in mean WTE are restricted to a larger number of riparian cells along the length of the river for each of the 90% probability scenarios (and around the upstream end of the ditch for 2050-45_{90}, repeated for RCP2.6_{90} in both time slices and 2050-6.0_{90}; Supplementary Material figures S7 and S8). Although reductions in both indices are projected elsewhere for all scenarios, spatial differentiation is evident, with larger declines on the floodplain compared to next to river. This is reflected in the mean values of mean WTE for the riparian and floodplain areas (Table 7). Declines in the former for 50% probability in the 2050s range between 0.04 m and 0.06 m (RCP2.6 and RCP8.5, respectively) compared to 0.09 m and 0.12 m (same RCPs) for the floodplain. These ranges, and differences between the riparian area and floodplain, increase into the future (2080s: 0.04 m–0.08 m vs 0.09 m–0.17 m). Declines in mean WTE increase (decrease) in magnitude for lower (higher) probability levels. At 10% probability differences across the floodplain become more evident with larger declines occurring towards the centre of the meadow and, in particular, along the north-eastern margin with the hillside (Fig. 9). Climate change-driven declines are larger still for WTE-95 and follow the same inter-scenario trends. Across the riparian area the average decline for the 50% probability level in the 2050s ranges between 0.07 m and 0.10m, increasing to between 0.07 m and 0.14 m for the 2080s. Comparable ranges for the floodplain are declines of 0.20 m–0.25 m and 0.21 m–0.36 m, respectively. Extreme changes are associated with RCP2.6 and RCP8.5 (Table 7). The largest changes in WTE-95 occur between the ditch and floodplain-hillside margin. The extent of such changes are larger than those for mean WTE (Fig. 9, Supplementary Material figures S7 and S8).
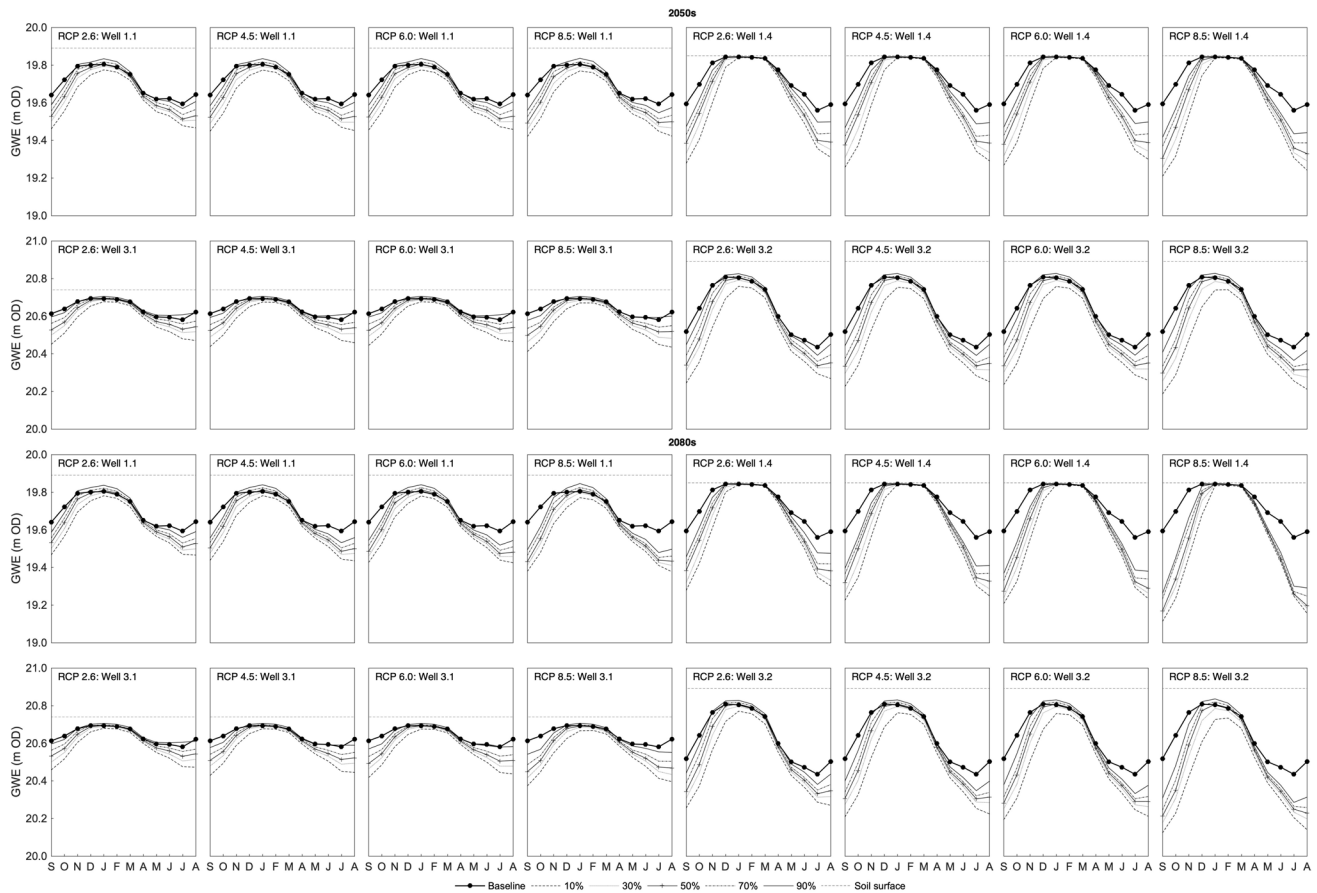
Fig. 8 Simulated mean monthly water table elevation (m OD) at four wells within Hunworth Meadow for the baseline and the UKCP18 scenarios for the 2050s and 2080s (Note: absolute y-axis ranges vary between wells at the downstream [wells 1.1 and 1.4] and upstream [wells 3.1 and 3.2] ends of the floodplain but cover the same range)

Changes in the highest water tables (i.e. WTE-5) are also dominated by declines although increases in mean WTE-5 for both the floodplain and riparian area are projected for at least the 90% probability scenarios (Table 7). However, in the case of the floodplain these increases, and those for 2080-26$_{70}$ and 2080-45$_{70}$, are all <1 cm, whilst declines for the remaining scenarios are no more than 0.03 m, and smaller still in most cases. Figure 9 (Supplementary Material figures S7 and S8) demonstrates the very limited changes in WTE-5 across the floodplain, especially for the 50% probability scenarios. At the higher probability level (90%), the increases that do occur on the floodplain are concentrated in the already wetter downstream end of meadow as well as around the ditch. These same areas are the focus of declines in WTE-5 for the 10% probability scenarios. The size of these declines is, however, smaller than those which occur for the same scenarios in the riparian area (mean declines of between 0.06 m and 0.07 m; Table 7). Declines along the river, especially in the upstream half of the site, are also evident for the 50% probability scenarios although they are, on average, no more than a few cm. Figure 9 shows widespread increases in WTE-5 across the riparian area for the highest (90%) probability scenarios. Whilst on average these increases are small

(no more than 0.03 m; Table 7), they are in many areas sufficient to bring WTE-5 to the elevation of the ground surface.

Climate change impacts on soil aeration stress and floodplain vegetation

Figure 10 maps mean SEV$_{as}$ across Hunworth Meadow derived from the ten years of the simulation period (2001–2010) as well as changes in these SEV$_{as}$ values from the baseline. In common with the approach employed for flood extent and water table elevations, results are shown for the baseline and 10%, 50% and 90% probabilitiess for RCP4.5 and RCP8.5. Absolute values of SEV$_{as}$ for all scenarios in the 2050s and 2080s are shown in Supplementary Material figures S10 and S11, respectively, whilst the corresponding changes from the baseline are shown in Supplementary Material figures S12 (2050s) and S13 (2080s). These four supplementary figures also show the corresponding results derived from the annual SEV$_{as}$ values for 2002 and 2007, identified by Clilverd et al. (2016) as representative of dry and wet years, respectively (see discussion).

Table 6 Baseline and UKCIP18 scenario WTE-5, mean WTE and WTE-95 (m above OD) and number of days (% of total 3493 days) when scenario water table elevation is below baseline water table elevation at the location of two shallow wells (Well 1.1 and Well 1.4; see Fig. 1 for location) installed within Hunworth Meadow. Shaded cells indicate reductions in water table elevation compared to the baseline and scenarios where over 50% of days experience lower water table elevations than the baseline

	2050s					2080s				
	10%	30%	50%	70%	90%	10%	30%	50%	70%	90%
Well 1.1										
WTE-5: Baseline 19.91										
2.6	19.87	19.89	19.90	19.92	19.93	19.87	19.89	19.91	19.92	19.93
4.5	19.86	19.89	19.90	19.92	19.93	19.86	19.89	19.91	19.92	19.93
6.0	19.86	19.89	19.90	19.92	19.93	19.86	19.89	19.90	19.92	19.93
8.5	19.86	19.89	19.90	19.91	19.93	19.85	19.89	19.90	19.92	19.93
Mean WTE: Baseline 19.70										
2.6	19.61	19.64	19.66	19.67	19.70	19.62	19.64	19.66	19.67	19.70
4.5	19.61	19.63	19.65	19.67	19.69	19.60	19.63	19.65	19.66	19.68
6.0	19.61	19.64	19.65	19.67	19.70	19.61	19.64	19.65	19.67	19.70
8.5	19.59	19.62	19.64	19.66	19.68	19.57	19.60	19.62	19.64	19.66
WTE-95: Baseline 19.47										
2.6	19.34	19.37	19.38	19.40	19.43	19.34	19.36	19.38	19.39	19.42
4.5	19.34	19.36	19.38	19.39	19.42	19.32	19.34	19.35	19.37	19.39
6.0	19.34	19.36	19.38	19.40	19.43	19.31	19.33	19.34	19.35	19.37
8.5	19.31	19.34	19.35	19.37	19.40	19.28	19.29	19.30	19.31	19.32
Days (% of 3493 total) when scenario WTE < baseline WTE										
2.6	3426 (98)	3256 (93)	2850 (82)	2369 (68)	1586 (45)	3402 (97)	3202 (92)	2615 (75)	2190 (63)	1626 (47)
4.5	3437 (98)	3283 (94)	2876 (82)	2421 (69)	1727 (49)	3409 (98)	3186 (91)	2650 (76)	2286 (65)	1881 (54)
6.0	3435 (98)	3273 (94)	2893 (83)	2394 (69)	1682 (58)	3423 (98)	3199 (92)	2709 (78)	2336 (67)	1949 (56)
8.5	3448 (99)	3306 (95)	2897 (83)	2489 (71)	1949 (56)	3444 (99)	3268 (94)	2815 (81)	2488 (71)	2084 (60)
Well 1.4										
WTE-5: Baseline 19.85										
2.6	19.85	19.85	19.85	19.85	19.85	19.85	19.85	19.85	19.85	19.86
4.5	19.85	19.85	19.85	19.85	19.85	19.85	19.85	19.85	19.85	19.85
6.0	19.85	19.85	19.85	19.85	19.85	19.85	19.85	19.85	19.85	19.85
8.5	19.85	19.85	19.85	19.85	19.85	19.85	19.85	19.85	19.85	19.85
Mean WTE: Baseline 19.73										
2.6	19.59	19.63	19.65	19.67	19.69	19.60	19.62	19.65	19.66	19.68
4.5	19.58	19.62	19.64	19.66	19.69	19.57	19.60	19.62	19.64	19.65
6.0	19.59	19.62	19.64	19.66	19.69	19.59	19.62	19.64	19.66	19.69
8.5	19.56	19.59	19.62	19.64	19.66	19.52	19.54	19.56	19.58	19.60
WTE-95: Baseline 19.34										
2.6	19.05	19.08	19.08	19.11	19.18	19.03	19.06	19.07	19.09	19.15
4.5	19.02	19.06	19.08	19.10	19.16	18.98	19.01	19.02	19.03	19.05
6.0	19.04	19.07	19.08	19.10	19.17	18.97	18.98	18.99	18.99	19.01
8.5	18.98	19.01	19.03	19.04	19.09	18.90	18.90	18.90	18.89	18.89
Days (% of 3493 total) when scenario WTE < baseline WTE										
2.6	3253 (93)	3027 (87)	2685 (77)	2341 (67)	1937 (55)	3191 (91)	2926 (84)	2534 (73)	2225 (64)	1929 (55)
4.5	3268 (94)	3065 (88)	2716 (78)	2399 (69)	1984 (57)	3225 (92)	2906 (83)	2575 (74)	2326 (67)	2101 (60)
6.0	3260 (93)	3046 (87)	2713 (78)	2380 (68)	1982 (57)	3254 (93)	2932 (84)	2648 (76)	2414 (69)	2163 (62)
8.5	3288 (94)	3061 (88)	2792 (80)	2487 (71)	2136 (61)	3285 (94)	3021 (96)	2763 (79)	2545 (73)	2302 (66)

Changes in soil aeration stress for all scenarios are quantified in Table 8, which provides mean values for the previously defined riparian and floodplain areas of the mean ten-year SEV_{as} as well as the percentage of the total number of MIKE SHE grid cells within each area in which these SEV_{as} values increase or decrease from the baseline. Supplementary Table S2 add the corresponding data derived from the annual SEV_{as} values in 2002 and 2007 (see discussion).

Baseline aeration stress varies across Hunworth Meadow, with the largest values of ten-year mean SEV_{as} (above 5 m weeks) being concentrated on the floodplain and, in particular, around the ditch and the lowest elevation downstream end of the site (ten-year SEV_{as} >8 m weeks in some locations; Fig. 10). In contrast, the riparian area is characterised by relatively lower aeration stress, with baseline ten-year SEV_{as} over much of the former
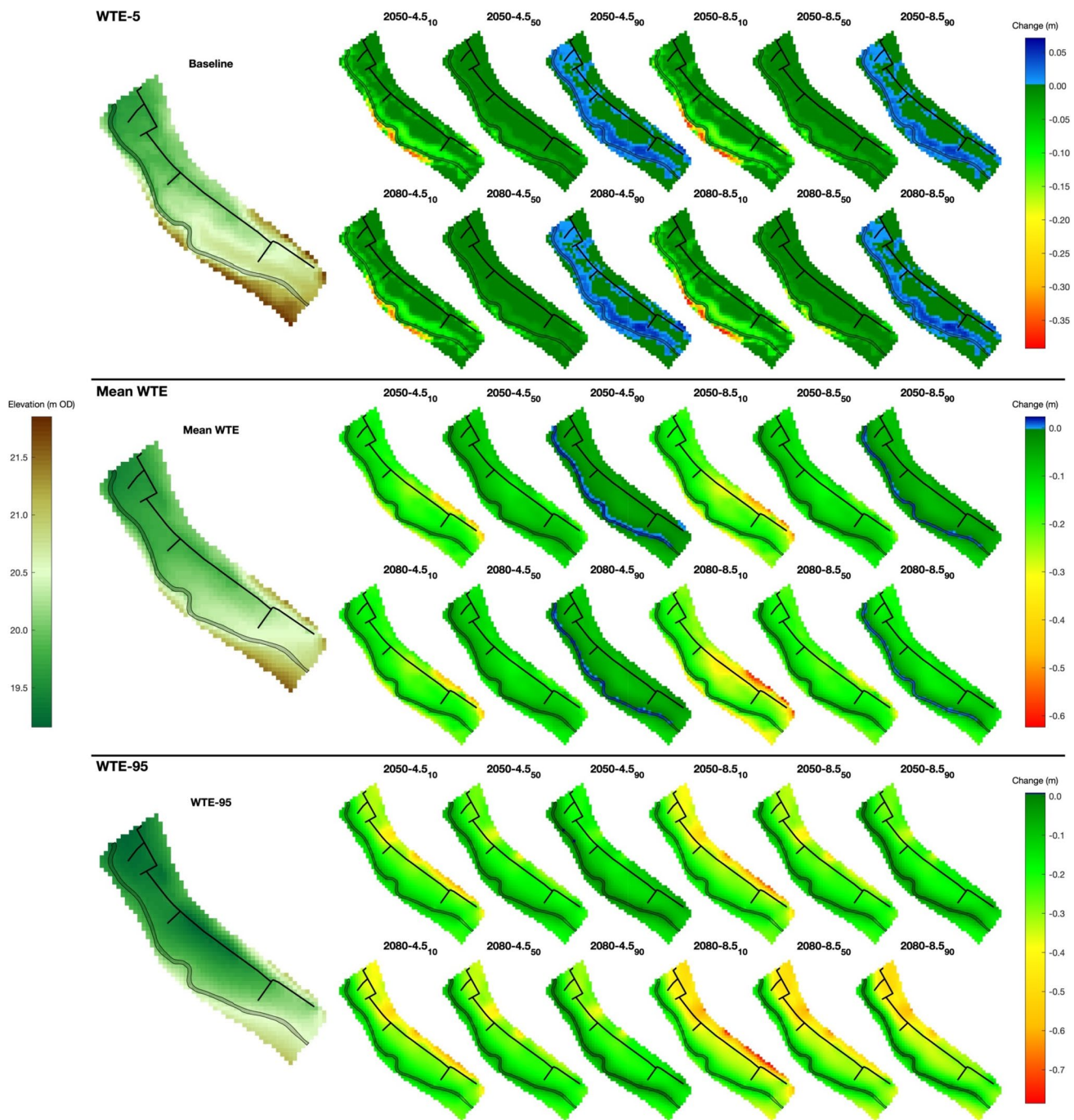
Fig. 9 Baseline WTE-5, mean WTE and WTE-95 (m OD) across Hunworth Meadow and the immediate area on either side of the River Glaven and change in these indices for 10%, 50% and 90% probability levels and the RCP4.5 and RCP8.5 scenarios in the 2050s and 2080s

embankment being less then 3 m weeks. On average baseline ten-year SEV_{as} for MIKE SHE cells on the floodplain is 1.2 m weeks (33%) larger than the corresponding value for the riparian area (Table 8).

The dominance of climate change-driven drying of Hunworth Meadow is clearly demonstrated by overwhelming declines in aeration stress. For the floodplain, mean values of

the ten-year SEV_{as} decline for all scenarios (Table 8). Similar declines are projected for the riparian area, although four 90% probability scenarios (three in the 2050s, one in the 2080s) are associated with either no change or very small increases. With the exception of the 90% probability scenarios, the vast majority (>98%) of MIKE SHE cells on both the floodplain and riparian area experience declines in

Table 7 Mean baseline and UKCIP18 scenario WTE-5, mean WTE and WTE-95 (m above OD) across the MIKE SHE grid cells covering the riparian area and the floodplain. The extents of these two areas are indicated in Supplementary Material Figure S9. Shaded cells indicate reductions compared to the baseline

	2050s					2080s				
	10%	30%	50%	70%	90%	10%	30%	50%	70%	90%
Riparian area										
WTE-5: Baseline 20.31										
RCP 2.6	20.25	20.28	20.30	20.31	20.33	20.26	20.29	20.30	20.32	20.34
RCP 4.5	20.25	20.28	20.30	20.31	20.33	20.26	20.28	20.30	20.32	20.34
RCP 6.0	20.25	20.28	20.30	20.31	20.33	20.25	20.28	20.30	20.31	20.34
RCP 8.5	20.24	20.27	20.29	20.31	20.33	20.24	20.27	20.29	20.31	20.33
Mean WTE: Baseline 20.13										
RCP 2.6	20.04	20.07	20.09	20.10	20.13	20.05	20.07	20.09	20.11	20.13
RCP 4.5	20.03	20.06	20.08	20.10	20.13	20.03	20.06	20.08	20.10	20.12
RCP 6.0	20.04	20.07	20.08	20.10	20.13	20.03	20.06	20.07	20.09	20.11
RCP 8.5	20.02	20.05	20.07	20.09	20.12	20.00	20.03	20.05	20.07	20.10
WTE-95: Baseline 19.94										
RCP 2.6	19.83	19.85	19.86	19.88	19.91	19.83	19.85	19.86	19.88	19.90
RCP 4.5	19.82	19.84	19.86	19.88	19.90	19.80	19.83	19.84	19.86	19.88
RCP 6.0	19.82	19.85	19.86	19.88	19.90	19.80	19.82	19.83	19.85	19.87
RCP 8.5	19.80	19.82	19.84	19.86	19.88	19.77	19.79	19.80	19.81	19.83
Floodplain										
WTE-5: Baseline 20.28										
RCP 2.6	20.26	20.27	20.27	20.28	20.28	20.26	20.27	20.27	20.28	20.28
RCP 4.5	20.26	20.27	20.27	20.28	20.28	20.26	20.27	20.27	20.28	20.28
RCP 6.0	20.26	20.27	20.27	20.28	20.28	20.26	20.27	20.27	20.28	20.28
RCP 8.5	20.25	20.27	20.27	20.28	20.28	20.25	20.27	20.27	20.28	20.28
Mean WTE: Baseline 20.08										
RCP 2.6	19.92	19.97	19.99	20.02	20.05	19.93	19.97	19.99	20.02	20.05
RCP 4.5	19.91	19.96	19.99	20.01	20.05	19.90	19.95	19.97	19.99	20.02
RCP 6.0	19.91	19.96	19.99	20.01	20.05	19.88	19.93	19.96	19.98	20.01
RCP 8.5	19.87	19.93	19.97	19.99	20.03	19.83	19.88	19.91	19.94	19.97
WTE-95: Baseline 19.70										
RCP 2.6	19.44	19.48	19.50	19.53	19.57	19.44	19.47	19.50	19.52	19.56
RCP 4.5	19.42	19.47	19.50	19.52	19.57	19.39	19.43	19.45	19.47	19.49
RCP 6.0	19.43	19.47	19.50	19.53	19.57	19.38	19.41	19.42	19.44	19.46
RCP 8.5	19.38	19.42	19.45	19.47	19.51	19.31	19.33	19.34	19.35	19.36

ten-year SEV_{as}. For the riparian area, however, most cells experience increases in this SEV_{as} value for the four 90% probability scenarios, accounting for no change or small increases in the overall mean ten-year SEV_{as}. The number of cells with positive changes does, however, decline with magnitude of radiative forcing. A similar decline in the number of floodplain cells with positive changes in ten-year SEV_{as} is evident for the 90% probability level, but only a minority of cells (<10% and <2% for RCP8.5) experience changes in this direction.

In accordance with trends for groundwater, ten-year SEV_{as} declines progressively as radiative forcing increases and probability level declines (Table 8). Declines for floodplain cells in the 2050s for 50% probability are in the range 1.2–1.5 m weeks (25–30% reductions from the baseline), with RCP2.6 and RCP8.5 accounting for the extremes. This compares to declines of 1.9–2.2 m weeks (38–44%) and 0.4–0.8 m weeks (9–16%) for the two extreme probabilities (10% and 90%, respectively). Larger declines tend to be projected further into the future, although differences for RCP2.6 are small and sometimes larger for the 2050s. Declines for the 50% probability level in the 2080s range between 1.2 and 1.8 m weeks (24–37%; RCP2.6 and RCP8.5). These inter-scenario trends are repeated for the riparian area, although absolute and percentage declines are smaller than those for the floodplain with declines for the 50% probability being in the range 0.61–0.75 m weeks (16–20%) for the 2050s and 0.56–0.95 m weeks (15–25%) for the 2080s. The smallest declines for a given scenario are concentrated within upstream riparian MIKE SHE cells although they expand both downstream and onto the floodplain at higher probability levels (Fig. 10). Conversely, some of the floodplain areas which experience the highest baseline ten-year SEV_{as} values (i.e. the far downstream end of the floodplain or adjacent to the ditch and hillside) experience the largest declines for each scenario.

Potential implications of changing soil aeration stress for vegetation are summarised in Table 9 and Fig. 11. The

former provides the percentage of the total number of riparian and floodplain MIKE SHE cells in which ten-year SEV_{as} is within the ranges suitable for each NVC community. These results are provided for the baseline and all climate change scenarios. The distribution of cells with suitable hydrological conditions for each community for the baseline and 10% 50% and 90% RCP4.5 and RCP8.5 scenarios is shown in Fig. 11 (results for all scenarios in the 2050s and 2080s are shown in Supplementary Material figures S14 and S15, respectively).

Under the baseline, suitable hydrological conditions for MG4 floodplain meadow, which is relatively intolerant of aeration stress, are concentrated close to the river, especially in the area of the former embankment (Fig. 11). Of the 116 riparian MIKE SHE cells, 35 (30%) have baseline ten-year SEV_{as} values suitable for this community. This contrasts to 7% of floodplain cells (although given the larger extent of this part of the model domain the absolute number of cells is larger; 47). Cells on the floodplain with aeration stress suitable for MG4 are concentrated just beyond the former embankment as

well as adjacent to the hillside at the upstream end of the meadow. Under climate change, and in response to declining aeration stress, the extent of the area with ten-year SEV_{as} suitable for MG4 increases in both the riparian area and floodplain for all scenarios with the single exception of 2050-2.6$_{90}$ (a decrease of a single cell for the floodplain). At the 50% probability level, a consistent 42% and between 41–46% of riparian cells are suitable for MG4 in the 2050s and 2080s, respectively (Table 9). This compares to 10% and 11–15% for the floodplain, demonstrating the continued importance of the area adjacent to the river for this community (Fig. 11). Even at 10% probability, associated with the largest increases in extent of suitability for MG4, there are only a few isolated cells in the centre of the floodplain that could support this community. The main driver of increases in MG4 suitability is an expansion of the zone adjacent to the river, both away from the channel and towards the downstream end of the floodplain. At least half of cells in the riparian zone have ten-year SEV_{as} suitable for MG4 across the extreme low probability scenarios.
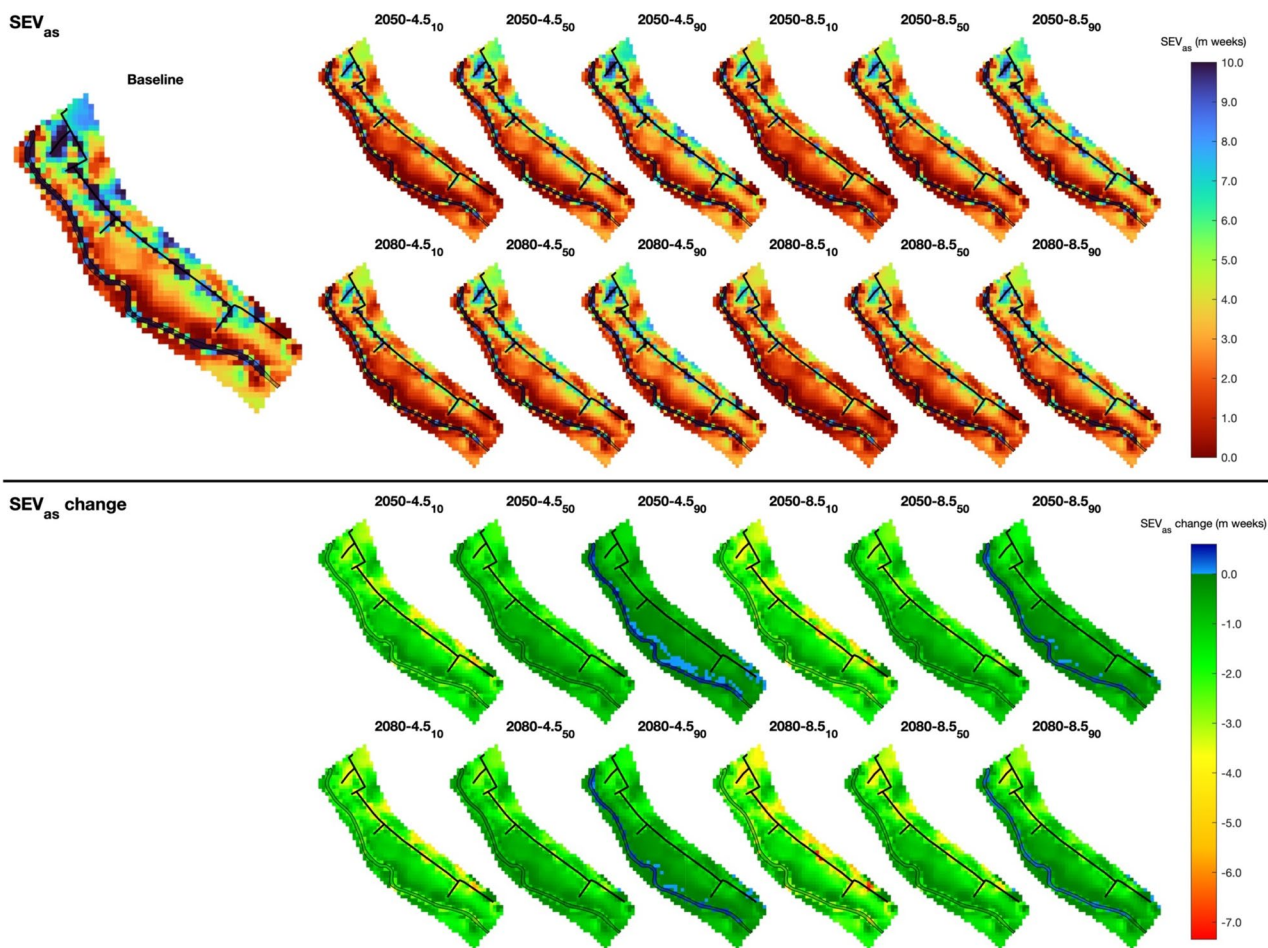
Fig. 10 Simulated mean sum exceedance values for aeration stress (SEV_{as}; m weeks) within Hunworth Meadow across all ten years (2001–2010) of the simulation period for the baseline and 10%, 50% and 90% probability levels for the RCP4.5 and RCP8.5 scenarios in the 2050s and 2080s

Table 8 Mean ten-year (2001–2010) SEV_{as} (m weeks) for the baseline and each UKCIP18 scenario across the MIKE SHE grid cells covering the riparian area (2 grid cells from the river) and the floodplain; percentage of cells (riparian cells total: 116, floodplain cells total: 692) with increases and decreases in SEV_{as} (Note: where these do not sum to 100 the remaining cells experience no change). The extents of the two areas are indicated in Supplementary Material Figure S9. Shaded cells indicate reductions in SEV_{as} compared to the baseline

	2050s					2080s				
	10%	30%	50%	70%	90%	10%	30%	50%	70%	90%
Riparian area - Baseline: 3.73										
RCP 2.6	2.58	2.92	3.12	3.40	3.76	2.64	2.94	3.16	3.40	3.75
	0 / 99	0 / 99	0 / 99	0 / 99	66 / 34	0 / 99	0 / 99	0 / 99	0 / 99	58 / 41
RCP 4.5	2.52	2.86	3.09	3.34	3.73	2.51	2.83	3.04	3.27	3.60
	0 / 99	0 / 99	0 / 99	0 / 99	50 / 49	0 / 99	0 / 99	0 / 99	0 / 99	21 / 78
RCP 6.0	2.55	2.87	3.09	3.36	3.75	2.46	2.76	2.97	3.20	3.54
	0 / 99	0 / 99	0 / 99	0 / 99	60 / 40	0 / 99	0 / 99	0 / 99	0 / 99	17 / 82
RCP 8.5	2.39	2.72	2.98	3.23	3.61	2.27	2.57	2.78	3.00	3.36
	0 / 99	0 / 99	0 / 99	0 / 99	22 / 77	0 / 99	0 / 99	0 / 99	0 / 99	9 / 91
Floodplain - Baseline: 4.88										
RCP 2.6	3.02	3.45	3.69	4.02	4.46	3.12	3.47	3.73	3.99	4.38
	0 / 99	0 / 99	0 / 99	0 / 99	10 / 90	0 / 99	0 / 99	0 / 99	0 / 99	9 / 90
RCP 4.5	2.93	3.35	3.64	3.91	4.38	2.91	3.28	3.51	3.74	4.07
	0 / 99	0 / 99	0 / 99	0 / 99	7 / 93	0 / 99	0 / 99	0 / 99	0 / 99	2 / 97
RCP 6.0	2.97	3.38	3.64	3.95	4.40	2.83	3.17	3.39	3.62	3.94
	0 / 99	0 / 99	0 / 99	0 / 99	8 / 91	0 / 99	0 / 90	0. / 99	0 / 99	1 / 98
RCP 8.5	2.72	3.14	3.43	3.70	4.12	2.50	2.87	3.06	3.27	3.56
	0 / 99	0 / 99	0 / 99	0 / 99	2 / 98	0 / 99	0 / 99	0 / 99	0 / 99	1 / 99

Changes in the extent of suitable conditions for both MG7C and MG8 again differ between the riparian area and the floodplain. For all scenarios, declining aeration stress across the floodplain drives an expansion in the extent of suitable conditions for both communities. MG7C flood pasture is less tolerant to prolonged high water tables (Table 1) and under baseline conditions could be supported on 17% of floodplain cells which are predominantly located in a band perpendicular to the river and closer to the channel than the ditch (Fig. 11). The potential extent of this community increases to 27% (29% for RCP8.5) of floodplain cells for the 50% probability scenarios in the 2050s. More variable increases of between 26% and 30% of the floodplain are projected for this probability level in the 2080s. Much of this expansion is associated with a widening of the band of suitable SEV_{as}, most notably midway down the floodplain where it extends to the ditch. There is also an expansion of suitable conditions beyond the ditch towards the hillside. The extent of suitable aeration stress for MG7C does tend to increase (decrease) with lower (higher) probability level, although differences are relatively small, with similar changes across different radiative forcing scenarios for a given probability. The greater tolerance of MG8 water meadow to aeration stress results in a larger part of the floodplain (38%; Table 1) having suitable conditions under the baseline. There is a particular concentration in the centre of the floodplain both at its upstream end and middle section. The area with suitable aeration stress under climate change tends to shift further away from the river towards and beyond the ditch, as well as into the lower section of the floodplain. These areas were characterised by baseline ten-year SEV_{as} values that exceeded the upper tolerable limits for MG8. Inter-scenario differences in suitable conditions for this community are relatively subtle. Across all scenarios 42–50% (44–52%) of floodplain cells have ten-year SEV_{as} appropriate for this community in the 2050s (2080s). Under baseline conditions, riparian cells which are suitable for MG7C and MG8 (16% and 25% of the total, respectively; Table 9) are concentrated towards the downstream end of the site and even there occur only in isolated patches. Climate change-driven declines from already relatively low baseline aeration stress compared to the floodplain is responsible for reductions in suitability for these two communities across the riparian area for all but most 90% probability scenarios (no change or an increase of a single cell). Given the relatively small number of suitable cells for the baseline, declines in terms of number of cells are in single figures (except for 2080-8.5$_{90}$ for MG8), albeit with progressively larger declines projected for lower probability levels.

The baseline distribution of suitability for MG13 inundation grassland and AG/Cx water meadow are very similar (Fig. 11). Given the higher minimum SEV_{as} values for both of these communities, indicative of tolerance to prolonged high water tables, cells with suitable aeration stress are concentrated in the wetter parts of the floodplain, in particular around the ditch and towards the downstream end of the site. Across the floodplain, 23% and 26% of cells have suitable SEV_{as} values for these two communities, respectively (Table 9). The extent of suitable conditions for MG13 on the floodplain declines for most cscenarios, the exceptions being either one (2050s) or all (2080s) of the 70% probability scenarios and all of the 90% probability

Table 9 Baseline and scenario percentages of riparian and floodplain MIKE SHE grid cells with ten-year SEV_{as} values in the suitable range for five NVC vegetation communities (the extents of the two areas are indicated in Supplementary Material Figure S9; riparian cells total: 116, floodplain cells total: 692). Shaded cells indicate reductions compared to the baseline

| | 2050s | | | | | 2080s | | | | |
	10%	30%	50%	70%	90%	10%	30%	50%	70%	90%
Riparian area										
MG4 – Baseline: 30										
RCP 2.6	50	43	42	36	30	50	42	41	36	30
RCP 4.5	52	47	42	36	30	51	46	42	37	32
RCP 6.0	51	46	42	36	30	52	48	42	39	35
RCP 8.5	55	50	42	39	32	59	50	46	42	36
MG7C – Baseline: 16										
RCP 2.6	10	11	14	16	16	10	13	13	16	16
RCP 4.5	11	9	14	12	16	11	10	14	12	17
RCP 6.0	10	9	14	14	16	12	10	15	14	16
RCP 8.5	14	9	13	13	17	13	10	12	15	16
MG8 – Baseline: 25										
RCP 2.6	20	20	22	20	24	20	21	22	20	25
RCP 4.5	19	20	22	20	25	20	20	22	22	25
RCP 6.0	19	20	22	20	25	20	20	21	22	25
RCP 8.5	17	20	21	22	25	16	20	21	23	22
MG13 – Baseline: 10										
RCP 2.6	4	10	11	12	10	4	10	12	13	10
RCP 4.5	4	10	11	12	10	3	9	9	11	13
RCP 6.0	4	10	11	13	10	4	9	10	12	14
RCP 8.5	4	6	9	11	10	4	3	6	10	11
AG/Cx – Baseline: 14										
RCP 2.6	7	7	9	11	14	7	7	10	11	13
RCP 4.5	7	8	9	12	13	6	7	8	10	11
RCP 6.0	7	8	9	12	13	7	8	8	10	11
RCP 8.5	7	7	7	9	11	7	7	7	7	10
Floodplain										
MG4 – Baseline: 7										
RCP 2.6	16	12	10	8	7	15	11	9	8	7
RCP 4.5	17	13	10	9	7	16	13	10	9	7
RCP 6.0	16	13	10	8	7	17	13	11	9	7
RCP 8.5	18	14	11	9	7	21	15	13	10	8
MG7C – Baseline: 17										
RCP 2.6	28	28	27	23	18	27	28	26	24	19
RCP 4.5	28	28	27	25	19	29	28	28	26	22
RCP 6.0	28	29	27	24	19	28	29	29	28	24
RCP 8.5	27	28	29	27	22	27	30	30	30	29
MG8 – Baseline: 38										
RCP 2.6	46	47	47	47	42	46	47	49	47	44
RCP 4.5	44	48	48	48	43	45	49	48	50	47
RCP 6.0	45	47	48	48	43	44	48	49	51	49
RCP 8.5	42	47	48	50	47	44	49	50	51	52
MG13 – Baseline: 23										
RCP 2.6	18	20	20	23	25	19	21	21	23	25
RCP 4.5	19	21	22	23	24	20	22	23	23	24
RCP 6.0	18	21	21	22	24	19	22	23	23	24
RCP 8.5	18	20	21	22	24	17	19	21	23	24
AG/Cx – Baseline: 26										
RCP 2.6	19	21	22	24	29	20	22	22	24	28
RCP 4.5	18	20	21	23	28	18	21	22	22	26
RCP 6.0	18	21	21	24	28	17	20	22	22	24
RCP 8.5	16	19	21	21	26	13	16	18	20	22

scenarios in both time slices (<2% increases). Declines in suitability for AG/Cx are less equivocal with small (<3%) increases being limited to all (2050s) and two (2080s) 90% probability scenarios. Where declines in extent of suitable conditions for MG13 and AG/Cx are projected, they follow the broad trends for water table elevation and SEV_{as} with the magnitude of reductions increasing as probability level declines whilst, in general, larger declines are projected for higher radiative

forcing. When declines in suitability are projected for both communities, AG/Cx is subject to the larger reductions with, for example, declines for the 50% probability level being in the range 4–5% (4–8%) for the 2050s (2080s) compared to 2–3% (<1–2%) for MG13. Declines for AG/Cx for the 10% probability scenarios are at most 10% and 13% in the 2050s and 2080s, respectively (RCP8.5), compared to 5% and 6% for MG13 under the same scenarios. Declining habitat suitability for these communities is associated with a loss of cells relatively close to the river and within the upper third of the meadow close to the ditch (Fig. 11). Cells with appropriate ranges in SEV_{as} become more concentrated on the other side of the ditch and towards the base of the hillside. Under baseline conditions, just 10% and 14% of riparian cells (12 and 16 cells) have suitable SEV_{as} ranges for MG13 and AG/Cx, respectively, with their location being largely coincident with the river channel. AG/Cx is projected to consistently decline in the riparian area with the one exception of no change for 2050s-2.6$_{90}$ (Table 9). In contrast, whilst the extent of suitability for MG13 declines for all 10% and some 30–50% probability scenarios, increases are projected for some of the higher probability level scenarios (no change for others). However, such increases amount to a few cells (no more than four) and as such, the riparian area remains largely unsuitable in terms of aeration stress for both MG13 and AG/Cx.

Discussion

Climate change-driven modifications to hydrometeorological conditions are characteristically associated with uncertainty that may include differences in both magnitude and direction of change (e.g. IPCC 2014, 2018; Arnell and Gosling 2013; Do et al. 2020). In the current study this uncertainty, especially in terms of direction of change, is most evident in the UKCP18 projections for precipitation. Across the 40 scenarios, increases in mean annual precipitation are projected in 24 cases (60%), with the remaining 16 scenarios (40%) projecting declines. Declines for all of the 10–50% probability scenarios, alongside the general increase in the size of these declines with increasing radiative forcing and lower probability level, replicate the results obtained by Thompson et al. (2017b) using UKCP09. The size of the declines projected by UKCP09 and UKCP18 are generally similar for a given probability level, albeit with those for the most recent projections being slightly larger. For example, mean changes which are as likely as not to be exceeded (i.e. 50% probability) across the three SRES-based UKCP09 scenarios were equivalent to declines of around 2% (both time slices) from the baseline (Thompson et al. 2017b). The corresponding values for the four RCP-based UKCP18 projections from the current study indicate declines of 4% and 3%,

respectively. Differences of no more than a few percentage points are replicated for the declines in the two lower probability levels. In contrast, for the two highest probability levels, projected increases in mean annual precipitation were larger for UKCP09 than for UKCP18; mean increase for the 90% level being 22% (2050s) and 26% (2080s) for the former compared to 16% and 19% for the latter. As a result, across all 30 (UKCP09) and 40 (UKCP18) scenarios, the total range of potential change, and hence, this particular source of uncertainty, is larger for the earlier set of projections (-27–30%, range 57% compared to -26–21%, range 47%). The seasonal distribution of precipitation changes are very similar for UKCP09 and UKCP18. At the 50% probability, both are characterised by increases between October and April with declines in the remaining months reflecting the dominant projected trend for the UK to experience wetter winters and drier summers (e.g. Jenkins et al. 2009; Lowe et al. 2018; Met Office 2021). At this probability level, the largest monthly increases (November) are greater for UKCP18 (2050s: 10–12%, 2080s: 14–22%) than for UKCP09 (4–11% and 13–15%, respectively). In contrast, the earlier scenarios project larger declines in summer (e.g. reductions in July/August of 20–30% and 24–40 for the 2050s and 2080s compared to the declines reported herein of 18–24% and 19–32%). Both sets of scenarios exibit constriction (expansion) in the period of increasing precipitation with lower (higher) probability level.

There is much less uncertainty in the direction of change in PET, with small declines in annual totals (<5%) being limited to the lowest (10%) probability (very likely to be exceeded), replicating earlier results for Hunworth based on UKCP09 (Thompson et al. 2017b). The more consistent direction of change in evapotranspiration is supported by many climate change impact studies that have employed ensembles of projections and reflects the overwhelming dominance of increasing temperature (e.g. IPCC 2013; Thompson et al. 2013; Jiménez Cisneros et al. 2014; Ho et al. 2016; Chan et al. 2020; Emiru et al. 2022). In the context of uncertainty related to evapotranspiration, it is appropriate to note that the approach employed in the current study replicated that used by Thompson et al. (2017b), only differing in its use of the newest UK climate projections. This avoids potential uncertainty associated with perturbing different meteorological inputs to one PET scheme (e.g. Thompson et al. 2009; Zhang et al. 2013; Lai et al. 2022) or the use of alternative PET schemes (Kingston et al. 2009; Thompson et al. 2014; Dallaire et al. 2021), both of which can impact simulated hydrometeorological responses to the same climate change scenarios. Whilst for a given probability level, mean increases in annual PET were larger (smaller declines for the 10% probability) for UKCP09 (Thompson et al. 2017b), differences are small with mean changes for scenarios of a given probability differing by no more than 3

Fig. 11 Simulated extent of suitable ten-year SEV_{as} values for five NVC vegetation communities within Hunworth Meadow for the baseline and 10%, 50% and 90% probability levels for the RCP4.5 and RCP8.5 scenarios in the 2050s and 2080s
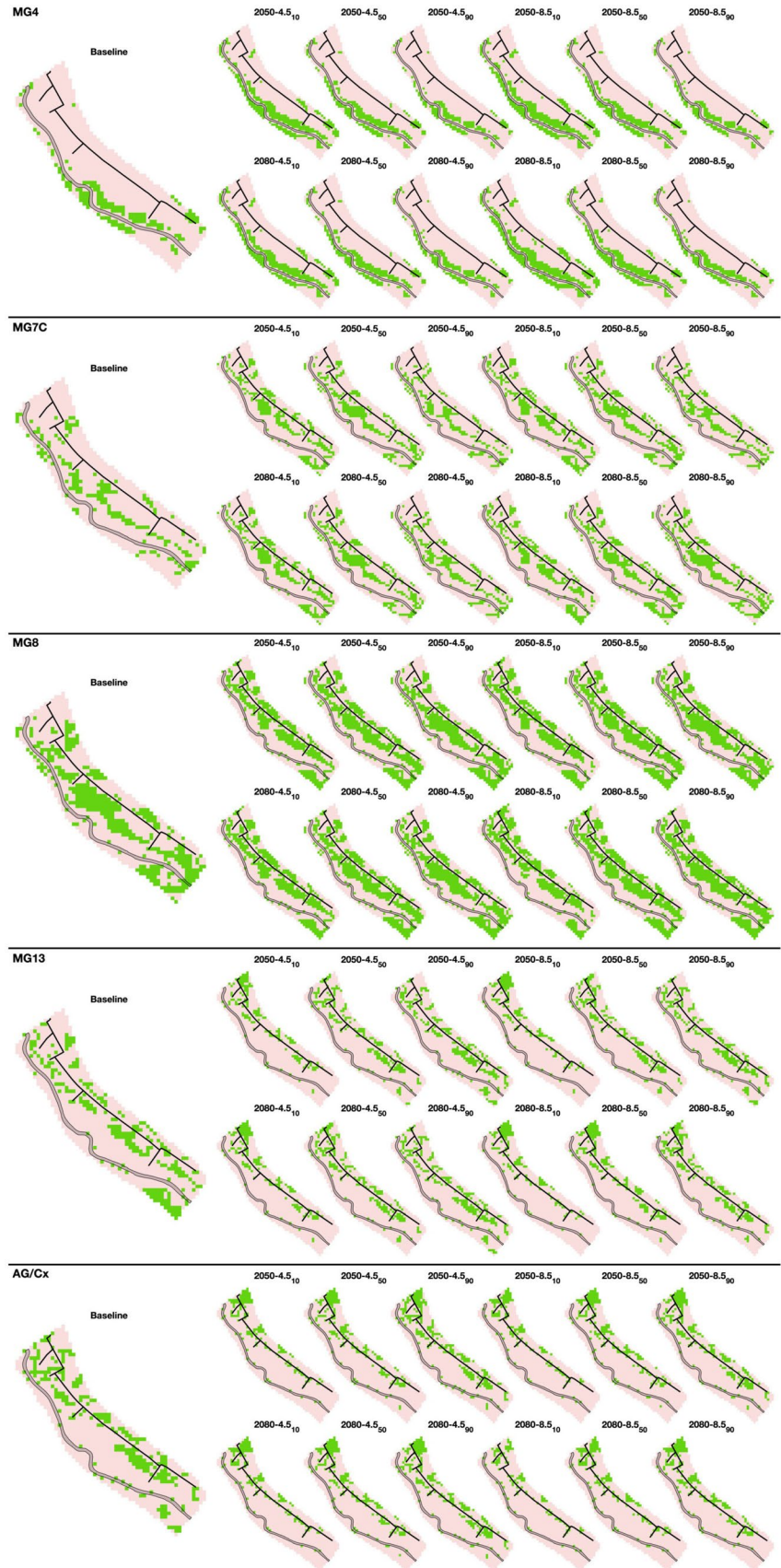
percentage points between UKCP09 and UKCP18. Across the 30 / 40 scenarios the overall ranges of change in annual PET are similar, albeit slightly larger for UKCP18 (-2–41%, range 43% for UKCP09 compared to -4–43%, range 47% for UKCP18). Similarly, the seasonal distribution of changes, and their overall range, are very similar with both sets of scenarios projecting the largest increases in summer (especially July and August).

Elevated potential evapotranspiration for most UKCP18 projections offsets the majority of increases in mean annual precipitation that are projected for the 70% and 90% probability scenarios with consequent reductions in net precipitation compared to the baseline. This includes four of the 90% probability scenarios which contrasts to the earlier UKCP09 results for which net precipitation increased for all scenarios of this extreme probability. Where increases in net precipitation are projected for UKCP18 scenarios, they are smaller in size than those for UKCP09 (mean increase 4% compared to 11%). As discussed by Thompson et al. (2017b), since projections for the 90% probability level are very unlikely to be exceeded, the annual net precipitation figures highlight the dominant drying trend for Hunworth Meadow and the River Glaven catchment under both the previous UKCP09 and current UKCP18 scenarios. Across the 10–70% probability scenarios reductions in annual net precipitation in the 2050s tend to be larger (by on average around 2%) for UKCP18 whilst this reverses for the 2080s (declines for UKCP09 are on average 2% larger than those for UKCP18). The dominant drying trend under both sets of projections is further confirmed by the similar declines in the number of months when precipitation exceeds PET.

Near consistent elevated evapotranspiration across ensembles of climate change scenarios that include both increases and decreases in precipitation have previously been shown to reduce uncertainty in the direction of hydrological changes, including increasing the proportion of scenarios that produce declines in river flow, although these impacts can vary spatially over larger catchments (e.g. Singh et al. 2010; Thompson et al. 2013; Ho et al. 2016). This can, in turn, enhance drying trends for floodplain wetlands by reducing the extent of flooding and potentially offsetting, or at least reducing, the impacts of any increases in direct precipitation (Thompson et al. 2017a). The use of net precipitation to infer such hydrological impacts is, however, a simplification, given the potential for actual evapotranspiration to fall below potential rates as soil moisture declines, a process that is represented within both the NAM and MIKE SHE models used herein (e.g. House et al. 2016a). Scenario river discharge as simulated by the first of these models is nonetheless dominated by declines, with a very slight increase in frequency of negative changes in flow metrics for UKCP18 compared to UKCP09. The former is associated with declines in mean discharge for all 10–70% probability

scenarios, whilst Thompson et al. (2017b) showed that three of the six 70% probability scenarios projected small increases for UKCP09. Beyond these scenarios, increases in mean, high (Q5) and low (Q95) discharges are limited for both the earlier and current projections to the 90% probability level, and as such are very unlikely to be exceeded. The increases for the current study are all between 9 and 11 percentage points smaller than those established from the older generation of climate projections. UKCP09-UKCP18 differences in the projected declines in the three river discharge metrics for the remaining scenarios (i.e. 10–70% probability) are smaller (all by less than 4 percentage points), echoing the similarly smaller differences previously discussed for precipitation and net precipitation. In general, more recent projections produce larger declines for the 2050s, whilst this reverses for the 2080s, although for both sets of projections there is the expected increase in the absolute magnitude of changes further into the future (e.g. Jobst et al. 2018). Very similar changes in discharge for UKCP09 and UKCP18 at the central (i.e. 50%) probability level echo the findings of Kay et al. (2020), to our knowledge the only other study to have compared the impacts on simulated river flow using these two generations of UKCIP projections (although this earlier study only considered the 2050s for RCP4.5 and RCP8.5). The largest changes in discharge are simulated in summer and early autumn (June–October), coinciding with the period of declining precipitation and the largest increases in PET. As a result, declines in low flows (Q95) are, in percentage terms, larger than those for high flows (Q5) as well as mean flows. This enhanced sensitivity of low flows to climate change replicates previous studies undertaken at both the catchment (e.g. Thompson 2017b; Chan et al. 2020) and global scales (e.g. Giuntoli et al. 2015; Thompson et al. 2021). There is also an overall increase in the seasonal range in discharge within the River Glaven as reported for catchments elsewhere in the UK (e.g. Fowler and Kilsby 2007; Johnson et al. 2009; Kay 2021).

As discussed by Thompson et al. (2017b), it should be noted that the projected changes in discharge of the River Glaven are based on the assumption that rainfall-runoff characteristics within the catchment are unaltered. Whilst this is a common assumption applied in many hydrological impact studies of climate change (e.g. Döll and Zhang 2010; Gosling et al. 2016; Do et al. 2020; Emiru et al. 2022), catchment vegetation and land use can exert important controls on runoff (Brown et al. 2005; Monger et al. 2022). A changing climate is likely to induce changes in natural vegetation and, particularly important across much of the UK and typified by the Glaven catchment, agricultural practices that may include alternative crop species, planting times, irrigation and machinery use, as well as grazing regimes (e.g. Bindi and Olesen 2011; Arnell and Freeman 2021). These practices may also be impacted by policy changes that themselves will be influenced by global

climate change and associated mitigation efforts (Olesen and Bindi 2002; Fellmann et al. 2018). Whilst these knock-on impacts are beyond the scope of the current study, they do represent sources of uncertainty in projected discharge of the River Glaven and the subsequent impacts on the catchment's floodplains including Hunworth Meadow.

Declines in the frequency with which the two threshold discharges employed herein are exceeded for the UKCP18 scenarios are very similar to those previously established using UKCP09, at least for 10–50% probability levels, and illustrate the dominant trend towards drier conditions. For example, across the eight UKCP18 50% probability scenarios the larger threshold associated with widespread inundation is exceeded either four (five scenarios) or three (three scenarios) times compared to the eight for the baseline. Similarly, four of the corresponding six earlier UKCP09 scenarios led to this threshold being exceeded four times with the remaining two producing three individual exceedances (Thompson 2017b). At the 10% probability level, all UKCP18 and UKCP09 scenarios produced a single event that exceeds the larger threshold. It is appropriate to acknowledge that despite declines from the baseline even for this most extreme scenario, some overbank inundation is retained whereas prior to embankment removal the larger channel capacity likely prevented its occurrence (Clilverd et al. 2013). Close correspondence between results for the two generations of climate projections is maintained for the smaller threshold discharge linked to flooding of the riparian area. The mean number of days when this discharge is exceeded for each of the 10–50% probabilities for the two sets of projections differ by no more than two (one for the number of individual events). Differences between the two generations of projections are larger for the higher probability scenarios. Declines in discharge compared to some increases (70% probability) or smaller increases (90% probability) for the most recent projections compared to UKCP09 reduces the frequency of threshold discharge exceedance. For example, whilst all but one UKCP18 90% probability scenario produces one additional event that exceeds the larger threshold discharge, all of the corresponding UKCP09 scenarios projected an additional two events. Similarly, the mean number of days (individual events) when the lower threshold discharge is exceeded are lower for UKCP18 compared to UKCP09 by 13 and 42 days (6 and 16 events) for the 70% and 90% probability scenarios, respectively. Three UKCP09 70% probability scenarios projected increased frequency of this lower threshold being exceeded compared to scenario-wide declines for UKCP18.

Comparing simulated (or observed) river discharges (or levels – see Duranel et al. 2007) with specific thresholds provides a relatively simple method to assess the potential for floodplain inundation under different scenarios (Clilverd et al. 2016; Addy and Wilkinson 2021). It is important to recognise, however, that the flood response to a given magnitude event at an individual site will vary with a number of factors that include antecedent soil moisture, groundwater levels and surface water extent (Jung et al. 2004; Byrne et al. 2019; Marchand et al. 2022). These will influence the ability of soils to accommodate infiltrating water, the potential for the water table to rise to the surface thereby initiating groundwater flooding, and the propagation of the flood across the floodplain (e.g. Acreman and Holden 2013; Hester et al. 2016; Saksena and Merwade 2017). Antecedent conditions will themselves vary between scenarios, as will the magnitude of change in river discharge. The combined impact of these factors can be better represented within coupled hydrological / hydraulic models such as MIKE SHE / MIKE 11 (see Thompson et al. 2004), although such physically-based, fully distributed models do impose large data demands which may be problematical for floodplain wetlands not subject to the intensive field investigations and monitoring programmes applied to Hunworth Meadow (e.g. Hollis and Thompson 1998). These interactions are likely responsible for variability in changes in simulated flood extent for an individual scenario across the eight events discussed above. Irrespective of this inter-event variability, declines in flood extent within Hunworth Meadows dominate, with small increases restricted to just nine (<3%) of the total 320 scenario-event combinations (i.e. 40 scenarios × eight events). Given that these increases are restricted to the 90% probability, associated with changes that are very unlikely to be exceeded, climate change is projected to overwhelmingly reduce floodplain inundation, corroborating the simpler threshold discharge exceedance analysis. In accordance with the projected changes in the hydrometeorological data used to force the MIKE SHE / MIKE 11 model, the magnitude of these declines is larger as probability level declines and radiative forcing increases.

These trends are replicated when detailed assessments for the two events considered herein are compared with those that are available for UKCP09 (Thompson et al. 2017b). In the first event (18/07/2001), associated with the largest discharge within the record from the Hunworth gauging station, the more recent projections produce very slightly smaller declines in total flood extent (by on average just under 1 percentage point). Whilst all of the UKCP09 90% probability scenarios projected small increases in total inundated area, the new results show that two of the eight UKCP18 scenarios project declines. When increases in flood extent are projected, they are smaller for UKCP18, but again only slightly (mean difference across all scenarios is just over 1 percentage point). All of the scenarios in both sets of projections produce declines in total inundated area for the smaller event (28/05/2007). These declines are, however, larger for the more recent projections (by on average 11 percentage points). Notwithstanding these differences,

the spatial distributions of surface water and their variable depths during the two example flood events are very similar and demonstrate consistent trends across both sets of climate change projections. These include the progressive concentration of inundation, especially relatively deep water, towards the downstream end of the floodplain and in association with the ditch. Some of the lowest sections of the floodplain are below the elevation of the lowered river bank, with drainage in this area further restricted by the embankment that demarcates the downstream end of the floodplain and the blocked ditch that runs beneath it. These characteristics contribute to the retention of some surface water (which may result from a combination of river bank overtopping or the water table intercepting the surface - see below) in these areas even under the most extreme drying scenarios (e.g. 10% probability). Further changes in the hydrological conditions in this part of the floodplain could potentially result from future drain unblocking and/or the installation of culverts beneath the embankment, interventions that have been considered by the landowner in the past. This would require a re-evaluation of the climate change scenarios using a revised MIKE SHE / MIKE 11 model incorporating appropriate hydraulic structures that can be represented within the modelling system (e.g. Thompson 2004; Rahim et al. 2012).

MIKE SHE results for specific locations demonstrate that under both baseline and scenario conditions there are contrasting water table regimes close to the river and on the floodplain, justifying the approach of separately reviewing climate change impacts on these two areas. Whilst strong seasonality, characterised by water tables close to or at the surface in winter and subsequent drawdowns through spring and summer, is evident across the model domain, groundwater levels are much more dynamic close to the river. As discussed by Clilverd et al. (2016), this contrast in simulated water tables matches observations from dip wells installed on Hunworth Meadow. Short-lived rises and falls in water table in the riparian area reflect the influence of seepage from and to the river in response to changes in river discharge, as well as localised inundation that has been facilitated by embankment removal. These results are in accordance with conceptual models and earlier numerical modelling of floodplain hydrology (Bates et al. 2000; Burt et al. 2002). Seepage from the river outside periods of high discharge are most likely responsible for the smaller summer water table drawdowns close to the channel (e.g. Duval and Hill 2006). This seepage has less effect further from the river and, as a result, baseline summer drawdowns are larger.

Climate change is projected to both lower water table elevations across Hunworth Meadow and enhance their seasonality. The dominant driver of enhanced seasonality is an increase in the magnitude of summer drawdowns rather than changes in peak winter water levels. All 40 scenarios project reductions in WTE-95 (representing low water table conditions) for the four well locations reviewed in detail, as well as for the mean WTE-95 for floodplain and riparian MIKE SHE grid cells, although there are some spatial variations in the magnitude of these changes (discussed below). The corresponding mean water tables similarly decline in the vast majority of cases (no change for some 90% probability scenarios). Summer drawdowns and general reductions in mean water table level increase in size with a decline in probability, an increase in radiative forcing and the more distant time slice. The resulting increases in the overall range of water table levels replicates other climate change impact studies for UK wetlands (Dawson et al. 2003; Acreman et al. 2009; Thompson et al. 2009; Herrera-Pantoja et al. 2012). Results for UKCP18 presented herein are also very similar to those for UKCP09 (Thompson et al. 2017b). In the vast majority of cases, mean baseline-scenario changes in the three water table elevation metrics (WTE-5, mean WTE, WTE-95) for a given probability level for the two wells that feature in Table 6 differ by <1 cm between the two sets of projections. Larger differences, but still not exceeding 7 cm, are restricted to the 90% probability and result from larger declines in low water table levels (i.e. WTE-95) for UKCP18.

There are some differences between simulated impacts of climate change on water table levels on the floodplain and riparian area. On the floodplain, absolute peak levels are barely impacted, although the duration of the highest water tables does contract for all but the highest probability levels. Peak winter water table levels on the floodplain are essentially coincident with the ground surface, so that any small gains projected for the highest probability scenarios likely partially account for the modest increases in flood extent discussed above. The original embankments along the river may have restricted drainage of surface water accumulating by processes that include groundwater flooding, an impact analogous to drainage congestion as described by Choudhury et al. (2004) and Singh et al. (2022). Embankment removal has probably facilitated drainage across the meadow once river levels decline so that the potential for increases in peak water table levels are limited and short-lived across most of the floodplain. Low-lying areas towards the downstream end of the meadow where drainage is limited are likely exceptions. Peak water table elevations (again as indicated by WTE-5) closer to the river do tend to vary more between scenarios compared to those on the floodplain, although the overall range of change is still small (-7cm–3cm for the mean of riparian area cells). Larger declines (increases) in high water table levels closer to the river compared to the floodplain for the lowest (highest) probability scenarios likely reflect the influence of changes in peak river discharges (i.e. Q5) and consequent modifications to seepage from the river to the hyporheic zone and localised inundation. This aligns with observations

elsewhere that have shown more dynamic river-groundwater fluxes in near-channel floodplain environments (e.g. Welsh et al. 2020; Marchand et al. 2022), such that peak water table levels in these areas are more sensitive to climate change-induced modifications to stream discharge.

Whilst summer water tables are projected to decline across the riparian area and the floodplain, the magnitude of declines is smaller in the former (e.g. at least half the size when comparing WTE-95 for wells 1.1 and 1.4 across all scenarios). This suggests that even under the most extreme climate change scenarios, the modifying influence of river-groundwater exchanges discussed above (and see Bates et al. 2000; Burt et al. 2002) is retained close to the channel. As for the baseline conditions, this influence diminishes with distance from the river so that summer drawdowns are larger on the floodplain, with the balance between precipitation and evapotranspiration being a dominant driver of groundwater levels (see also Thompson et al. 2009). Whilst, as a result, the magnitudes of declines in low water table elevation across much of the floodplain are relatively uniform for most scenarios, there are some particularly large declines adjacent to the hillside especially at the upstream end of the meadow. These are most obvious for the 10–50% probability scenarios. Under baseline conditions, the water table is relatively high in this area, probably in response to a combination of subsurface flows originating from the hillside and the backing up of these upland-floodplain exchanges in response to high water tables on the floodplain (Burt et al. 2002; Jung and Burt 2004). Drier floodplain conditions in response to climate change would likely reduce this backing-up whilst subsurface flows from the hillside, especially in summer when the conditions indicated by WTE-95 are encountered, will decline, given that the whole model domain is subject to the same revised precipitation and PET. These changes would account for the relatively large declines in summer water table elevations in this part of the floodplain.

Hydrological conditions within floodplains, and other wetlands, exert important controls on plant and animal communities (e.g. Ausden et al. 2001; Baker et al. 2009, Wheeler et al. 2009; Keddy 2010). As a result, modifications to water level regimes due to climate change (or as a result of other factors such a river regulation) will induce biological responses. Potential ecological impacts of hydrological changes can be inferred by the magnitude of changes in water level / discharge regimes alone using methods such as the Range of Variability Approach / Indicators of Hydrological Alteration (see Richter et al. 1996; Acreman and Dunbar 2004; Laize and Thompson 2019). Indeed, one recent study has employed this method to assess risks of ecological change within extensive floodplain wetlands due to a large ensemble of modified climates (Thompson et al. 2021b). However, a more robust approach is to compare projected hydrological conditions against water

level (or flow; House et al. 2017) requirements of specific species or communities, assuming they are available, in order to determine the extent to which these conditions are out of range (Wheeler et al. 2009; House et al. 2016a). The current study employed an index that summarises root zone aeration stress resulting from high water tables (SEV_{as}) since previous research has established that relatively subtle differences in water table depth across floodplains, including those on the River Glaven, may give rise to different plant communities (Gowing et al. 2002a, 2002b; Dwire et al. 2006; Clilverd et al. 2022). Whilst the earlier climate change impact assessment for Hunworth Meadow based on the UKCP08 projections included a very preliminary analysis of SEV_{as} changes at specific well locations (Thompson et al. 2017b), the current study provides a site-wide analysis that includes a comparison of simulated aeration stress with tolerance ranges for five floodplain / wet grassland plant communities which might be expected at this site (Gowing et al. 2002a, 2002b).

SEV_{as} regimes on the floodplain and riparian area under baseline conditions are distinctly different, as are the declines in soil aeration stress in response to climate change. Despite smaller drawdowns closer to the river compared to the floodplain, baseline aeration stress is lower as a result of the more dynamic water table regime that is characterized by relatively high frequency rises and falls in response to river flows as described above. In contrast, on the floodplain, near permanent saturation at the surface through the earlier part of the growing season produces higher SEV_{as} values despite the larger summer drawdowns. As a result, more of the riparian area is shown to be suitable for communities that are relatively intolerant to aeration stress, most notably MG4 floodplain meadow, whilst the vast majority of the floodplain is too wet (high soil aeration stress) for this community, a finding supported by botanical evidence provided by Clilverd et al. (2016) and Clilverd et al. (2022). Baseline conditions on the floodplain are, in contrast, more suitable for communities adapted to low root zone oxygen concentrations (in particular MG13 inundation grassland and AG/Cx water meadow, but also MG8 water meadow). These communities, especially MG13 and AG/Cx, are much less likely to be supported within the riparian area. Root zone aeration stress is projected to decline for the vast majority of climate change scenarios. Declines in SEV_{as} are smaller over the riparian area so that the already relatively drier areas experience smaller changes in soil aeration stress. On the floodplain, changes in SEV_{as} translate to increases in suitable conditions for MG4, MG7C and MG8 for all scenarios (except one 90% probability scenario for MG4) although it should be noted that in most cases the majority of the area is still too wet for these three communities, which are considered to be inhibited by $SEV_{as} > c.1, 3$

and 4 m weeks, respectively. Conversely, the extent of the area with appropriate SEV_{as} values for communities most adapted to low soil oxygen status (MG13 and AG/Cx) are projected to decline for all but the most extreme (and hence extremely unlikely) high probability scenarios. Declines in suitable conditions for those communities adapted to low oxygen conditions are more obvious on the riparian area that is already characterised by low baseline SEV_{as} values. The only community projected to experience increases in suitable conditions beyond the equivalent of a few MIKE SHE grid cells is MG4 (all scenarios), a species-rich hay meadow community of high conservation importance.

The approach used herein employs the mean of the annual SEV_{as} values from each of the ten years of the model simulation period and, as such, assumes it is the average root zone soil aeration stress that determines suitability for the different vegetation communities. In reality, of course, hydrological conditions under baseline conditions vary year to year, as evidenced by the inter-annual variability in simulated water table levels. Similarly, under climate change the magnitude of changes in water table elevation and resulting soil aeration stress also display interannual variations. In general, absolute changes in SEV_{as} in wet years are larger than those in dry years, although they follow the broad spatial trends such as being larger on the floodplain compared to the riparian area (see Supplementary Material figures S12, S13 and Table S2). Given that the time scales for wet grassland community assembly vary between a few years to decades (e.g. Mountford and Manchester 1999; Wheeler et al. 2004), alternating wet and dry years compared to sequences of a number of wet years followed by dry years may, therefore, have different impacts on individual species and competitive balances within the plant communities (e.g. Gowing et al. 1997).

Whilst water table elevation and resulting aeration stress undoubtedly play important roles in structuring wetland plant communities (see also Robertson et al. 2001; Gaberščik et al. 2018; Keddy and Campbell 2020), a range of other factors, themselves linked to hydrological changes, may influence the botanical composition of Hunworth Meadow in response to climate change. For example, SEV_{as} based on water table depth alone does not account for water source and its chemical characteristics, providing some uncertainty in the botanical changes likely on Hunworth Meadow. Clilverd et al. (2016) and Clilverd et al. (2022) demonstrated that during high flow periods, floodwaters within the River Glaven were oxygen-rich. Passive diffusion of dissolved oxygen from the water column into submerged terrestrial plants may provide an important source of oxygen (Mommer et al. 2004) potentially reducing aeration stress

resulting from high water tables. This could be important across the riparian area, already subject to relatively low values of SEV_{as}, given the evidence that river-hyporheic zone exchanges continue under climate change. Although embankment removal facilitated more exchanges between river and floodplain (Clilverd et al. 2016), the current study has shown that climate change is projected to reduce flooding from the river, so that the influx of oxygen-rich water will also likely reduce. Similarly, given the dominance of agriculture within the Glaven catchment, floodwaters and the sediment they transport input elevated nutrient loads to the river's floodplains with implications for plant communities (e.g. Beltman et al. 2007; Michalcová et al. 2011; Zelnik and Čarni 2013). Whilst the supply of nutrients via this route has likely increased following embankment removal (Clilverd et al. 2013) with potential impacts on the distribution of plant types on the meadow (Clilverd et al. 2022), the current study suggests that reduced river-floodplain inundation due to climate change might reverse enhanced nutrient supply. Furthermore, the dominance of drier conditions on the floodplain will likely change nutrient availability within the soil. This could include enhancing nitrogen availability via increased mineralization and nitrification, and limiting phosphorous availability through P-adsorption (Zeitz and Velty 2002; Baldwin and Mitchell 2000). With soil fertility being an additional driver of plant species composition across wet grasslands in general (e.g. Wheeler et al. 2004), and Hunworth Meadow in particular (Clilverd 2006; Clilverd et al. 2022), such hydrologically moderated changes in nutrient availability may further impact upon changes in the site's vegetation communities.

The approach adopted herein assumes that vegetation species are readily able to respond to changing hydrological conditions when in reality this will depend upon existing seed banks on the site or in the wider catchment. A botanical study by Wotherspoon (2008) demonstrated that a number of wet meadows along the River Glaven harbored a much higher plant diversity than Hunworth Meadows. Such species pools could potentially provide sources of hydrochorically deposited propagules (e.g. Merritt et al. 2010; Nilsson et al. 2010) although, as noted by Clilverd (2006), this would require that the embankments that remain along some of these sites do not limit seed dispersal. The dominant declines in river discharge projected herein might limit this dispersal whilst less frequent inundation of Hunworth Meadown for most scenarios is likely to reduce the potential for waterborne introductions of propagules. As a result, species introductions such as via green hay and/or seed introduction from local meadows that support target species or communities may be necessary (e.g. Bissels et al. 2004; Walker et al. 2004; Baasch et al. 2016).

Conclusions

This study has updated and expanded the assessment of climate change impacts on Hunworth Meadow, a site previously restored via removal of an embankment isolating the floodplain from its river. With increased recognition of the importance of river-floodplain re-connection to river restoration success (Friberg et al. 2016), it is critical that longer-term climate change impacts on hydrological outcomes are assessed based on the most up-to-date climate change predictions. For Hunworth Meadow the combination of a high resolution, fully distributed MIKE SHE / MIKE 11 model of the meadow and a NAM rainfall-runoff model of the catchment enabled translation of projected changes in meteorological drivers (precipitation and PET, the latter driven by modified temperature, relative humidity and solar radiation) to hydrological impacts including river discharge, floodplain inundation and shallow water table levels. Climate changes for 40 scenarios (20 for both the 2050s and 2080s) were taken from UKCP18, the current UK probabilistic climate projections. Since the methodology follows an earlier study employing the previous generation of projections, UKCP09, the study is one of only a small number to re-evaluate climate change impacts on wetlands using updated projections that reflect ongoing developments in global climate change research.

Drier climatic conditions dominate the UKCP18 projections. Although there is uncertainty in the direction of change in precipitation, at an annual level the majority (60%) of scenarios project declines that increase in magnitude with lower probability level, enhanced radiative forcing and more distant time slice. Mean declines for the 50% probability, as likely as not to be exceeded, are 2.1% (2050s) and 2.6% (2080s). Most scenarios project increased winter precipitation and declines in summer. There is a much more consistency in the direction of change in PET with increases being projected for all but the 10% probability scenarios (small declines). The magnitude of elevated PET grows with probability level, radiative forcing and into the future. On average, increases for the 50% probability level are 10% (2050s) and 14% (2080s) above the baseline. The largest increases in PET are projected for summer months. Declines in annual net precipitation are projected for all scenarios apart from four 90% probability scenarios. Additionally, declines in the number of months with positive net precipitation are projected for all scenarios. These changes are very similar to those projected by UKCP09, although there is a tendency towards slightly larger declines (smaller increases) in precipitation and smaller increases in PET.

Declines dominate river discharge with reductions in mean discharge projected for all 10–70% probability levels, a higher frequency of declines compared to UKCP09. Differences in the magnitude of changes between the current study and those of UCKP09 are, however, small (<4 percentage points). For the 50% probability level, declines for UKCP18 are in the range 13–16% (2050s) and 10–18% (2080s). Peak (Q5) and low (Q95) flows are similarly projected to decline for the majority of scenarios with, in percentage terms, the latter being subject to larger declines with a resultant increase in the seasonality of river flow. The frequency with which bankfull discharges are exceeded declines for all but seven of the eight 90% probability scenarios. At the 50% probability, the incidence of these exceedance events is at least halved. Flood extent within Hunworth Meadow is projected to decline for the vast majority (<97%) of events / scenarios, although there is considerable inter-event variability in the size of these declines with antecedent conditions likely having a considerable influence.

Simulated shallow water tables within the meadow demonstrate the dominance of future drier conditions with declines in mean, WTE-5 and WTE-95 at individual wells and on average across the site being projected for all scenarios. These results are very similar to those using the earlier UKCP09 projections. Climate change-driven increases in summer drawdowns are larger on the floodplain; mean declines in WTE-95 for floodplain MIKE SHE cells for the 50% probability level equal 0.22 m (2050s) and 0.28 m (2080s), over twice as large as the declines for riparian cells. Peak winter water tables on the floodplain still intercept the ground surface with very little difference in WTE-5 across all scenarios. Closer to the river, the smaller drawdowns under both baseline and scenario conditions, alongside an overall more dynamic water table regime, are driven by exchanges with the river, and there are some small (-0.07–0.03m) scenario differences in WTE-5.

Evaluation of SEV_{as}, a measure of root zone soil aeration stress, provides a means of assessing potential botanical implications of changing hydrological conditions. Despite larger summer drawdowns, high baseline water tables on the floodplain through the early growing season are responsible for higher aeration stress compared to the riparian area (mean ten-year SEV_{as}: 4.88 m weeks vs 3.73 m weeks). Suitable conditions for vegetation communities that are relatively intolerant of aeration stress, most notably MG4 floodplain meadow, are therefore largely absent from the floodplain instead being concentrated in the riparian area. Conversely, a larger part of the floodplain has SEV_{as} values within the tolerable range for communities more able to withstand prolonged waterlogging, most notably MG8 water meadow, but also MG13 inundation grassland and AG/Cx water meadow. Declines in mean SEV_{as} for the floodplain are projected for all 40 climate change scenarios. At the 50% probability level these are equivalent to 1.28 m weeks (26%) and 1.45 m weeks (30%) for the 2050s and 2080s. Although this is largely repeated for the riparian area, the magnitudes of the declines are smaller (in absolute terms half the size of those on the

floodplain for the 50% probability), with small increases projected for four 90% probability scenarios. Lower aeration stress on the floodplain increases the extent of suitable conditions for MG4, MG7C flood pasture and MG8 whilst reducing the potential extent of MG13 and AG/Cx. Suitable conditions for MG4 also expand on the already dry embankment, whilst they either deteriorate or remain unchanged for the other communities. Whilst modified hydrological conditions in response to climate change will exert important controls on floodplain vegetation, additional factors will include changing nutrient delivery and availability within the soil as well as seed dispersal, all of which may be further impacted by shifts in the hydrology of the floodplain and its wider catchment.

Data availability The datasets employed in the current study are available from the corresponding author on reasonable request.

Code availability The MIKE SHE / MIKE 11 hydrological / hydraulic modelling system is commercially available from DHI Group (https://www.mikepoweredbydhi.com/products/mike-she)

Declarations

Competing interests The authors have no relevant financial or non-financial interests to disclose.

References

Acreman MC, Blake JR, Booker DJ, Harding RJ, Reynard N, Mountford JO, Stratford CJ (2009) A simple framework for evaluating regional wetland ecohydrological response to climate change with case studies from Great Britain. Ecohydrology 2:1–17

Acreman MC, Blake JR, Mountford O, Stratford C, Prudhomme C, Kay A, Bell V, Gowing D, Rothero E, Thompson JR, Hughes A, Barkwith A, van de Noort R (2012) Guidance on using wetland sensitivity to climate change tool-kit. A contribution to the Wetland Vision Partnership. Centre for Ecology and Hydrology, Wallingford, UK

Acreman MC, Dunbar MJ (2004) Defining environmental river flow requirements – a review. Hydrol Earth Syst Sci 8:861–876

Acreman MC, Holden J (2013) How wetlands affect floods. Wetlands 33:773–786

Acreman MC, Riddington R, Booker DJ (2003) Hydrological impacts of floodplain restoration: a case study of the River Cherwell. Hydrol Earth Syst Sci 7:75–85

Addy S, Wilkinson ME (2021) Embankment lowering and natural self-recovery improves river-floodplain hydro-geomorphic connectivity of a gravel bed river. Sci Total Environ 770:144626

Al-Khudhairy D, Thompson JR, Gavin H, Hamm NAS (1999) Hydrological modelling of a drained grazing marsh under agricultural land use and the simulation of restoration management scenarios. Hydrol Sci J 44:943–971

Antheunisse AM, Loeb R, Lamers LPM, Verhoeven JTA (2006) Regional differences in nutrient limitation in floodplains of selected European rivers. River Res Appl 22:1039–1055

Arnell NW, Freeman A (2021) The effect of climate change on agro-climatic indicators in the UK. Clim Chang 165:40

Arnell NW, Gosling SN (2013) The impacts of climate change on river flow regimes at the global scale. J Hydrol 486:351–364

Ausden M, Sutherland WJ, James R (2001) The effects of flooding lowland wet grassland on soil macroinvertebrate prey of breeding wading birds. J Appl Ecol 38:320–338

Baasch A, Engst K, Schmiede R, May K, Tischew S (2016) Enhancing success in grassland restoration by adding regionally propagated target species. Ecol Eng 94:583–591

Baldwin DS, Mitchell AM (2000) The effects of drying and re-flooding on the sediment and soil nutrient dynamics of lowland river–floodplain systems: a synthesis. Regul Rivers Res Manag 16:457–467

Barber KR, Leeds-Harrison PB, Lawson CS, Gowing DJG (2004) Soil aeration status in a lowland wet grassland. Hydrol Process 18:329–334

Baker C, Thompson JR, Simpson M (2009) Hydrological dynamics I: surface waters, flood and sediment dynamics. In: Maltby E, Barker T (eds) The Wetlands Handbook. Wiley-Blackwells, Chichester, pp 120–168

Bates BC, Kundzewicz ZW, Wu S, Palutikof JP (eds) (2008) Climate change and water, Technical paper of the Intergovernmental Panel on Climate Change. IPCC Secretariat, Geneva, Switzerland

Bates PD, Stewart MD, Desitter A, Anderson MG, Renaud J-P, Smith JA (2000) Numerical simulation of floodplain hydrology. Water Resour Res 36:2517–2529

Beltman B, Willems JH, Güsewell S (2007) Flood events overrule fertiliser effects on biomass production and species richness in riverine grasslands. J Veg Sci 18:625–634

Bernhardt ES, Palmer MA, Allan JD, Alexander G, Barnas K, Brooks S, Carr J, Clayton S, Dahm C, Follstad-Shah J, Galat D, Gloss S, Goodwin P, Hart D, Hassett B, Jenkinson R, Katz S, Kondolf GM, Lake PA et al (2005) Synthesizing U.S. River Restoration Efforts. Science 308:636–637

Bindi M, Olesen JE (2011) The responses of agriculture in Europe to climate change. Reg Environ Chang 11(Supplement 1):151–158

Bissels S, Hölzel N, Donath TW, Otte A (2004) Evaluation of restoration success in alluvial grasslands under contrasting flooding regimes. Biol Conserv 118:641–650

Blackwell M, Maltby E (eds) (2006) Ecoflood Guidelines: How to use floodplains for flood risk reduction. European Commission, Brussels

Brown AE, Zhang L, McMahon TA, Western AW, Vertessy RA (2005) A review of paired catchment studies for determining changes in water yield resulting from alterations in vegetation. J Hydrol 310:28–61

Burt TP, Bates PD, Stewart MD, Claxton AJ, Anderson MG, Price DA (2002) Water table fluctuations within the floodplain of the River Severn, England. J Hydrol 262:1–20

Byrne CF, Stone MC, Morrison RR (2019) Scalable flux metrics at the channel-floodplain interface as indicators of lateral surface connectivity during flood events. Water Resour Res 55:9788–9807

Canadell J, Jackson RB, Ehleringer JR, Mooney HA, Sala OE, Schulze ED (1996) Maximum rooting depth for vegetation types at the global scale. Oecologia 108:583–595

Castellarin A, Di Baldassarre G, Brath A (2010) Floodplain management strategies for flood attenuation in the river Po. River Res Appl 27:1037–1047

Champkin JD, Copp GH, Sayer CD, Clilverd HM, George L, Vilizzi L, Goddard MJ, Clarke J, Walker AM (2018) Responses of fishes and lampreys to the re-creation of meanders in a small English chalk stream. River Res Appl 34:34–43

Chan WCH, Thompson JR, Taylor RG, Nay AE, Ayenew T, MacDonald AM, Todd MC (2020) Uncertainty assessment in river flow projections for Ethiopia's Upper Awash Basin using multiple GCMs and hydrological models. Hydrol Sci J 65:1720–1737

Choudhury NY, Paul A, Paul BK (2004) Impact of costal embankment on the flash flood in Bangladesh: a case study. Appl Geogr 24:241–258

Chubarova NP (1972) Computation of the height of capillary rise of water in different genetic types of bound soils. Soil Mech Found Eng 9:25–27

Clilverd HM (2016) Hydroecological monitoring and modelling of river-floodplain restoration in a UK lowland river meadow. PhD thesis, UCL, London

Clilverd HM, Thompson JR, Heppell CM, Sayer CD, Axmacher JC (2013) River-floodplain hydrology of an embanked lowland Chalk river and initial response to embankment removal. Hydrol Sci J 58:627–650

Clilverd HM, Thompson JR, Heppell CM, Sayer CD, Axmacher JC (2016) Coupled hydrological/hydraulic modelling of river restoration impacts and floodplain hydrodynamics. River Res Appl 32:1927–1948

Clilverd HM, Thompson JR, Sayer CD, Heppell CM, Axmacher JC, Stratford CJ, Burningham H (2022) Simulated effects of floodplain restoration on plant community types. Appl Veg Sci 24:e12697

Dallaire G, Poulin G, Arsenault R, Brissette F (2021) Uncertainty of potential evapotranspiration modelling in climate change impact studies on low flows in North America. Hydrol Sci J 66:689–702

Dai Z, Amatya DM, Sun G, Trettin CC, Li G, Li L (2010) A comparison of MIKE SHE and DRAINMOD for modeling forested wetland hydrology in coastal South Carolina, USA. XVIIth World Congress of the International Commission of Agricultural Engineering. Quebec, Canada, Canadian Society for Bioengineering

Das BM (2002) Principles of geotechnical engineering, 5th Edition. Brooks/Cole, Pacific Grove, California

Dawson TP, Berry PM, Kampa E (2003) Climate change impacts on freshwater wetland habitats. J Nat Conserv 11:25–30

DHI (2007) MIKE SHE User Manual. DHI – Water & Environment, Hørsholm, Denmark

DHI (2009) MIKE 11 a modelling system for rivers and channels: reference manual. DHI Water and Environment, Hørsholm

Do HX, Zhao F, Westra S, Leonard M, Gudmundsson L, Boulange JES, Chang J, Ciais P, Gerten D, Gosling SN, Muller Schmier H, Stacke T, Telteu C-E, Wada Y (2020) Historical and future changes in global flood magnitude–Evidence from a model–observation investigation. Hydrol Earth Syst Sci 24:1543–1564

Döll P, Zhang J (2010) Impact of climate change on freshwater ecosystems: A global-scale analysis of ecologically relevant river flow alterations. Hydrol Earth Syst Sci 14:783–799

Duranel AJ, Acreman MC, Stratford CJ, Thompson JR, Mould DJ (2007) Assessing hydrological suitability of the Thames floodplain for species-rich meadow restoration. Hydrol Earth Syst Sci 11:170–179

Duranel A, Thompson JR, Burningham H, Durepaire P, Garambois S, Wyns R, Cubizolle H (2021) Modelling the hydrological interactions between a fissured granite aquifer and a valley mire in the Massif Central, France. Hydrol Earth Syst Sci 25:291–319

Duval TP, Hill AR (2006) Influence of stream bank seepage during low-flow conditions on riparian zone hydrology. Water Resour Res 42:W10425

Dwire KA, Boone Kauffman J, Baham JE (2006) Plant species distribution in relation to water-table depth and soil redox potential in montane riparian meadows. Wetlands 26:131–146

Eglington SM, Bolton M, Smart MA, Sutherland WJ, Watkinson AR, Gill JA (2010) Managing water levels on wet grasslands to improve foraging conditions for breeding northern lapwing Vanellus vanellus. J Appl Ecol 47:451–458

Emiru NC, Recha JW, Thompson JR, Belay A, Aynekulu E, Manyevere A, Demissie TD, Osano PM, Hussein J, Molla MB, Mengistu GM, Solomon D (2022) Impact of climate change on the hydrology of the Upper Awash River Basin. Ethiopia Hydrology 9:3

FAO (2013) Crop Water Information: Wheat (WWW) Food and Agriculture Organization of the United Nations (FAO) Water and Development Unit, Rome Italy (wwwfaoorg/nr/water/cropinfo_wheathtml; 21 September 2013)

Fellmann T, Witzke P, Weiss F, Van Doorslaer B, Drabik D, Huck I, Salputra G, Jansson T, Leip A (2018) Major challenges of integrating agriculture into climate change mitigation policy frameworks. Mitig Adapt Strateg Glob Chang 23:451–468

Fowler HJ, Kilsby CG (2007) Using regional climate model data to simulate historical and future river flows in northwest England. Clim Chang 80:337–367

Friberg N, Angelopoulos NV, Buijse AD, Cowx IG, Kail J, Moe TF, Moir H, O'Hare MT, Verdonschot PFM, Wolter C (2016) Effective river restoration in the 21st Century: From trial and error to novel evidence-based approaches. Adv Ecol Res 55:535–611

Gaberščik A, Krek JL, Zelnik I (2018) Habitat diversity along a hydrological gradient in a complex wetland results in high plant species diversity. Ecol Eng 118:84–92

Gardner EA, Burningham H, Thompson JR (2019) Impacts of climate change and hydrological management on a coastal lake and wetland system. Ir Geogr 52:21–48

Giuntoli I, Vidal JP, Prudhomme C, Hannah DM (2015) Future hydrological extremes: the uncertainty from multiple global climate and global hydrological models. Earth Syst Dynam 6:267–285

Gowing DJG, Gilbert JC, Youngs EG, Spoor G (1997) Water Regime Requirements of the Native Flora with particular reference to ESAs. Final report to the Ministry of Agriculture, Fisheries and Food (MAFF Commissioned Project BD0209), Silsoe College, Cranfield University, Silsoe, UK

Gowing DJG, Spoor G, Mountford O (1998b) The influence of minor variations in hydrological regime on grassland plant communities: implications for water management. In: Joyce CB, Wade PM (eds) European wet grasslands: biodiversity, management and restoration. Wiley, Chichester, pp 217–227

Gowing DJG, Tallowin JRB, Dise NB, Goodyear J, Dodd ME, Lodge RJ (2002a) A review of the ecology, hydrology and nutrient dynamics of floodplain meadows in England. English Nature Research Reports - No. 446, English Nature, Peterborough, UK

Gowing DJG, Youngs EG, Barber KR, Rodwell JS, Prosser MV, Wallace HL Mountford JO, Spoor G (2002b) The water regime requirements and the response to hydrological change of grassland plant communities. DEFRA report BD1310, Cranfield University, Silsoe, UK

Gowing DJG, Youngs EG, Gilbert JC, Spoor G (1998a) Predicting the effect of change in water regime on plant communities. In: H. Wheater and C. Kirby (Eds). Hydrology in a changing environment, Volume I. John Wiley, Chichester, UK, 473–483

Gosling SN, Zaherpour J, Mount NJ, Hattermann FF, Dankers R, Arheimer B, Breuer L, Ding J, Haddeland I, Kumar R, Kundy D, Liu J, van Griensven A, Veldkamp TIE, Vetter T, Wang X, Zhang X (2017) A comparison of changes in river runoff from multiple global and catchment-scale hydrological models under global warming scenarios of 1°C, 2°C and 3°C. Clim Chang 141:577–595

Hammersmark CT, Cable Rains M, Mount JF (2008) Quantifying the hydrological effects of stream restoration in a montane meadow Northern California USA. River Res Appl 24:735–753

Hafezparast M, Araghinejad S, Fatemi SE (2013) A conceptual rainfall-runoff model using the auto calibrated NAM models in the Sarisoo River. Hydrol Curr Res 4:148. https://doi.org/10.4172/2157-7587.1000148

Henriksen HJ, Troldborg L, Højberg AJ, Refsgaard JC (2008) Assessment of exploitable groundwater resources of Denmark by use of ensemble resource indicators and a numerical groundwater–surface water model. J Hydrol 348:224–240

Herbst M, Rosier PT, Morecroft MD, Gowing DJ (2008) Comparative measurements of transpiration and canopy conductance in two mixed deciduous woodlands differing in structure and species composition. Tree Physiol 28:959–970

Herrera-Pantoja M, Hiscock K, Boar R (2012) The potential impact of climate change on groundwater-fed wetlands in eastern England. Ecohydrology 5:401–413

Hester ET, Guth CR, Scott DT, Jones CN (2016) Vertical surface water–groundwater exchange processes within a headwater floodplain induced by experimental floods. Hydrol Process 30:3770–3787

Ho JT, Thompson JR, Brierley CB (2016) Projections of hydrology in the Tocantins-Araguaia Basin, Brazil: uncertainty assessment using the CMIP5 ensemble. Hydrol Sci J 61:551–567

Hollis GE, Thompson JR (1998) Hydrological data for wetland management. Water Environ J 12:9–17

Hough MN, Jones RJA (1997) The United Kingdom Meteorological Office Rainfall and Evaporation Calculation System: MORECS version 2.0 – an overview. Hydrol Earth Syst Sci 1:227–239

House AR, Thompson JR, Acreman MC (2016a) Projecting impacts of climate change on hydrological conditions and biotic responses in a chalk valley riparian wetland. J Hydrol 534:178–192

House AR, Thompson JR, Roberts C, de Smeth K, Old G, Acreman MC (2017) Projecting impacts of climate change on habitat availability in a macrophyte dominated chalk river. Ecohydrology 10(4) eco.1823

House AR, Thompson JR, Soresnson JPR, Roberts C, Acreman MC (2016b) Modelling groundwater/surface-water interaction in a managed riparian chalk valley wetland. Hydrol Process 30:447–462

Hulme M, Jenkins GJ, Lu X, Turnpenny JR, Mitchell TD, Jones RG, Lowe J, Murphy JM, Hassell D, Boorman P, McDonald R, Hill S (2002) Climate change scenarios for the United Kingdom: the UKCIP02 Scientific Report. Tyndall Centre for Climate Change Research, School of Environmental Sciences, University of East Anglia, Norwich, UK

IPCC (2000) Special Report on Emissions Scenarios (SRES): A special report of Working Group III of the Intergovernmental Panel on Climate Change. Cambridge University Press, Cambridge

IPCC (2013) Climate Change 2013: The Physical Science Basis. Working Group I Contribution to the Fifth Assessment Report of the Intergovernmental Panel on Climate Change [Stocker, T.F., Qin, D. Plattner, G.-K., Tignor, M., Allen, S.K., Boschung, J., eNauels, A., Xia, Y., Bex, V. and Midgley, P.M. (eds)]. Cambridge University Press, Cambridge, UK and New York, NY, USA

IPCC (2014) Climate Change 2014: Synthesis Report. Contribution of Working Groups I, II and III to the Fifth Assessment Report of the Intergovernmental Panel on Climate Change [Core Writing Team, R.K. Pachauri and L.A. Meyer (eds)]. IPCC, Geneva, Switzerland

IPCC (2018) Summary for Policymakers. In: Global Warming of 1.5°C. An IPCC Special Report on the impacts of global warming of 1.5°C above pre-industrial levels and related global greenhouse gas emission pathways, in the context of strengthening the global response to the threat of climate change, sustainable development, and efforts to eradicate poverty [Masson-Delmotte, V., P. Zhai, H.-O. Pörtner, D. Roberts, J. Skea, P.R. Shukla, A. Pirani, W. Moufouma-Okia, C. Péan, R. Pidcock, S. Connors, J.B.R. Matthews, Y. Chen, X. Zhou, M.I. Gomis, E. Lonnoy, T. Maycock, M. Tignor, and T. Waterfield (eds.)]. Cambridge University Press, Cambridge, UK and New York, NY, USA

Jenkins GJ, Murphy JM, Sexton DMH, Lowe JA, Jones P, Kilsby CG (2009) UK Climate Projections: Briefing Report. Met Office Hadley Centre, Exeter

Jiménez Cisneros BE, Oki T, Arnell NW, Benito G, Cogley JG, Döll P, Jiang T, Mwakalila SS (2014) Freshwater resources. In: Climate Change 2014: Impacts, Adaptation, and Vulnerability. Part A: Global and Sectoral Aspects. Contribution of Working Group II to the Fifth Assessment Report of the Intergovernmental Panel on Climate Change [Field, C.B., V.R. Barros, D.J. Dokken, K.J. Mach, M.D. Mastrandrea, T.E. Bilir, M. Chatterjee, K.L. Ebi, Y.O. Estrada, R.C. Genova, B. Girma, E.S. Kissel, A.N. Levy, S. MacCracken, P.R. Mastrandrea, and L.L. White (eds)]. Cambridge University Press, Cambridge, UK and New York, USA, 229–269

Jobst AM, Kingston DG, Cullen NJ, Schmid J (2018) Intercomparison of different uncertainty sources in hydrological climate change projections for an alpine catchment (upper Clutha River, New Zealand). Hydrol Earth Syst Sci 22:3125–3142

Johnson AC, Acreman MC, Dunbar MJ, Feist SW, Giacomello AM, Gozlan RE, Hinsley SA, Ibbotson AT, Jarvie HP, Jones JI, Longshaw M, Maberly SC, Marsh TJ, Neal C, Newman JR, Nunn MA, Pickup RW, Reynard NS, Sullivan CA et al (2009) The British river of the future: How climate change and human activity might affect two contrasting river ecosystems in England. Sci Total Environ 407:4787–4798

Jones CN, Ameli A, Neff BP, Evenson GR, McLaughlin DL, Golden HE, Lane CR (2019) Modeling connectivity of non-floodplain wetlands: insights, approaches, and recommendations. J Am Water Resour Assoc 55:559–577

Jung M, Burt TP, Bates PD (2004) Toward a conceptual model of floodplain water table response. Water Resour Res 40:W12409

Junk WJ, Bayley PB, Sparks RE (1989) The flood pulse concept in river floodplain systems. In: D.P. Doge, ed. Proceedings of the International Large River Symposium. Canadian Special Publication of Fisheries and Aquatic Sciences, Vol. 106, 110−127. Ottawa, Canada

Kay AL (2021) Simulation of river flow in Britain under climate change: Baseline performance and future seasonal changes. Hydrol Process 35:e14137

Kay AL, Watts G, Wells SC, Allen S (2020) The impact of climate change on U.K. river flows: A preliminary comparison of two generations of probabilistic climate projections. Hydrol Process 34:1081–1088

Keddy PA (2010) Wetland Ecology: Principles and Conservation. Cambridge University Press, Cambridge

Keddy PA, Campbell D (2020) The Twin Limit Marsh model: a non-equilibrium approach to predicting marsh vegetation on shorelines and in floodplains. Wetlands 40:667–680

Kingston DG, Todd MC, Taylor RG, Thompson JR, Arnell NW (2009) Uncertainty in the estimation of potential evapotranspiration under climate change. Geophys Res Lett 36:L20403

Kundzewicz ZW, Mata LJ, Arnell NW, Döll P, Kabat P, Jiménez B, Miller KA, Oki T, Sen Z, Shiklomanov IA (2007) Freshwater resources and their management. In: Parry ML, Canziani OF, Palutikof JP, van der Linden PJ, Hanson CE (eds) Climate change 2007: impacts, adaptation and vulnerability. Contribution of Working Group II to the Fourth Assessment Report of the Intergovernmental Panel on Climate Change. Cambridge University Press, Cambridge, pp 173–210

Laize CLR, Thompson JR (2019) R implementation of the Ecological Risk due to Flow Alteration (ERFA) method (R / Shiny Code). NERC Environmental Information Data Centre, Wallingford

Lai C, Chen X, Zhong R, Wang Z (2022) Implication of climate variable selections on the uncertainty of reference crop evapotranspiration projections propagated from climate variables projections under climate change. Agric Water Manag 259:107273

Lowe JA, Bernie D, Bett P, Bricheno L, Brown S, Calvert D, Clark R, Eagle K, Edwards T, Fosser G, Fung F, Gohar L, Good P, Gregory J, Harris G, Howard T, Kaye N, Kendon E, Krijnen J et al (2018) UKCP18 Science Overview Report. Met Office Hadley Centre, Exeter

Madsen H (2000) Automatic calibration of a conceptual rainfall-runoff model using multiple objectives. J Hydrol 235:276–288

Madsen H (2003) Parameter estimation in distributed hydrological catchment modelling using automatic calibration with multiple objectives. Adv Water Resour 26:205–216

Maltby EB, Ormerod S, Acreman MC, Blackwell M, Durance I, Everard M, Morris J, Spray C, Biggs J Boon P, Brierley B, Brown L, Burn A, Clarke S, Diack I, Duigan C, Dunbar M, Gilvear D, Gurnell A, Jenkins A, Large A, Maberly S, Moss B, Newman J, Robertson A, Ross M, Rowan J, Shepherd M, Skinner A, Thompson JR, Vaughan I, Ward R (2011) Freshwaters – Openwaters, Wetlands and Floodplains In: The UK National Ecosystem Assessment Technical Report. UK National Ecosystem Assessment, UNEP-WCMC, Cambridge, UK, 295–360

Marchand J-P, Biron P, Buffin-Bélanger T, Larocque M (2022) High-resolution spatiotemporal analysis of hydrologic connectivity in the historical floodplain of straightened lowland agricultural streams. River Res Appl 38:1061–1079

Merritt DM, Nilsson C, Jansson R (2010) Consequences of propagule dispersal and river fragmentation for riparian plant community diversity and turnover. Ecol Monogr 80:609–626

Met Office (2021) UK Climate Projections: Headline Findings. Met Office, Exeter

Meynell PJ, Thien NG, Ni DV, Triet T, van der Schans M, Shulman D, Thompson JR, Barzen J, Shepherd G (2012) An integrated fire and water management strategy using the ecosystem approach: Tram Chim National Park, Vietnam. In: Gunawardena ERN, Gopal B, Kotagama HB (eds) Ecosystems and Integrated Water Resources Management in South Asia. Routledge, New Delhi, India and Abingdon, pp 199–228

Michalcová D, Gilbert JC, Lawson CS, Gowing DJG, Marrs RH (2011) The combined effect of waterlogging, extractable P and soil pH on α-diversity: a case study on mesotrophic grasslands in the UK. Plant Ecol 212:879–888

Mommer L, Pedersen O, Visser EJW (2004) Acclimation of a terrestrial plant to submergence facilitates gas exchange under water. Plant Cell Environ 27:1281–1287

Monger F, Bond S, Spracklen DV, Kirkby MJ (2022) Overland flow velocity and soil properties in established semi-natural woodland and wood pasture in an upland catchment. Hydrol Process 36:e14567

Monteith JL (1965) Evaporation and the environment. Symp Soc Exp Biol 19:205–234

Moorlock BSP, Hamblin RJO, Booth SJ, Kessler H, Woods MA, Hobbs PRN (2002) Geology of the Cromer District – a brief explanation of the geological map. Sheet Explanations of the British Geological Survey. 1:50 000 Sheet 131 Cromer (England and Wales). BGS, Nottingham, UK

Moss R, Edmonds J, Hibbard K, Manning MR, Rose SK, van Vuuren DP, Carter TR, Emori S, Kainuma M, Kram T, Meehl GA, Mitchell JFB, Nakicenovic N, Riahi K, Smith SJ, Stouffer RJ, Thomson AM, Weyant JP, Wilbanks TJ (2010) The next generation of scenarios for climate change research and assessment. Nature 463:747–756

Mountford JO and Manchester SJ (editors), Barratt DR, Dale LC, Dunbar FM, Green IA, Sparks TH, Treweek JR, Barber KR, Gilbert JC, Gowing DJG, Lawson CS, Morris J, Spoor G (1999) Assessment of the effects of managing water-levels to enhance ecological diversity. Final report to the Ministry of Agriculture, Fisheries and Food. MAFF Commissioned Project BD1301

Murphy JM, Sexton DMH, Jenkins GJ, Boorman PM, Booth BBB, Brown CC, Clark RT, Collins M, Harris GR, Kendon EJ, Betts RA, Brown SJ, Howard TP, Humphrey KA, McCarthy MP, McDonald RE, Stephens A, Wallace C, Warren R et al (2009) UK Climate Projections Science Report: Climate change projections. Met Office Hadley Centre, Exeter

Naiman RJ, Decamps H, McClain ME (2010) Riparia: ecology conservation and management of stream- side communities. Elsevier Academic Press, London

Nash IE, Sutcliffe IV (1970) River flow forecasting through conceptual models. J Hydrol 10:282–290

Nilsson C, Brown RL, Jansson R, Merritt DM (2010) The role of hydrochory in structuring riparian and wetland vegetation. Biol Rev 85:837–858

Nilsson C, Svedmark M (2002) Basic principles and ecological consequences of changing water regimes: riparian plant communities. Environ Manag 30:468–480

Olesen JE, Bindi M (2002) Consequences of climate change for European agricultural productivity, land use and policy. Eur J Agron 16:239–262

Okruszko T, Duel H, Acreman MC, Grygoruk M, Flörke M, Schneider C (2011) Broad-scale ecosystem services of European wetlands– Overview of current situation and future perspectives under different climate and water management scenarios. Hydrol Sci J 56:1501–1517

Pescott O, Wentworth J (2011) Postnote: natural flood management. Houses of Parliament Parliamentary Office of Science and Technology, London

Plum N (2005) Terrestrial invertebrates in flooded grassland: a literature review. Wetlands 25:721–737

Rahim B-EEA, Yusoff I, Jafri AM, Othman Z, Abdul Ghani A (2012) Application of MIKE SHE modelling system to set up a detailed water balance computation. Water Environ J 26:490–503

Rahman MM, Thompson JR, Flower RJ (2016) An enhanced SWAT wetland module to quantify hydraulic interactions between riparian depressional wetlands, rivers and aquifers. Environ Model Softw 84:263–289

Rahman MM, Thompson JR, Flower RJ (2020) Hydrological impacts of climate change on rice cultivated riparian wetlands in the Upper Meghna River Basin (Bangladesh and India). Hydrol Sci J 65:33–56

Ramsar Convention on Wetlands (2018) Global Wetland Outlook: State of the World's Wetlands and their Services to People. Ramsar Convention Secretariat, Gland

Ramsar Convention on Wetlands (2021) Global Wetland Outlook: Special Edition 2021. Ramsar Convention Secretariat, Gland

Refsgaard JC, Sørensen HR, Mucha I, Rodak D, Hlavaty Z, Banský L, Klucovska J, Topolska J, Takac J, Kosc V, Enggrob H, Engesgaard P, Jensen JK, Fiselier J, Griffioen J, Hansen S (1998) An integrated model for the Danubian Lowland – methodology and applications. Water Resour Manag 12:433–465

Richter BD, Baumgartner JV, Powell J, Braun DP (1996) A method for assessing hydrologic alteration within ecosystems. Conserv Biol 10:1163–1174

River Restoration Centre. 2023. UK Projects Map (https://www.therrc.co.uk/uk-projects-map; accessed 25 April 2023). The River Restoration Centre, Cranfield, UK

Robertson AI, Bacon P, Heagney G (2001) The responses of floodplain primary production to flood frequency and timing. J Appl Ecol 38:126–136

Rodwell JS (1992) British Plant Communities. Volume 3 - Grasslands and Montane Communities. Cambridge University Press, Cambridge, UK

Saksena S, Merwade V (2017) Integrated modeling of surface-subsurface processes to understand river-floodplain hydrodynamics in the Upper Wabash River Basin. Proceedings of the World Environmental and Water Resources Congress 2017: International Perspectives, History and Heritage, Emerging Technologies, and Student Papers, 60–68

Sayer CD (2014) Conservation of aquatic landscapes: ponds, lakes, and rivers as integrated systems. WIREs Water 1:573–585

Sieben WH (1965) Het verband tussen outwatering en opbrengst bij de jonge zavelgronden in de Noordoost- polder. Van Zee tot Land 40:1–117

Silvertown J, Dodd ME, Gowing DJG, Mountford JO (1999) Hydrologically defined niches reveal a basis for species richness in plant communities. Nature 400:61–63

Singh A, Naik M, Gaurav K (2022) Drainage congestion due to road network on the Kosi alluvial Fan, Himalayan Foreland. Int J Appl Earth Obs Geoinf 112:102892

Singh CR, Thompson JR, French JR, Kingston DG, Mackay AW (2010) Modelling the impact of prescribed global warming on runoff from headwater catchments of the Irrawaddy River and their implications for the water level regime of Loktak Lake, northeast India. Hydrol Earth Syst Sci 14:1745–1765

Smart J, Amar A, O'Brien M, Grice P, Smith K (2008) Changing land management of lowland wet grasslands of the UK: impacts on snipe abundance and habitat quality. Anim Conserv 11:339–351

Surridge BWJ, Baird AJ, Heathwaite AL (2005) Evaluating the quality of hydraulic conductivity estimates from piezometer slug tests in peat. Hydrol Process 19:1227–1244

Tattersfield P, McInnes R (2003) Hydrological requirements of Vertigo moulinsiana on three candidate Special Areas of Conservation in England (Gastropoda, Pulmonata: Vertiginidae). Heldia 5:135–147

Thompson JR (2004) Simulation of wetland water level manipulation using coupled hydrological/hydraulic modelling. Phys Geogr 25:39–67

Thompson JR (2012) Modelling the impacts of climate change on upland catchments in southwest Scotland using MIKE SHE and the UKCP09 probabilistic projections. Hydrol Res 43:507–530

Thompson JR, Crawley A, Kingston DG (2016) GCM-related uncertainty for river flows and inundation under climate change: the Inner Niger Delta. Hydrol Sci J 61:2325–2347

Thompson JR, Crawley A, Kingston DG (2017a) Future river flows and flood extent in the Upper Niger and Inner Niger Delta: GCM-related uncertainty using the CMIP5 ensemble. Hydrol Sci J 62:2239–2265

Thompson JR, Gavin H, Refsgaard A, Refstrup Sørenson H, Gowing DJ (2009) Modelling the hydrological impacts of climate change on UK lowland wet grassland. Wetl Ecol Manag 17:503–523

Thompson JR, Gosling SN, Zaherpour J, Laizé CLR (2021a) Increasing risk of ecological change to major rivers of the world with global warming. Earth's Future 911, e2021EF002048

Thompson JR, Green AJ, Kingston DG, Gosling SN (2013) Assessment of uncertainty in river flow projections for the Mekong River using multiple GCMs and hydrological models. J Hydrol 486:1–30

Thompson JR, Green AJ, Kingston DG (2014) Potential evapotranspiration-related uncertainty in climate change impacts on river flow: An assessment for the Mekong River basin. J Hydrol 510:259–279

Thompson JR, Iravani H, Clilverd HM, Sayer CD, Heppell CM, Axmacher JC (2017b) Simulation of the hydrological impacts of climate change on a restored floodplain. Hydrol Sci J 62:2482–2510

Thompson JR, Laizé CLR, Acreman MC, Crawley A, Kingston DG (2021b) Impacts of climate change on environmental flows in West Africa's Upper Niger Basin and the Inner Niger Delta. Hydrol Res 52(4):958–974

Thompson JR, Refstrup-Sørenson H, Gavin H, Refsgaard A (2004) Application of the coupled MIKE SHE / MIKE 11 modelling system to a lowland wet grassland in Southeast England. J Hydrol 293:151–179

Thorup-Kristensen K, Salmerón Cortasa M, Loges R (2009) Winter wheat roots grow twice as deep as spring wheat roots is this important for N uptake and N leaching losses? Plant Soil 322:101–114

Tickner D, Opperman JJ, Abell R, Acreman MC, Arthington AH, Bunn SE, Cooke SJ, Dalton J, Darwall W, Edwards G, Harrison I, Hughes K, Jones T, Leclère D, Lynch AJ, Leonard P, McClain ME, Muruven D, Olden JO et al (2020) Bending the curve of global freshwater biodiversity loss: An emergency recovery plan. BioScience 70:330–342

Tockner K, Stanford JA (2002) Riverine flood plains: present state and future trends. Environ Conserv 29:308–330

Toogood SE, Joyce CB, Waite S (2008) Response of floodplain grassland plant communities to altered water regimes. Plant Ecol 197:285–298

USDA (1986) Urban hydrology for small watersheds. United States Department of Agriculture Technical Release 55 (TR-55)

van Vuuren DP, Edmonds J, Kainuma M, Riahi K, Thomson A, Hibbard K, Hurtt GC, Kram T, Krey V, Lamarque J-F, Masui T, Meinshausen M, Nakicenovic N, Smith SJ, Rose SK (2011) The representative concentration pathways: an overview. Clim Chang 109:5–31

Viers JH, Fremier AK, Hutchinson RA, Quinn JF, Thorne JH, Vaghti MG (2012) Multiscale patterns of riparian plant diversity and implications for restoration. Restor Ecol 20:160–169

Walker KJ, Stevens PA, Stevens DP, Mountford JO, Manchester SJ, Pywell RF (2004) The restoration and re-creation of species-rich lowland grassland on land formerly managed for intensive agriculture in the UK. Biol Conserv 119:1–18

Ward JV (1998) Riverine landscapes: biodiversity patterns, disturbance regimes, and aquatic conservation. Biol Conserv 83:269–278

Ward JV, Stanford JA (1995) Ecological connectivity in alluvial river ecosystems and its disruption by flow regulation. Regul Rivers Res Manag 11:105–119

Welsh MK, Vidon PG, McMillan SK (2020) Stream and floodplain restoration impacts riparian zone hydrology of agricultural streams. Environ Monit Assess 192:85

Wesseling J, van Wijk WR (1975) Soil physical conditions in relation to drain depth. In: Luthin JN (ed) Drainage of Agricultural Lands. American Society of Agronomy, Madison, pp 461–504

Wheeler BD, Gowing DJG, Shaw SC, Mountford JO, Money RP (2004) Ecohydrological guidelines for lowland wetland plant communities. Environment Agency, Peterborough

Wheeler B, Shaw S, Tanner K (2009) A wetland framework for impact assessment at statutory sites in England and Wales. Environment Agency Science Report SC030232, Environment Agency, Bristol, UK

Wilby RL, Dessai S (2010) Robust adaptation to climate change. Weather 65:180–185

Wotherspoon K (2008) The influence of land management and soil properties on the composition of lowland wet meadow vegetation, with implications for restoration. M.Sc. thesis, Queen Mary, University of London, London

Wyżga B (2001) Impact of the channelization-induced incision of the Skawa and Wisłoka Rivers, southern Poland, on the conditions of overbank deposition. Regul Rivers Res Manag 17:85–100

Xi Y, Peng S, Clais P, Chen Y (2020) Future impacts of climate change on inland Ramsar wetlands. Nat Clim Chang 11:45–51

Zeitz J, Velty S (2002) Soil properties of drained and rewetted fen soils. J Plant Nutr Soil Sci 165:618–626

Zelnik I, Čarni A (2013) Plant species diversity and composition of wet grasslands in relation to environmental factors. Biodivers Conserv 22:2179–2192

Zhang D, Liu X, Hong H (2013) Assessing the effect of climate change on reference evapotranspiration in China. Stoch Env Res Risk A 27:1871–1881

Zotarelli L, Dukes MD, Morgan KT (2010) Interpretation of soil moisture content to determine soil field capacity and avoid over-irrigating sandy soils using soil moisture sensors. (WWW) Gainesville, Florida (http://edis.ifas.ufl.edu/ae460; 26 September 2012)